



Fakultät für Medizin

Applications of HBVenv-specific antibodies as research and therapeutic tools

Fenna Meret Kolbe

Vollständiger Abdruck der von der Fakultät für Medizin der Technischen Universität München zur Erlangung des akademischen Grades einer

Doktorin der Naturwissenschaften (Dr. rer. nat.)

genehmigten Dissertation.

Vorsitz: Prof. Kathrin Schumann, Ph.D.

Prüfer*innen der Dissertation:

1. Prof. Dr. Ulrike Protzer

2. Prof. Dr. Matthias Feige

Die Dissertation wurde am 15.03.2023 bei der Technischen Universität München eingereicht und durch die Fakultät für Medizin am 18.07.2023 angenommen.

Table of contents

Abstract	4
Zusammenfassung	6
Abbreviations	8
1 Introduction	10
1.1 The Hepatitis B Virus	10
1.1.1 Morphology and replication cycle	10
1.1.2 Course of infection and HBV-associated liver diseases	16
1.2 Prophylaxis and current treatment options	19
1.2.1 Prophylactic vaccine.....	19
1.2.2 Nucleos(t)ide analogues and PEGylated interferon.....	20
1.3 Novel therapeutic options for the treatment of chronic HBV infection	21
1.3.1 Adoptive T-cell transfer.....	21
1.3.2 Therapeutic vaccination.....	21
1.4 Innate and adaptive immunity in HBV infection	22
1.4.1 The innate immune system.....	22
1.4.2 Adaptive immunity.....	23
1.5 Monoclonal antibodies as therapeutic and biotechnological tools	28
1.6 DNA nanotechnology	28
1.7 Aim of thesis	29
2 Results	31
2.1 Determination of HBsAg “a”-determinant structure	31
2.1.1 Construct design	31
2.1.2 Structural properties of Fc-“a”-determinant constructs	33
2.1.3 Fc-“a”-determinant constructs show pH sensitivity	34
2.1.4 Fc-“a”-determinant folds correctly and forms higher oligomers	36
2.1.5 Assessment of antibody binding affinities using the Fc-“a”-determinant constructs ..	40
2.2 Fc-engineered antibodies to enhance antibody dependent cellular cytotoxicity (ADCC) 42	
2.2.1 Structural properties of Fc-engineered antibodies.....	42
2.2.2 Fc-engineered antibodies are successfully produced in HEK293T cells.....	45
2.2.3 Fc-engineered antibodies are successfully purified.....	45
2.2.4 Fc-engineered antibodies recognize HBsAg.....	48
2.2.5 Neutralization capacity of Fc-engineered antibodies is impaired	48
2.2.6 ADCC assessment via reporter cell line.....	50

2.3	DNA Nanoshells	52
2.3.1	Conjugated antibodies still recognize their targets	52
2.3.2	DNA nanoshells conjugated with anti-HBcAg antibodies efficiently engulf recombinant HBcAg	52
2.3.3	DNA nanoshells conjugated with anti-HBsAg antibodies efficiently neutralize HBV infection <i>in vitro</i>	53
2.3.4	DNA nanoshells need to be present at time of infection to facilitate neutralization <i>in vitro</i>	55
2.3.5	DNA nanoshells seem to be taken up by monocyte derived dendritic cells	56
3	Discussion	58
3.1	Fc-“a“-determinant	58
3.1.1	Design and production and of Fc-“a“-determinant constructs	58
3.1.2	Fc-“a“-determinant constructs take on physiological structure.....	60
3.1.3	Fc-“a“-determinant constructs can be used to obtain antibody binding kinetics.....	62
3.2	Fc-engineered antibodies	63
3.2.1	Design of Fc-engineered antibodies	63
3.2.2	Production and stability of Fc-engineered antibodies.....	64
3.2.3	Fc-engineered antibodies show less HBsAg-specificity and neutralization capacity than the wild type	65
3.2.4	Comparison of antibody therapy with other therapeutic approaches.....	66
3.3	DNA nanoshells	70
3.3.1	DNA nanoshells efficiently inactivate HBV <i>in vitro</i> when present at time of infection	70
3.3.2	Effective neutralization with Nanoshells requires less antibody.....	72
3.3.3	Potential other fields of application of DNA nanoshells.....	73
4	Final evaluation and outlook	74
5	Materials and Methods	75
5.1	Materials	75
5.1.1	Devices	75
5.1.2	Consumables	76
5.1.3	Chemicals and Reagents	77
5.1.4	Solutions and Buffers	80
5.1.5	Kits.....	81
5.1.6	Enzymes	82
5.1.7	Primers	82
5.1.8	Plasmids	82
5.1.9	Cell lines, bacterial and viral strains.....	84
5.1.10	Media	84

5.1.11	Antigens	85
5.1.12	Antibodies	86
5.1.13	Software	86
5.2	Methods	87
5.2.1	Cell culture and transfection of mammalian cells	87
5.2.2	HBV infection, neutralization and quantification of viral replication	88
5.2.3	Molecular cloning methods	90
5.2.4	Protein production and purity as well as functional analysis	92
5.2.5	Flow cytometry	95
5.2.6	Affinity measurements.....	95
5.2.7	ADCC assessment via NFAT reporter cell line	96
6	List of figures	97
7	List of tables	98
8	Bibliography	99
	Acknowledgements.....	114

Abstract

Worldwide approximately 269 million people are chronically infected with the hepatitis B virus (HBV), even though an effective prophylactic vaccine is available. Chronic hepatitis B (CHB) increases the risk of developing liver cirrhosis or hepatocellular carcinoma (HCC) which led to 820,000 deaths in 2019, and represents, according to WHO, a major health problem. Current therapeutic options are limited to nucleos(t)ide analogues (NUC) and pegylated interferon (PEG-IFN). Both therapies inhibit viral replication but fail to eliminate the virus from infected cells. This is due to persistence of a covalently closed circular DNA (cccDNA) derived from the HBV genome, which resides in the nucleus serving as template for viral transcription. Therefore, lifelong treatment is required. Currently, different therapeutic approaches to eliminate HBV cccDNA are under development. These include therapeutic vaccination, adoptive T-cell transfer and antibody therapies.

The aim of this study was to pave the way for development of further antibody-based therapeutics. To establish new therapeutic antibodies, a deep knowledge of the antigen structure is of utmost importance. In the context of HBV infection, most neutralizing antibodies are directed against the so called "a"-determinant which defines a region within the luminal loop of the viral surface antigen (HBsAg). Knowledge about the tertiary structure of the "a"-determinant is so far limited to predictive models. This is due to the complex structure of HBsAg, which harbors transmembrane domains, rendering protein crystallization and thereby protein structure determination difficult. The complexity of the antigen structure further hampers the characterization of antibody-antigen binding properties.

During the first part of this thesis, a protein was designed which should contribute to the functional characterization of HBsAg-specific antibodies and facilitate the structure determination of the "a"-determinant. For this, the "a"-determinant was fused to the Fc-part of an IgG antibody. This protein will be referred to as Fc-"a"-determinant. As the Fc-part is a dimer, the dimerization of the "a"-determinant essential for correct structure formation is promoted as well. Furthermore, employing an Fc-part facilitates protein purification via affinity chromatography. The Fc-"a"-determinant was expressed in HEK293T cells, purified and subjected to Western Blot and ELISA analysis for structural and functional characterization. The Fc-"a"-determinant could be used for binding affinity analyses of an HBsAg-specific antibody via microscale thermophoresis (MST), thereby portraying a tool for further functional characterization of HBsAg-specific antibodies. Unfortunately the Fc-"a"-determinant forms higher oligomers at concentrations ≥ 30 nM, impeding protein crystallization and subsequent structure determination.

Another aspect of this thesis was the design of HBsAg-specific antibodies that elicit a strong antibody dependent cell-mediated cytotoxicity (ADCC) without the risk of antibody-dependent enhancement of infection (ADE). For this, Fc-engineering was utilized to optimize a previously isolated human monoclonal, HBsAg-specific antibody for the binding to CD16, the natural killer cell receptor activating ADCC. Three antibody variants were designed, expressed in HEK293T cells and subsequently purified via a protein G column. All Fc-optimized antibodies showed a decreased antigen specificity in ELISA analyses and concomitant decreased neutralization capacity in HBV-infected HepG2-NTCP cells compared to the wildtype so that they turned out not to be suited for therapeutic use.

The final goal of this thesis was the establishment of a novel therapeutic approach for existing and newly emerging viral infections. For this, DNA nanoshells were designed via DNA origami, which were on the inside coated with HBV-specific antibodies. These nanoshells are supposed to encapsulate HBV in the circulation, thereby preventing infection. Neutralization assays with HBV-infected HepG2-NTCP cells showed a significantly enhanced neutralization capacity of the nanoshells when compared to antibodies alone. While further studies are needed to evaluate the clinical relevance of the nanoshells, this technology provides a novel approach to react to newly emerging viruses and to optimize the therapies of existing viral infections.

Zusammenfassung

Weltweit sind ungefähr 269 Millionen Menschen chronisch mit dem Hepatitis B Virus (HBV) infiziert, obwohl eine wirksame prophylaktische Impfung verfügbar ist. Chronische Hepatitis B (CHB) erhöht das Risiko an einer Leberzirrhose oder hepatozellulärem Karzinom (HCC) zu erkranken, was 2019 laut WHO weltweit zu 820.000 Todesfällen führte, und stellt somit ein großes Gesundheitsproblem dar. Bisherige Therapiemöglichkeiten beschränken sich auf die Verabreichung von Nukleos(t)id Analoga (NUC) und pegyliertem Interferon (PEG-IFN). Beide Therapien hemmen die Virusreplikation. Sie sind aber nicht in der Lage das Virus aus der infizierten Leber zu eliminieren. Der Grund hierfür ist die persistente Form des Hepatitis B Virus (HBV), die kovalent geschlossene zirkuläre DNA (cccDNA), die im Zellkern lokalisiert ist und als Template für die virale Transkription dient. Dadurch ist eine lebenslange Behandlung erforderlich. Verschiedene therapeutische Ansätze, die auf die Eliminierung der cccDNA zielen, sind in Entwicklung. Dazu gehören therapeutische Impfungen, ein adoptiver T-Zell Transfer und Antikörpertherapien.

Das Ziel dieser Studie war es, den Weg zur Entwicklung Antikörper-basierter Therapeutika zu ebnen. Um neue therapeutische Antikörper zu entwickeln, ist ein tiefes Verständnis der Antigenstruktur von äußerster Wichtigkeit. Im Kontext einer HBV-Infektion richten sich die meisten neutralisierenden Antikörper gegen die sogenannte "a"-Determinante, die einen Bereich des luminalen Loops des viralen Oberflächenantigens (HBsAg) definiert. Das Wissen über die Tertiärstruktur der "a"-Determinante beschränkt sich auf prädiktive Modelle. Dies lässt sich darauf zurückführen, dass das HBsAg Transmembran-Domänen beinhaltet, die eine Proteinkristallisation und anschließende Strukturbestimmung erschweren. Die komplexe Struktur des HBsAg führt weiterhin dazu, dass die Charakterisierung von Antikörper-Antigen Bindungen deutlich erschwert ist.

Im ersten Teil der Arbeit wurde ein Protein designt, das zur funktionellen Charakterisierung von HBsAg-spezifischen Antikörpern beitragen und die Strukturaufklärung der "a"-Determinante erleichtern soll. Hierfür wurde die "a"-Determinante an den Fc-Teil eines IgG Antikörpers kloniert. Das Protein wird im Folgenden als Fc-"a"-Determinante benannt. Da der Fc-Teil als Dimer vorliegt, wird in diesem Konstrukt die Dimerisierung der "a"-Determinante unterstützt, die seine Struktur mitbestimmt. Außerdem erleichtert der Fc-Teil die Reinigung des Proteins mittels Affinitätschromatographie. Die Fc-"a"-Determinante wurde in HEK293T Zellen exprimiert, aufgereinigt und mittels Western Blot und ELISA strukturell und funktionell charakterisiert. Mittels Microscale Thermophorese (MST) konnte die Fc-"a"-Determinante für die Bestimmung der Affinitätskonstanten eines HBsAg-spezifischen Antikörpers verwendet werden und trägt somit zur weiteren funktionellen Charakterisierung von HBsAg-spezifischen Antikörpern bei. Leider stellte sich

heraus, dass die Fc-“a“-Determinante bereits bei Konzentrationen ≥ 30 nM höhere Oligomere bildet, die die Proteinkristallisation und somit die Strukturaufklärung behindern.

Ein weiterer Aspekt dieser Arbeit war, HBsAg-spezifische Antikörpern so zu modulieren, dass sie die Fähigkeit erwerben, eine starke antikörperabhängige zellvermittelte Toxizität (ADCC) auszulösen, ohne dabei infektionsverstärkend zu wirken. Hierfür wurde ein bereits isolierter HBsAg-spezifischer monoklonaler Antikörper mittels Fc-Engineering für die Bindung an CD16, den ADCC-aktivierenden NK-Zell-Rezeptor, optimiert. Insgesamt wurden drei Antikörper designt, in HEK293T Zellen exprimiert und anschließend über eine Protein G Säule gereinigt. Alle drei Fc-optimierten Antikörper zeigten allerdings eine verringerte Antigenspezifität im ELISA und damit einhergehende eine verringerte Neutralisationskapazität in HBV-infizierten HepG2-NTCP Zellen im Vergleich zum Wildtyp, so dass sie für eine antivirale Therapie nicht nutzbar sind.

Das finale Ziel dieser Arbeit war die Etablierung eines neuen Therapieansatzes für diverse, bestehende und neu auftretende Virusinfektionen. Hierfür wurden DNA-Nanoshells mittels DNA-Origami hergestellt, welche mit HBV-spezifischen Antikörpern gekoppelt wurden. Diese Nanoshells sollen HBV in der Zirkulation abfangen, einkapseln und somit eine Infektion verhindern. Neutralisationsexperimente mit HBV-infizierten HepG2-NTCP Zellen zeigten eine signifikant höhere Neutralisationskapazität der Nanoshells im Vergleich zu den Antikörpern allein. Zwar sind weitere Studien nötig, um eine klinische Relevanz der Nanoshells zu beurteilen, doch stellt diese Technologie einen originellen Ansatz dar, um auf neu auftretende Viren zu reagieren und die Therapie von bereits bekannten Virusinfektionen zu optimieren.

Abbreviations

aa	Amino acid
ADCC	Antibody dependent cell-mediated cytotoxicity
ADE	Antibody dependent enhancement
APC	Antigen presenting cell
BCR	B-cell receptor
cccDNA	Covalently closed circular DNA
CH1-3	Constant heavy chain 1-3
CHB	Chronic Hepatitis B
DC	Dendritic cell
DNA	Desoxyribonucleinacid
DR	Direct repeats
dsIDNA	Double stranded linear DANN
EM	Electron microscopy
ER	Endoplasmatic reticulum
Fc region	Fragment crystallizable region
HBcAg	Hepatitis B virus core antigen
HBeAg	Hepatitis B virus earl antigen
HBsAg	Hepatitis B virus surface antigen
HBsAg-L	Large Hepatitis B virus surface antigen
HBsAg-M	Middle Hepatitis B virus surface antigen
HBsAg-S	Small Hepatitis B virus surface antigen
HBV	Hepatitis B Virus
HBVenv	Hepatitis B Virus envelope protein
HBx	Hepatitis B virus X-protein
HCC	Hepatocellular carcinoma
HPSG	Heparan sulfate proteoglycans
IFN	Interferon
IFNgamma	Interferon gamma
Ig	Immunoglobulin
IL2	Interleukin 2
ITL	Infiltrating tumor lymphocytes
kb	Kilo bases
LAG3	Lymphocyte-activation gene 3
M	Molar
m	Meter
mAb	Monoclonal antibody
MAVS	Mitochondrial antiviral-signaling protein
MHC	Major histocompatibility complex
mM	Millimolar
MVB	Multivescular body
NA	Nucleos(t)die analogues
NK	Natural killer cell
NLR	Nucleotide-binding oligomerization domain-like receptors

nM	Nanomolar
nm	Nanometer
NOD	Nucleotide-binding oligomerization domain
NPC	Nuclear pore complex
ORF	Open reading frame
PAMP	Pathogen-associated molecular pattern
PD1	Programmed cell death protein 1
PEG	Polyethylene glycol
pgRNA	Pre-genomic RNA
pi	Post infection
pM	Picomolar
pMHC	Peptide Major histocompatibility complex
preC-C	PreCore-Core
preS-S	PreSurface-Surface
PRR	Pattern recognition receptors
rcDNA	Relaxed circular DNA
RIG-I	Retinoic acid-inducible-gene-I
RLR	Retinoic acid-inducible-gene-I-like receptors
RNA	Ribonucleinacid
SVP	Subviral particles
TCR	T-cell receptor
TEM	Transmission electron microscopy
T_h1, T_h2, T_h17	T helper cell 1, 2, 17
TLR	Toll-like receptor
TNFα	Tumor necrosis factor α
T_{reg}	Regulatory T cell
V domain	Variable domain
V_H	Heavy chain variable region
V_L	Light chain variable region
WHO	World Health Organization

1 Introduction

1.1 The Hepatitis B Virus

This chapter covers the biological characteristics of the hepatitis B virus (HBV), including its morphology, replication cycle and the different courses of infection. While describing the morphology, particular attention will be paid on the structure of the viral surface antigens as they are of great importance for this thesis.

1.1.1 Morphology and replication cycle

1.1.1.1 Morphology

HBV is a partially double-stranded, enveloped DNA virus belonging to the family of Hepadnaviridae [Schaefer 2007]. As all members of this family, HBV is highly species-specific and hepatotropic [Magnius et al. 2020]. In 1965, *Blumberg et al.* discovered the Australian antigen, now referred to as Hepatitis B surface antigen (HBsAg), and its correlation to viral hepatitis [Blumberg et al. 1965]. Five years later, *Dane et al.* published electron microscopy data showing the existence of the infectious HBV virions, henceforth referred to as “Dane particles” [Dane et al. 1970]. The Dane particle is 42 nm in diameter and composed of an icosahedral core protein, enveloped by a lipid layer (Figure 1). The core protein (HBcAg) forms the shell of the HBV capsid which can be observed in two different variants. Capsids with a T = 3 symmetry are 30 nm in diameter, while capsids with a T = 4 symmetry are 34 nm in diameter. The capsid harbors the viral DNA, titled relaxed circular DNA (rcDNA), associated with a polymerase with reverse transcriptase activity. The surface of the viral envelope consists of the HBsAg, which includes small (-S), middle (-M) and large (-L) surface protein [Bruss 2007]. Furthermore, infected cells give rise to subviral particles (SVP), mainly consisting of S protein, reaching a diameter of 22 nm. These SVP do not contain viral DNA and are therefore not infectious and can exceed the number of infectious virions up to 10⁵-fold [Ganem and Prince 2004]. The S protein forms dimers that spontaneously assemble to SVP and provide its antigenic structure, herein referred to as HBsAg. Even though the amino-acid sequence is known, the exact structure of HBsAg is not resolved, yet, as crystallization efforts of SVP were not successful so far. A cryo-electron microscopy approach, however, led to a low-resolution image of HBsAg [Gilbert et al. 2005]. The folding pathway of HBsAg is partially characterized and reveals that the S protein consists of at least two transmembrane domains [Eble et al. 1986; Eble et al. 1987]. Further studies pointed towards the existence of two additional transmembrane domains, leading to the proposed monomeric structure of S protein (Figure 2) [Komla-Soukha and Sureau 2006; Suffner et al. 2018]. Directly after being synthesized, two S protein subunits each form dimers via disulfide-bridges and acquire antigenicity of HBsAg [Wunderlich and

Bruss 1996]. While about 50% of HBsAg found in patient sera is N-glycosylated at residue N146, this glycosylation does not affect the dimerization of the protein [Suffner et al. 2018] but may play an important role for antibody binding. How exactly the transition from S protein dimers to HBsAg SVP is mediated is still unclear, as no intermediate structures have been observed, yet. *Suffner et al.* proposed a model of how the homodimeric structure of S protein could be formed (Figure 2) [Suffner et al. 2018]. The luminal or antigenic loop, amino-acids 99 - 169, harbors the so-called “a”-determinant, which refers to the region between amino-acids 124-147, marks the part of S protein that is bound by most anti-HBsAg antibodies [Chiou et al. 1997; Romani et al. 2018] and is of great importance for this thesis.

Phylogenetically, HBV can be divided into 10 different genotypes (A-J) [Okamoto et al. 1988; Norder et al. 1992; Stuyver et al. 2000; Arauz-Ruiz et al. 2002; Tatematsu et al. 2009; Arankalle et al. 2010] and 4 serological subtypes (ayw, ayr, adw and adr). The serotypes are defined by different residues in the immunogenic loop of the S protein [Le Bouvier 1971; Bancroft et al. 1972; Okamoto et al. 1987]. Furthermore, the geographical distribution of the various subtypes is very diverse and the different geno- and serotypes have a major influence not only on the severity of the emerging illness, but also on the course of infection [Velkov et al. 2018].

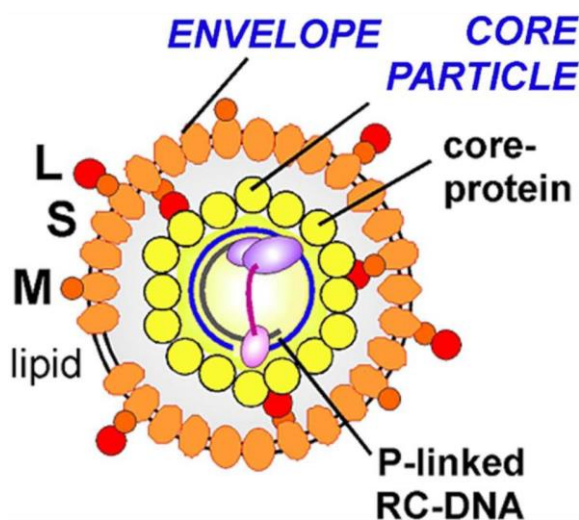


Figure 1. Structural properties of HBV. The infectious HBV particle, referred to as Dane particle, is composed of an encapsulated partially double stranded rcDNA, associated with a polymerase with reverse transcriptase activity. The icosahedral capsid is enveloped by a lipoprotein membrane, which consists of host lipids and hepatitis B envelope proteins – HbsAg-S, -M and -L. The whole virion is about 42 nm in diameter [Nassal 2015].

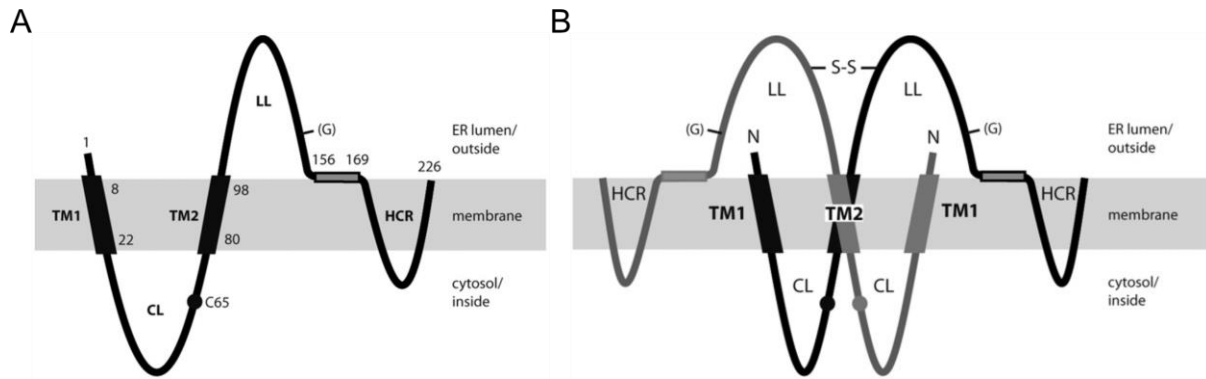


Figure 2. Proposed structure of HBsAg. (A) Monomeric S protein is composed of two transmembrane domains (TM1, TM2) and a putative HCR, that results in two additional transmembrane regions. The luminal or antigenic loop (aa 99-169) comprises the “a”-determinant (aa 124-147) that is the main epitope for neutralizing antibodies. Within the “a”-determinant a N-glycosylation site is present at N146. **(B)** Directly after synthesis, the S protein forms dimers which are stabilized by disulfide-bonds, thereby acquiring antigenicity of HBsAg [Suffner et al. 2018].

1.1.1.2 Genomic organization of the virus

With only 3.2 kilobases (kb) in length, the genome of HBV is highly organized and partitioned into 4 partially overlapping open reading frames (ORF), termed precore-core (preC-C), presurface-surface (preS-S), P and X (Figure 3), which are located on the coding minus strand (-). The plus strand (+) is incomplete and noncoding [Ganem and Prince 2004]. The relaxed circular configuration of the genome is preserved by the end regions which harbor two direct repeats (DR) of 11 nucleotides. Both of these, DR1 and DR2, are not only crucial for viral replication but play also an important role in the integration of HBV DNA into the host genome [Dejean et al. 1984]. By employing two in-frame initiation codons, the preC-C ORF encodes two different proteins, the core protein and the hepatitis B e antigen (HBeAg). Following core protein translation, initiated by the internal initiation codon, it assembles into the complete viral capsids. Utilizing the upstream initiation codon, the precursor of HBeAg is translated and further processed in the endoplasmic reticulum (ER) before generating mature HBeAg [Takahashi et al. 1983]. The P ORF partially overlaps the preC-C ORF and encodes the HBV DNA polymerase (P protein) with reverse transcriptase and RNase H activity. Within the P ORF, the preS-S ORF is located, utilizing three in-frame initiation codons to allow for translation of the proteins HBsAg-S, -M and -L, that assemble into the viral envelope. Finally, the X ORF overlaps the P ORF and regulates translation of HBV X protein (HBx) [Ganem and Prince 2004].

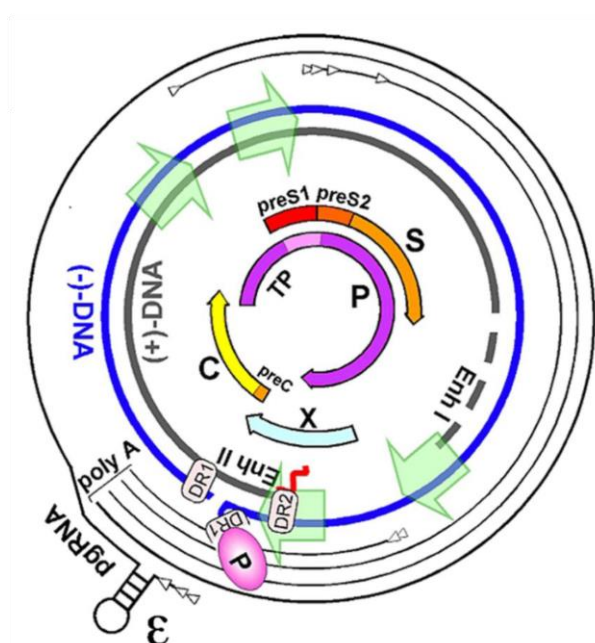


Figure 3. Genomic organization of HBV. As the genome of HBV is only 3.2 kb in length, it needs to be highly organized. It comprises four partially overlapping open reading frames (ORF) located on the (-) strand, namely PreC-C (orange/yellow arrow), PreS-S (red/orange arrow), P (violet arrow) and X (light blue arrow), giving rise to four pregenomic RNA (pgRNA) that encode seven viral proteins in total. Viral transcripts are depicted by the black outer lines with the transcription starting at positions indicated by the white arrowheads. The encapsidation signal on the pgRNA is depicted by ϵ and the green arrows symbolize promoters. TP marks the terminal protein domain of P protein. The end regions of the rcDNA utilize direct repeats (DR1, DR2) of 11 nucleotides each to enable viral replication and integration into the host genome. The (+) strand is non-coding with Enh I and Enh II depicting transcriptional enhancers [Nassal 2015].

1.1.1.3 Replication cycle

The replication cycle of HBV starts with the low-affinity attachment of the Dane particle to heparan sulfate proteoglycans (HPSG) on the target cell via HBsAg-S [Verrier et al. 2016], followed by binding to the sodium taurocholate receptor NTCP, mediated by HBsAg-L (Figure 4 (1-2)) [Yan et al. 2012]. Upon binding to NTCP, the virion enters the cell via endocytosis. Following pH decrease during translocation of the endosomes to different cellular compartments, the viral envelope fuses with the endosomal membrane, thereby releasing the viral capsid into the cytoplasm, which is subsequently transported to the nucleus [Ko et al. 2017]. After being translocated to the nucleus pore complex (NPC), the viral capsid disassembles, which leads to a release of HBV rcDNA and core proteins into the nucleus. In the nucleus, the rcDNA is converted to covalently closed circular DNA (cccDNA), which is organized in a chromatin-like minichromosome and serves as template for viral replication and gene expression, illustrating the persistent form of HBV [Nassal 2015]. The cccDNA is transcribed into four different HBV RNAs that are 3.5 kb, 2.4 kb, 2.1 kb and 0.7 kb in length, respectively [Tong and Revill 2016]. The 3.5 kb HBV RNA exists in two different forms, the precore mRNA and the pregenomic RNA (pgRNA) [Kramvis and Kew 1999]. Following transcription, the HBV RNAs are translocated into the

cytoplasm. The shortest of these RNAs is translated into HBx, which affects a variety of processes like activation of host and viral gene transcriptions, DNA repair, cell growth and apoptosis [Tong and Revill 2016]. The 3.5 kb precore mRNA is translated into the precore polypeptide, which is further processed at the ER to form mature HBeAg, which is released from the cell and serves as surrogate marker of HBV infection [Kramvis and Kew 1999; Tong and Revill 2016]. While a part of the 3.5 kb long pgRNA is translated into core and P protein, the untranslated pgRNA is encapsulated into the nucleocapsid, formed by the previously translated core protein. One part of the pgRNA containing nucleocapsids is shuttled back to the nucleus where they serve as stable pool of cccDNA, ensuring the persistence of the virus, the rest is enveloped by the envelope proteins, which are translated from the 2.4 kb and 2.1 kb HBV RNA, respectively [Tong and Revill 2016]. While the 2.4 kb HBV RNA is translated into HBsAg-L, the 2.1 kb HBV RNA serves as template for the translation of HBsAg-M and -S [Nassal 2015; Tong and Revill 2016]. After being synthesized, the HBsAg variants are further processed in the ER and the Golgi apparatus. The envelopment of nucleocapsids takes place at the membrane of multivesicular bodies (MVB) where two cytoplasmic domains of HBsAg interact with the nucleocapsid which in turn initiates the budding process. These enveloped nucleocapsids are then released and are able to infect more cells [Ko et al. 2017]. In addition to surrounding the nucleocapsids, the surface proteins also form two different kinds of subviral particles, with spherical particles being the majority, consisting mainly of HBsAg-S, and filamentous particles, which also contain HBsAg-M and -L [Bruss 2007]. While the filaments are secreted utilizing the same MVB pathway as the enveloped nucleocapsids, the spherical subviral particles are released via the Golgi pathway of the host cell [Ko et al. 2017].

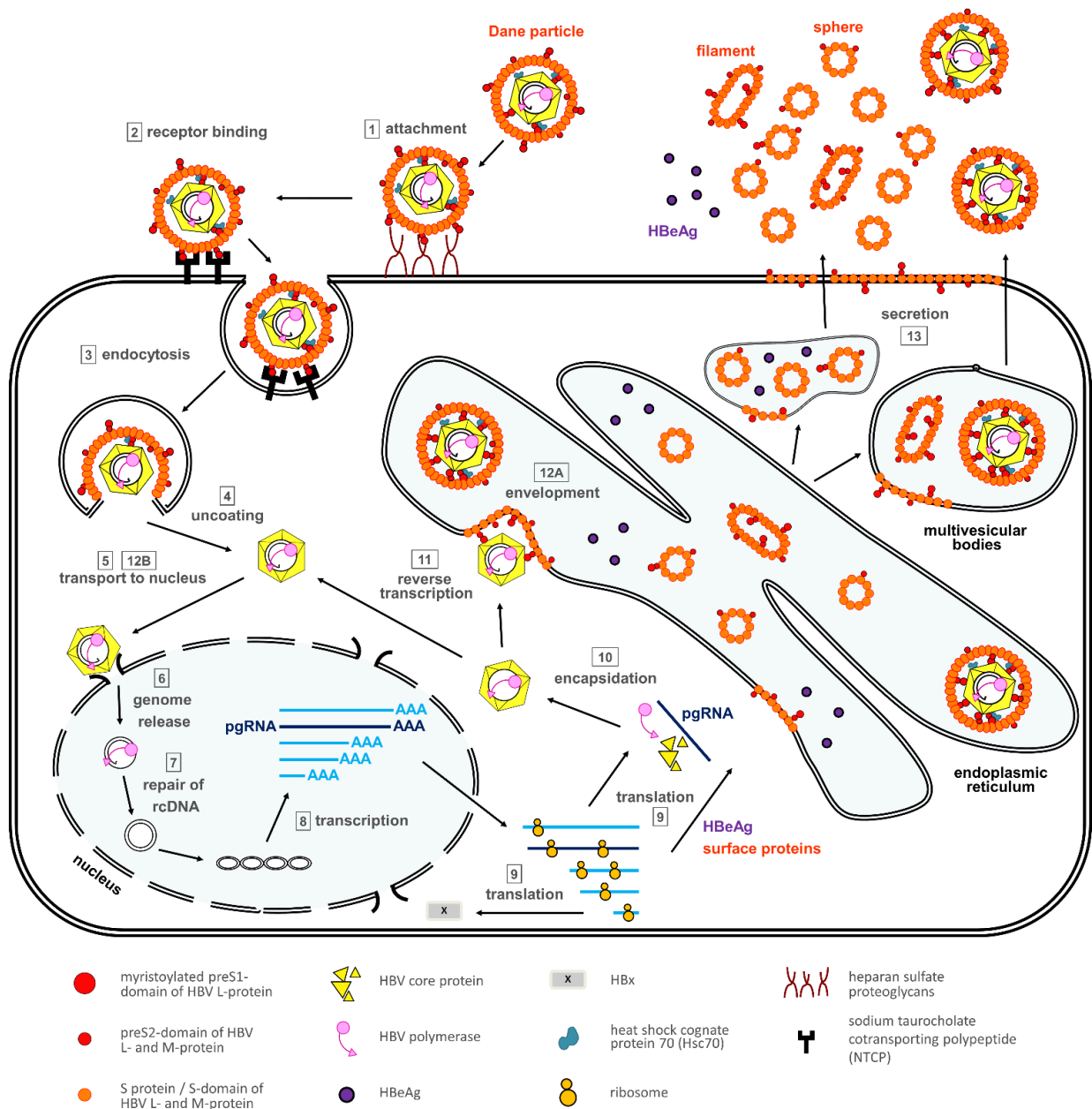


Figure 4. Replication cycle of HBV. (1) Dane particle attaches to HPSRG via HBSAg-S, followed by (2) binding to NTCP via HBSAg-L and (3) endocytosis. (4) The viral capsid is released into the cytoplasm and (5) transported to the NPC. (6) The viral genome is released into the nucleus, (7) rcDNA is converted into cccDNA, which in turn is (8) transcribed into the different pgRNA. (9) Upon translocating of the pgRNA into the cytoplasm, they are translated into their corresponding proteins. (10) The pgRNA is encapsidated by the newly synthesized core proteins, a part is (11) reverse transcribed into rcDNA and (12B) retransported to the nucleus to ensure a persistent pool of cccDNA. (12A) The other part of encapsidated pgRNA is enveloped by the synthesized envelope proteins, processed in the ER and (13) secreted via the MVB pathway to allow for subsequent infection of cells. SVP not containing viral DNA are secreted via both, the MVB and the Golgi pathway. From [Ko et al. 2017].

1.1.2 Course of infection and HBV-associated liver diseases

HBV is transmitted via blood, saliva, and other body fluids through sexual contact, as well as through perinatal transmission and injecting drug use. Upon infection with HBV, patients develop either acute hepatitis B, which is characterized by the transient presence of serum HBsAg and IgM anti-HBc, or chronic hepatitis B, which is marked by the persistence of serum HBsAg for more than 6 months [Juszczak 2000]. The course of infection hugely varies between patients and is influenced by the age and immune status of the individual. Compared to only 5-10% of infected adults, 90% of infected newborns develop a chronic infection state [Juszczak 2000]. This chapter will cover the differences between acute and chronic HBV infection as well as HBV-associated liver diseases, which can arise from chronic infection.

1.1.2.1 Acute HBV infection

While more than 95% of HBV-infected adults are able to spontaneously clear the infection within 3-6 months, this is true for only 5% of young children and newborns [Peeridogaheh et al. 2018; WHO 2022]. In areas such as Central Latin America, North America and Western Europe the prevalence is low, correlating with an acute course of infection which is mainly transmitted via unsafe sexual contact and injections with unsterile needles during drug abuse [Papastergiou et al. 2015; Peeridogaheh et al. 2018]. HBV has developed numerous ways to sufficiently suppress the innate immune response in infected hepatocytes, one of them being the interference with Toll-like receptor (TLR) signaling, and is therefore referred to as “stealth virus” [Yu et al. 2017]. Thus, acute HBV infection is mainly cleared by polyclonal and multispecific T cells that elicit both, cytolytic and noncytolytic functions [Thimme et al. 2003] and is accompanied by inflammation and necrosis of hepatocytes, thereby portraying a self-limiting disease that usually proceeds without symptoms [Chisari et al. 2010; Noordeen 2015; Peeridogaheh et al. 2018]. However, some patients develop an acute infection accompanied by symptoms such as jaundice which could lead to the progression of the infection to fulminant hepatitis, leading to acute liver failure, causing a mortality rate of acute Hepatitis B of about 0.5 – 1% [Peeridogaheh et al. 2018; WHO 2022].

During an acute HBV infection, HBsAg, HBeAg and viral DNA as well as high ALT levels can be detected in the patients’ serum [Krugman et al. 1979], with serum HBeAg and DNA being markers for active viral replication and therefore infectivity [Liang and Ghany 2002]. The natural course of acute HBV infection is characterized by the clearance of serum HBeAg and undetectable DNA levels, followed by clearance of HBsAg and seroconversion to anti-HBc IgM antibodies [Perrillo et al. 1983; Liang 2009]. Anti-HBs antibodies develop late in infection and persist even after recovery, thereby serving as marker for HBV immunity [Tabor et al. 1981]. While the exact role of HBeAg in HBV infection is still

not fully understood, it has been correlated to a higher risk of developing hepatocellular carcinoma [Yang et al. 2002]. Therefore, persistent levels of serum HBeAg during acute HBV infection indicates the necessity of treatment to prevent further progression of the disease [Liang 2009]. Furthermore, while an individual is being considered as not infected, when there is no serum HBsAg detected and HBV no longer resides in the blood, cccDNA still persists in the nuclei of hepatocytes and presents an inactive form of the virus which could be reactivated when administering immunosuppressive medication. This needs to be taken into consideration when treating patients that have cleared an HBV infection [Etienne et al. 2022].

1.1.2.2 Chronic HBV infection

Chronicity of HBV infection occurs in 2-6% of adults and 90% of newborns, highlighting the necessity of a mature adaptive immune system in order to clear the infection. The transmission route preceding the development of a chronic state of hepatitis B is usually maternally during the first three trimesters of pregnancy and during the perinatal period [Peeridogaheh et al. 2018]. In areas with a high infection prevalence, such as Asia, sub-Saharan Africa, the Pacific Islands and parts of the Balkan regions, the course of infection is mainly chronic [Papastergiou et al. 2015]. In contrast to acute hepatitis B, chronic HBV infection is characterized by high titer serum levels of HBsAg, HBeAg and viral DNA even after several months. An infection is regarded as chronic when HBsAg is detected in serum for more than 6 months [Liang 2009]. While most cases do not portray any liver damage, some patients develop liver fibrosis and cirrhosis, which ultimately leads to a higher risk of developing hepatocellular carcinoma (HCC) [Peeridogaheh et al. 2018]. Contrasting the strong and multispecific T-cell response that can be observed in patients with acute Hepatitis B, a chronic infection portrays a weak and unspecific T-cell response by an exhausted T-cell population which fails to eliminate infected hepatocytes [Maini et al. 2000; Bertoletti and Gehring 2006]. Available treatment for chronic hepatitis B (CHB) is limited to pharmaceuticals that only inhibit viral replication, thereby stalling the infection but being unable to eradicate the virus from the infected hepatocytes due to the residing cccDNA, the persistent form of HBV. Each year, 1.5 million new CHB cases are reported and in 2019, roughly 296 million people were chronically infected with HBV. CHB increases the risk of developing liver cirrhosis or hepatocellular carcinoma (HCC), resulting in estimated 820,000 deaths per year, highlighting the need of a curative treatment [WHO 2022].

1.1.2.3 HBV-associated hepatocellular carcinoma

Following chronic HBV infection, HCC can develop which is the third leading cause of cancer-related deaths [Sung et al. 2021]. While a preceding liver cirrhosis greatly enhances the risk of establishing HCC, and a cirrhotic state of the liver could be observed in 80-90% of patients, some individuals

develop HCC without a foregoing cirrhosis [Forner et al. 2012; Peeridogaheh et al. 2018]. Furthermore, the incidence of HCC in a cirrhotic state of CHB has been reported to be more than 8.5 fold higher than in a non-cirrhotic state [Tarao et al. 2019]. There are three mechanisms that are known to induce development of HCC which will be described in the following. The first mechanism is the expression of viral proteins, especially HBx. While the exact mode of action of HBx is not fully understood, yet, it is probably a crucial factor for HBV replication. It has also been reported to interfere with p53, a transcription factor which is involved in DNA-repair, cell cycle control and induction of apoptosis and therefore often referred to as guardian of the genome. Especially this interaction of HBx with p53 is thought to drive HCC development [Su et al. 1998; Peeridogaheh et al. 2018]. The second mechanism which is associated with HCC development is the integration of viral genome into the host genome, which occurs in 85-90% of HCC cases [Peeridogaheh et al. 2018]. Integration can take place when virions that contain HBV double stranded linear DNA (dsDNA) infect a cell. Upon release of viral dsDNA, it is integrated at double-stranded DNA breaks during the cellular repair mechanism. This form of integrated HBV shows to be replication deficient [Peeridogaheh et al. 2018]. While the exact role of integrated HBV DNA in HCC development is still not fully understood, there are a few theories to explain the relationship. Firstly, as a result of genome integration, the expression patterns and functions of host genes could be altered, leading to a favoring of HCC development. The integrated form of HBV DNA has been reported to give rise to HBsAg which in turn could develop into infectious particles that are secreted [Tu et al. 2021]. Furthermore, an instability of chromosomes has been reported [Peeridogaheh et al. 2018]. The last mechanism to drive HCC development is the increased hepatocyte division which occurs to compensate for the loss of infected hepatocytes. Additionally, because of the persistent state of inflammation, there is an increase of genetic damages, which is known to be crucial for cancer progression [Peeridogaheh et al. 2018].

1.2 Prophylaxis and current treatment options

While current treatments only suppress viral replication and are not able to eradicate the virus from the body, there is also a prophylactic vaccine available which is highly efficient. This chapter will introduce the prophylactic vaccine and the different treatment options that are used in the clinics right now, highlighting their respective benefits and disadvantages.

1.2.1 Prophylactic vaccine

The first recombinant prophylactic vaccine against hepatitis B, Recombivax HB, has been licensed in 1986 [Food and Drug Administration 1987; Bucci 2020]. Two other vaccines, Energix-B and Heplisav-B, have been approved by the FDA afterwards [Food and Drug Administration 1988, 2017]. Both, Recombivax HB and Energix-B contain HBsAg-S, have been shown to be safe and very effective in reducing cases of HBV infection and are approved for people of all ages [Food and Drug Administration 1987, 1988; FDA 04.24.2019, 2019]. Vaccination is especially recommended for infants by the World Health Organization (WHO) [WHO 2022]. Heplisav-B also contains HBsAg with CpG as adjuvant and is approved for use in adults of 18 years and older [Food and Drug Administration 2017]. The vaccines help to establish a broad immunity against all genotypes of HBV (A-H) by neutralizing antibodies directed against the viral surface antigen [Romanò et al. 2015] and have been shown to provide long-term protection [Gabbuti et al. 2007].

However, as soon as a chronic infection has been established, the vaccine is not effective anymore and other treatments are needed. In order to achieve sufficient protection via a vaccine, neutralizing antibodies are of utmost importance. For HBV, the part that is targeted by neutralizing antibodies is the hydrophilic, luminal loop of HBsAg, also referred to as “a”-determinant [Romanò et al. 2015]. Any changes in this region may lead to mutants escaping the immune system because the neutralizing antibodies do not recognize their original target anymore, which in turn leads to an insufficient treatment with antibodies [Peeridogaheh et al. 2018]. A variety of escape mutants is known and most of them harbor mutations in the “a”-determinant region [Romanò et al. 2015; Qin and Liao 2018; Tarafdar et al. 2022]. Some of them are known to structurally alter the “a”-determinant, while the mode of action of other mutants is not fully understood, yet [Romanò et al. 2015; Lazarevic et al. 2019]. This is partly due to the fact, that the actual structure of the “a”-determinant region is not known. To fully understand the mechanism of immune escape through certain mutations, the structure of HBsAg, especially the “a”-determinant, needs to be resolved and the binding characteristics of neutralizing antibodies to the “a”-determinant need to be studied more thoroughly. This knowledge could also aid the development of further treatment options that can not only prevent

HBV infection but also clear an existing chronic infection by eradicating the persistent form of HBV, the cccDNA.

1.2.2 Nucleos(t)ide analogues and PEGylated interferon

Nucleos(t)ide analogues (NUC) display antiviral efficacy, are administered orally and are used for the treatment of chronic HBV infection [Papatheodoridis et al. 2002]. They act by interfering with the viral polymerase. Upon phosphorylation, they are structurally similar to nucleotides and get incorporated into growing DNA strands. As they act as chain terminators, ultimately, this leads to the disengagement of the polymerase of the DNA, thereby preventing viral replication [Fung et al. 2011]. While NUC treatment is well tolerated, very effective in stalling the virus spread and a finite treatment in HBeAg-negative patients is feasible, discontinuation of the medication can lead to recurrence of the infection and subsequent establishment of cirrhosis and HCC [Fung et al. 2011; Lok et al. 2016; Chien and Liaw 2022]. Therefore, patients stopping NUC treatment need to be carefully monitored in order to assure safety [Chien and Liaw 2022].

Similar to NUCs, treatment with PEGylated interferon (PEG-IFN) leads to a sufficient inhibition of viral spread but not to an eradication of the virus. It acts as an antiviral, antiproliferative and immunomodulatory agent whose lifetime in the cell is prolonged by the modification with PEG [Ye and Chen 2021]. While treatment with PEG-IFN might lead to a long-term suppression of the virus even after discontinuation of treatment, it is also accompanied by more severe side effects [Brunetto and Bonino 2014; Tseng et al. 2014]. Therefore, there is an urgent need for a therapeutic therapy which does not only suppress the viral replication, but ultimately eradicates the virus from the host cell. The obvious target for drug development in this direction is the cccDNA which serves as template for viral replication and is therefore referred to as the persistent form of HBV. While it is difficult to target the cccDNA directly, as it resides in the cell, therapy with antibodies which target infected cells and elicit a strong antibody effector function, such as antibody dependent cell-mediated cytotoxicity (ADCC), seems to be a promising approach to tackle this challenge.

1.3 Novel therapeutic options for the treatment of chronic HBV infection

This chapter covers treatment options for chronic HBV infection which are in development. This includes adoptive T-cell transfer and therapeutic vaccination.

1.3.1 Adoptive T-cell transfer

Since CHB is characterized by a scarce T-cell response and T cells have been shown to silence and destabilize cccDNA in infected hepatocytes, adoptive T-cell transfer is a promising therapeutic approach [Wisskirchen et al. 2019]. Here, T cells that are redirected to HBV envelope proteins are administered to the patients to replenish the pool of functional T cells. This in turn leads to the induction of a strong T-cell response against HBV-infected cells which enables the clearance of infected cells and thereby also the eradication of cccDNA. A similar approach, namely transfer of bone marrow stem cells from HBV immune donors, led to viral clearance in CHB patients [Ilan et al. 1993; Lau et al. 1997; Ilan et al. 2000]. However, the number of target cells is very high which might lead to severe side effects when following this therapeutic approach. This is why studies have been performed to also include a safe-guard mechanism in the generated T cells. First *in vivo* analyses revealed that T cells co-expressing HBV specific receptors and a safety switch such as iC9 are able to reliably recognize and eradicate infected hepatocytes without showing hepatotoxicity [Klopp et al. 2021]. Overall, adoptive T-cell transfer is a promising approach to tackle the challenge of treating CHB, but more studies are needed to rule out any possible side effects and co-treatment with other antiviral components, such as antibodies, to already lower the viral load in patients may be more efficient.

1.3.2 Therapeutic vaccination

Another approach for the treatment of CHB is a therapeutic vaccination. TherVacB, a heterologous prime-boost vaccination schedule has been developed in our lab. The vaccination strategy is a protein prime vaccination followed by a modified vaccinia virus Ankara (MVA) boost vaccination which has been shown to efficiently induce strong anti-HBV immune responses [Backes et al. 2016]. Simultaneous siRNA mediated knockdown of PD-L1 expression showed enhanced efficacy of the TherVacB approach [Bunse et al. 2022]. A similar effect was observed when virus antigen expression was knocked down prior to vaccination, resulting in efficient restoration of T cells and induction of HBV specific immune responses [Michler et al. 2020]. Additionally, combinational treatment with CpG after vaccination showed to enhance CD8 T-cell functions in the liver of HBV-transgenic mice [Kosinska et al. 2019].

1.4 Innate and adaptive immunity in HBV infection

The following chapter describes the basic principles of the immune system in order to defend the host from various pathogens. It will cover the differences between innate and adaptive immunity and describe in further detail T- and B-cell mediated immunity. Particular focus will be led on the roles of innate and adaptive immunity in HBV infection.

1.4.1 The innate immune system

Innate immunity is the first line of defense when encountering a pathogen. It comprises anatomic and chemical but also cellular barriers. To defend against a variety of microbes and pathogens, the first layer of defense – the anatomical barrier – is crucial. Anatomical barriers are skin, the oral mucosa, the respiratory epithelium and the intestines. These already prevent pathogens entering the body. When this barrier is not sufficient and a pathogen finds its way into the body, it will come across the next barrier: complement and other microbial proteins like C3, defensins and RegIIIγ. Should these barriers also be insufficient, the third line of defense – the innate immune cells – comes into play. These consist of macrophages, granulocytes and natural killer cells [Murphy and Weaver 2017].

In the scope of viral infections, pathogen recognition receptors (PRR) recognize the pathogen-associated molecular patterns (PAMP) of the entering virus, which leads to the activation of a signaling cascade. PAMPs, like viral nucleic acids, are recognized by different PRRs, such like TLR, retinoic acid-inducible-gene-I (RIG-I)-like receptors (RLR) and nucleotide-binding oligomerization domain (NOD)-like receptors (NLR) [Koyama et al. 2008]. Usually, PRRs then recruit adaptor proteins, such as mitochondrial antiviral-signaling protein (MAVS), which in turn leads to activation of the transcription factor NF-κB, subsequently triggering the production of IFN and inducing the innate immune response, which ultimately leads to elimination of infected cells and free viruses [Koyama et al. 2008]. In HBV infection, however, this immune activation is circumvented by the virus utilizing a variety of different strategies [Xu et al. 2021]. While activation of different TLRs has been shown to be crucial for a sufficient defense against HBV [Isogawa et al. 2005], other studies suggested that HBV is suppressing the activation of the TLR signaling pathway to escape the immune system [Wu et al. 2009]. Another study showed the ability of HBV to suppress RIG-I-MAVS signaling, illustrating yet another way of HBV to escape the immune system [Zhou et al. 2021]. Additionally, it was demonstrated that HBeAg can inhibit NF-κB phosphorylation, which presumably is one factor leading to immune escape and HBV persistence [Yu et al. 2017]. All these findings highlight different strategies of HBV to evade the detection of the host innate immunity, which further emphasizes the crucial role of a strong adaptive immune response mediated by B and T cells.

1.4.2 Adaptive immunity

In contrast to the innate immune system, the adaptive immune system needs to learn how to defend against different pathogens, which makes it much more specific than the innate immune response. It can be further divided into B and T cell mediated immunity which will be distinguished in the following, with special focus on their regarding roles in chronic HBV infection. Furthermore, general antibody effector functions such as ADCC and antibody dependent enhancement (ADE) will be highlighted.

1.4.2.1 T-cell mediated immunity

After leaving the thymus, matured T cells recirculate between the blood and secondary lymphoid organs before encountering their specific antigen [Gowans and Knight 1964; Marchesi and Gowans 1964]. T cells express a variety of antigen-binding receptors, the T-cell receptors (TCR). Each naïve T cell expresses one single TCR type [Wucherpfennig et al. 2010]. In order for the T cell to proliferate and differentiate, it is dependent on certain signals from antigen presenting cells (APC), such as dendritic cells (DC), macrophages and B cells [Guy et al. 2013]. APCs are specialized in taking up pathogens to subsequently process and present antigens in form of peptides on the major histocompatibility complex (MHC) [Murphy and Weaver 2017]. There are two main classes of MHC, class I and class II. MHC I molecules are expressed by nearly every cell type, while MHC II molecules are expressed on APCs only [Wieczorek et al. 2017]. Therefore, MHC I molecules are important for the presentation of processed viral proteins after a cell has been infected by a virus and MHC II molecules present phagocytosed peptides from the extracellular environment [Murphy and Weaver 2017]. These peptide-MHC complexes (pMHC) are recognized by the TCR on T cells which leads to their activation and subsequent proliferation and differentiation [Guy et al. 2013]. T cells are generally divided into two subgroups, depending on whether they express the cell-surface protein CD4 or CD8. Both proteins play major roles in the recognition of MHC molecules and are referred to as co-receptors due to their necessity in T-cell function and signaling [Murphy and Weaver 2017]. While CD4 recognizes a region of MHC II, CD8 recognizes a region of MHC I. Therefore, CD4⁺ T cells mainly function in the defense against antigens derived from the extracellular surroundings, while CD8⁺ T cells mainly act in an antiviral manner. Upon recognition of pMHC with the aid of CD4⁺ or CD8⁺, T cells elicit a variety of functions. The most direct function of a T cell is its cytotoxicity. CD8⁺ T cells differentiating into cytotoxic T cells recognize infected cells, release effector molecules such as perforin, granzymes, granulysins and Fas ligand, which in turn leads to the activation of an endogenous apoptotic pathway of the infected cells [Murphy and Weaver 2017]. CD4⁺ T cells mainly differentiate into effector T cells, being divided into four major groups, namely helper T cell 1, -2 and -17 and regulatory T cells (T_h1, T_h2 T_h17 and T_{reg}) [Wan and Flavell 2009]. All of these subsets are specialized

for different functions and produce different effector molecules. T_H1 cells activate macrophages, T_H2 cells are important for the defense against parasites and induce B-cell proliferation as well as isotype switching, while T_H17 cells recruit neutrophils to the infection site, thereby promoting inflammation. T_{reg} cells mainly produce suppressive cytokines and help maintaining self-tolerance and homeostasis [Wan and Flavell 2009].

1.4.2.2 T-cell mediated immunity in the context of CHB

As already pointed out in 1.1.2, the course of HBV infection largely depends on the presence of a strong and multispecific T-cell response towards infected hepatocytes. While $CD4^+$ T cells efficiently aid the activation of an HBV specific $CD8^+$ T-cell response during an acute HBV infection, this is not true in a chronic infection [Buschow and Jansen, Diahann T. S. L. 2021]. It has been shown that $CD4^+$ T cells in CHB patients express programmed-death 1 (PD-1) and lymphocyte activation gene 3 (LAG-3) to a much higher degree than in healthy individuals, and also lose the capability to secrete cytokines such as $IFN\gamma$, IL-2 and $TNF\alpha$, thereby failing to elicit their helper function [Dong et al. 2019]. Coexpression of PD-1 And LAG-3 is a well-known characteristic of infiltrating tumor lymphocytes (ITL) that leads to T-cell exhaustion [Du et al. 2020]. As a consequence, exhausted $CD4^+$ T cells are incapable of inducing the antiviral $CD8^+$ T-cell response which would be required for clearance of the infection [Chisari et al. 2010]. The exact mechanism how CHB leads to an exhausted T-cell population is not fully understood, yet. However, it has been shown that released serum HBeAg suppresses both, the humoral and the T-cell response to HBcAg *in vivo*, suggesting a immunomodulatory role of HBeAg [Chen et al. 2004]. Since high levels of serum HBsAg are detected in CHB patients, it might have a similar modulatory function as HBeAg by acting as high dose tolerogen, thereby suppressing immune elimination of infected hepatocytes [Webster et al. 2004]. Lastly, even if its function is not fully understood, it is known that overexpression of HBV X protein can inhibit cellular proteasome activity which could in turn interfere with the processing and presentation of antigens on MHC molecules [Hu et al. 1999; Chisari et al. 2010]. Taking together, HBV is equipped with a variety of immunosuppressive functions which still need to be further studied in the future to reliably counteract an infection.

1.4.2.3 B-cell mediated immunity

The B cell mediated or humoral immune response relies on the activation of B cells, which in turn leads to the production of immunoglobulins (Ig) that are specific for a certain pathogen. B cells are produced in bone marrow cells and circulate in the lymphatic system after maturation until they encounter a pathogen. In order to recognize antigens, B cells express surface immunoglobulins, also referred to as B-cell receptors (BCR) [LeBien and Tedder 2008]. These BCR act in two different ways when binding to an antigen. First, when recognizing an antigen of a microbe, the BCR activates a signaling cascade.

Second, the BCR can also aid to internalize the antigen, process it and present it on MHC II in order for effector T cells to recognize the antigen [Murphy and Weaver 2017]. After being activated, B cells eventually differentiate into plasma or memory cells, that are capable to secrete pathogen-specific soluble Igs which are then referred to as antibodies. Upon encountering a pathogen repeatedly, antibodies are produced and secreted. They bind the pathogens and elicit an immune response [Murphy and Weaver 2017].

1.4.2.3.1 Structural properties of antibodies

Antibodies, or immunoglobulins (Igs), are secreted by B cells and represent the soluble form of the BCR. They form a Y-shape, with the two arms of the Y being the variable regions (V regions) which harbor the antigen binding sites and the stem of the Y being the constant or crystallizable region (C region) which is not as variable and interacts with FcγRs on cells [Murphy and Weaver 2017]. These Igs can be divided into five major classes, namely IgG, IgA, IgD, IgE and IgM, all of which elicit different functions and differ in their organization of the C region [Encyclopedia Britannica 2022]. While the different antibody classes are noteworthy, for a detailed description of the structural properties, only IgG molecules will be explained as they are the most important ones for this thesis.

IgG antibodies are dimeric molecules that consist of two different forms of polypeptide chains, two heavy chains (H) with 50 kDa each and two light chains (L) with 25 kDa each, resulting in a total mass of IgG of roughly 150 kDa. Each heavy chain consists of one variable domain (V_H) and three constant domains (C_{H1} - C_{H3}), while the light chain only consist of one variable and one constant domain (V_L and C_L) (Figure 5) [Gorshtein 2022]. Both, heavy and light chain, are co-translationally translocated into the endoplasmatic reticulum (ER), and protein folding is already initiated before the translation is completed [Bergman and Kuehl 1979]. Upon formation of the C_{H3} domain, the dimerization of the heavy chains is induced, which is further supported by the disulfide bridges within the hinge region. At this point, all constant regions, except for C_{H1} , are formed. The light chains will form separately and association of light with heavy chains induces folding of the C_{H1} domain [Feige et al. 2010].

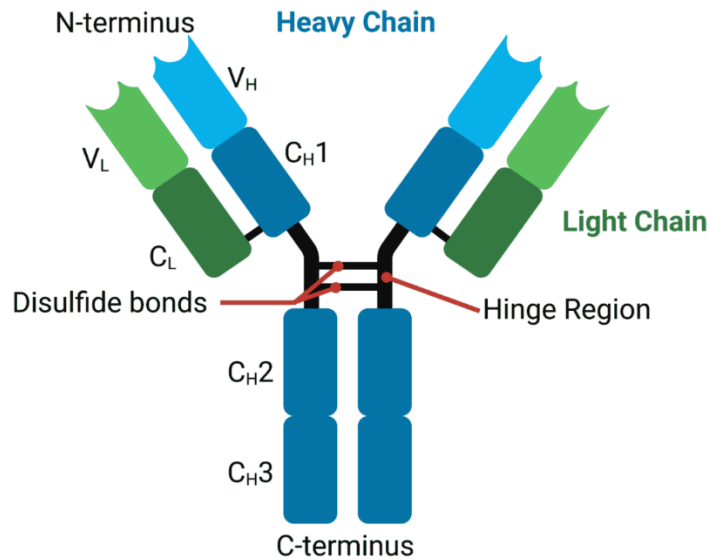


Figure 5 Structural properties of an IgG1 molecule. IgG1 is composed of two heavy (blue) and two light chains (green) which are paired via disulfide bonds within the hinge region (black lines). The variable regions on the tip of the Y-shape are the antigen binding sites (V_H, V_L), while the stem of the Y binds to effector molecules expressed on cells [Gorshtein 2022].

1.4.2.3.2 Antibody dependent cell-mediated cytotoxicity (ADCC)

One important effector mechanism of antibodies is antibody dependent cell-mediated cytotoxicity which allows for sufficient killing of target cells that express a certain antigen. Upon opsonization of the target cell, which describes the binding of antibodies to target cells, natural killer (NK) cells recognize the Fc-part of the antibody via their CD16 Fc-receptor [Perussia et al. 1983; Murphy and Weaver 2017]. This receptor recognizes IgG1 and IgG3 subclasses [Galon et al. 1997]. Following antibody recognition, NK cells release perforin and granzymes which subsequently induces an apoptotic pathway in the target cell, ultimately leading to cell death [Murphy and Weaver 2017].

1.4.2.3.3 Antibody dependent enhancement (ADE)

In some cases, antibodies do not only help to eradicate pathogens, but can also help them to circumvent immune responses and enter their target cells. This mechanism is referred to as antibody dependent enhancement (ADE) [Hawkes and Lafferty 1967]. This phenomenon occurs when antibodies are able to recognize their target but are incapable of eliminating the pathogen. The pathogen is then covered with antibodies which makes it invisible to the other immune cells, allowing for the uptake in target cells which is then followed by an enhanced replication of the pathogen [Hawkes and Lafferty 1967; Murphy and Weaver 2017]. As already stated above, FcγR on NK cells recognize IgG subclasses 1 and 3 [Galon et al. 1997], leading to the conclusion that opsonization of a pathogen by these IgG subclasses would not lead to a subsequent event of ADE. Along this line, it has

been shown that IgG2a antibodies recognizing the same target as their IgG1 counterparts are able to enhance viral infection while the IgG1 antibodies did not [Hohdatsu et al. 1994]. This shows that for the potential development of antiviral antibodies, not only the antigenicity but also the IgG subclass is of importance in order to prevent unwanted side effects such as ADE.

1.4.2.4 B-cell mediated immunity in the context of CHB

While the impaired T-cell response in CHB has been thoroughly studied over the last decades, little effort has been made to study the impact of B cells during chronic HBV infection, even though they make up a great portion of the adaptive immune system. Within the last few years, more data has been obtained to reveal the role of B-cell mediated immunity in the context of CHB. After differentiation into plasma cells, B cells are known to produce antibodies against HBsAg, HBcAg and HBeAg during HBV infection, all of which have been shown to prevent reinfection with HBV, thereby portraying an important defense mechanism [Gehring and Protzer 2019]. Similar to the alterations in T-cell populations, B cells also show an increased expression pattern of PD-1 in CHB patients which in turn inhibits the antibody production [Burton et al. 2018; Salimzadeh et al. 2018]. Furthermore, it could be shown that HBVenv specific B cells are not only scarce in CHB patients, but also that constant exposure of the antigen to the BCR, B cells show deficiencies in their maturation process [Salimzadeh et al. 2018; Le Bert et al. 2020]. Finally, the ability of antibodies to clear the HBV infection varies and is mainly dependent on its antigen epitope. Only antibodies recognizing the unique “a”-determinant structure of HBsAg are able to neutralize and clear the virus [Sureau 2016; Zhang et al. 2016; Kang et al. 2018]. It has also been shown that some antibodies, while able to eradicate circulating HBsAg from the periphery, they were not able to clear the liver from viral particles [Zhang et al. 2011]. As the “a”-determinant seems to be the epitope that drives successful neutralization of the virus and infected cells, thorough knowledge about this region would be of high value to understand the mechanisms that underlie viral clearance mediated by B cells.

1.5 Monoclonal antibodies as therapeutic and biotechnological tools

Monoclonal antibodies (mAbs) are used to treat a various amount of diseases, including some variants of cancer [Zahavi and Weiner 2020]. Therefore, the assumption to use them to treat CHB is evident. While neutralizing mAbs have been shown to successfully reduce viral load and lower serum antigen levels, in the case of CHB no complete treatment including cccDNA eradication has been observed, yet [Zhang et al. 2016]. However, they could be used in combination therapies in order to maximize the effect of other treatments such as the ones described above. Furthermore, mAbs are not only useful in therapeutic approaches, they can also be used in basic biotechnological research to help understanding functional mechanisms. Often, mAbs or antibody fragments are employed to resolve protein structures via co-crystallization as they can aid as stabilizing agents or folding chaperones [Griffin and Lawson 2011].

1.6 DNA nanotechnology

DNA nanotechnology has been on the rise for a few years now and describes the methodology of utilizing DNA to design and construct synthetic structures and has already been used in drug delivery, bioimaging and biophysics [Seeman 1982; Dey et al. 2021]. This method is very versatile and nearly every structure can be designed with DNA [Gerling et al. 2015]. In principle, the final target structure is translated into the folding route of a long single stranded DNA which will be the main strand to form the desired structure, the scaffold [Dey et al. 2021]. Then, so called staples, small single-stranded DNA strands that aid the folding of its respective scaffold are designed and produced [Ke et al. 2012]. For this, several softwares are available to support the correct DNA designing strategy [Benson et al. 2015; Veneziano et al. 2016; Jun et al. 2019]. Once, the desired DNA nanostructure is achieved, it can be analyzed and characterized via imaging techniques like transmission electron microscopy (TEM). The imaging with TEM, however, comes with the drawback of high vacuum and dehydration conditions which might lead to alterations in the 3D structure of the construct. To overcome this issue, cryo electron microscopy (cryo EM) is sometimes preferred as it keeps the structure intact [Dey et al. 2021]. Using different kinds of linkers, these DNA scaffolds can then also be altered by introducing proteins such as antibodies or aptamers to further facilitate a certain function that relies on specificity [Madsen and Gothelf 2019]. This approach portrays a promising concept for the capture of viruses in order to prevent infection.

1.7 Aim of thesis

Even though prophylactic vaccines exist, acute as well as chronic HBV infection is still a major health problem worldwide. Current licensed therapies are limited to PEG-Ifny and NAs, both of which are not able to completely eradicate the virus from the host due to its persistent form, namely cccDNA. While there are many promising therapeutic approaches in development, including a therapeutic vaccine and adoptive T-cell therapy, they also come with different drawbacks. Therapeutic vaccination seems to be especially efficient in low titer mice, while adoptive T-cell transfer comes with the obstacle of targeting too many cells, thereby encountering the challenge of hepatotoxicity. Both approaches would therefore benefit from the co-treatment with monoclonal antibodies directed against HBV envelope proteins with a strong ability to induce antibody effector functions such as ADCC in order to lower serum antigen levels and eliminate infected target cells. While HBV specific monoclonal antibodies can be determined by B-cell screening from vaccinated donors, there is also the possibility to design new antibodies *de novo*. To do this, however, thorough knowledge of the structure of the target protein is necessary to be able to model the antigenic site of the antibodies in a perfect way. For HBsAg, however, only the amino-acid sequence is known and predictions of its respective structure have been made. Due to the properties of HBsAg no crystal structure has been obtained, yet. In order to build a fundamental knowledge for the future *de novo* design of antibodies directed against HBV envelope proteins, this thesis describes a newly designed construct which allows for an easy expression and purification of the antigenic loop of HBsAg. It can be used for co-crystallization with HBsAg-specific antibodies, thereby enabling structure determination. While this construct only comprises the antigenic loop and therefore no determination of the whole structure is possible, it consists of the most important part for antibody-antigen interactions. By generating a deeper understanding of the structural properties of this region, antibodies against HBV can be generated with a focus on a strong binding due to steric properties. Furthermore, already described antibodies directed against HBsAg are targeted for Fc-engineering in order to elicit a higher ADCC. In a previous thesis, mAbs have been characterized that show strong neutralizing abilities but only a limited ability to induce ADCC [Wolff 2020]. With the help of Fc-engineering, alterations have been made to generate even more potent antibodies to fight CHB. Lastly, one big part of this thesis describes a novel approach for antibody applications. In cooperation with the Dietz lab in Garching, DNA nanomolecules were designed that can be conjugated with different virus binders, for instance antibodies or aptamers. These nanomolecules then form cages which in turn are capable to engulf the virus, thereby inhibiting infection of cells [Sigl et al. 2021]. With this approach, antibodies do not need to be neutralizing by themselves as they only need to recognize their targets. As the recent SARS-CoV2 pandemic showed, sometimes antiviral antibodies are not neutralizing and therefore are not practical in therapeutic

approaches. With the DNA nanocages, however, also non-neutralizing antibodies could be employed. The overall aim of this thesis is therefore to not only establish a basis for the development of new antibodies, but to also enhance the antibody effector functions of already existing antibodies and to highlight different and novel application possibilities of already existing antibodies in order to fight CHB.

2 Results

2.1 Determination of HBsAg “a”-determinant structure

2.1.1 Construct design

Upon infection with HBV, its antigen HBsAg is secreted, forming subviral particles and filaments, which attenuates the immune response towards the virus. The development of antibodies directed against HBsAg is a promising approach to overcome acute and even chronic hepatitis B. The “a”-determinant is located within the antigenic loop of the HBsAg S protein and portrays the antibody binding site of neutralizing antibodies against HBV. Since the “a”-determinant of HBsAg is crucial for antibody-binding studies and further development of novel antibodies but the structure has not been resolved, a protein was designed to facilitate structure determination. The antigenic loop of the S protein (residues 99-169), which includes the “a”-determinant (residues 124-147) was fused to the Fc domain of an IgG antibody to provide a scaffold enabling both, a correct “a”-determinant formation and a convenient purification via affinity chromatography using a protein G column. The IgG Fc domain forms homodimers via disulfide bridges, facilitating the putative dimerization of the “a”-determinant [Suffner et al. 2018]. Additionally, by eliminating the transmembrane domains of the S protein, protein crystallization and therefore structure determination was expected to be more feasible. Four different versions of this protein, referred to as Fc-“a”-determinant, were designed, expressed, and purified in this study (Figure 6). Their structural as well as biological properties will be discussed in this chapter.

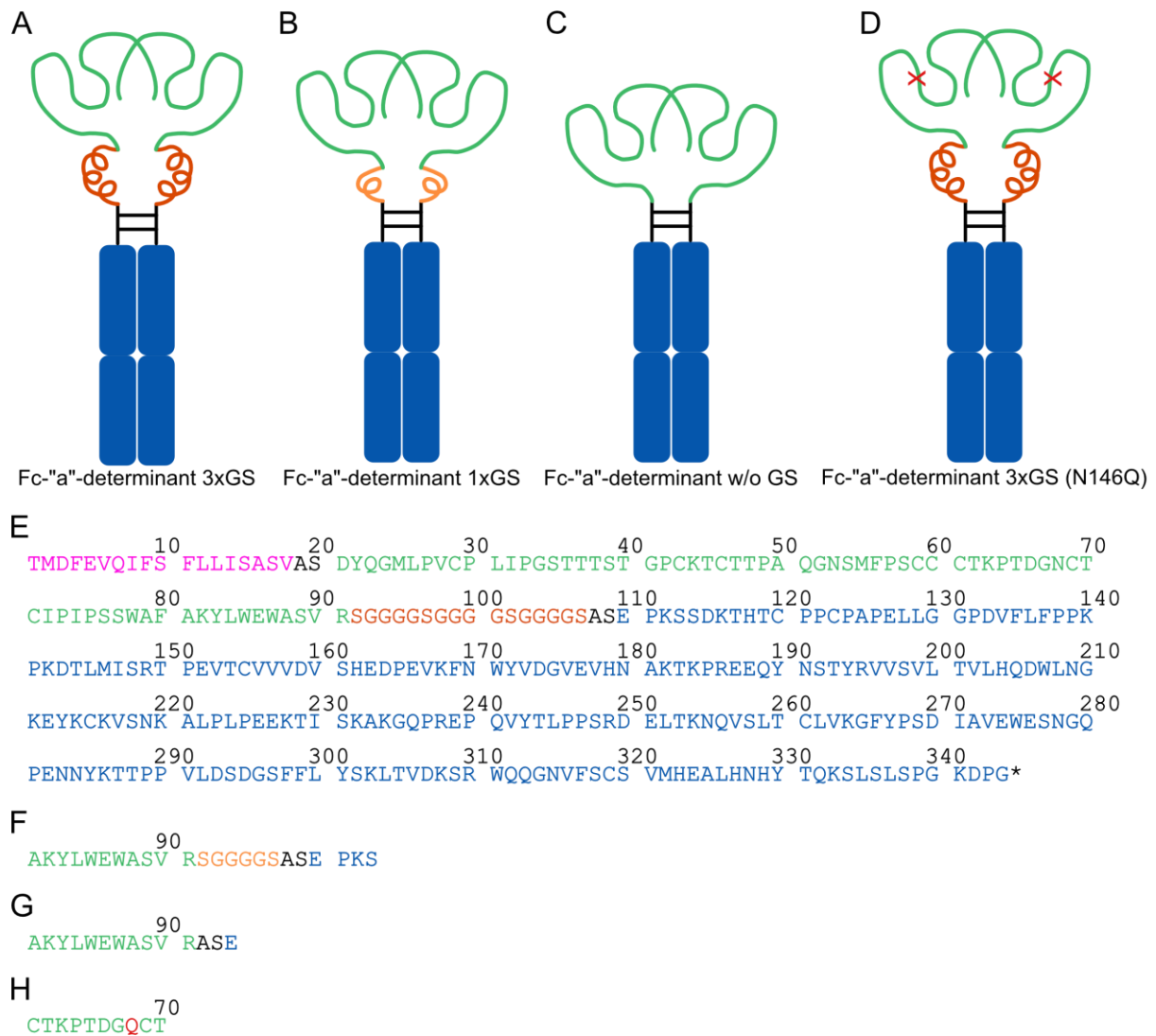


Figure 6 Schematic representation of Fc-"a"-determinant constructs. All Fc-"a"-determinant constructs consist of the CH2, CH3 and hinge regions of an IgG antibody. The antigenic loop of S protein (residues 99-169) is fused to the hinge region via a **(A)** 3xG₄S linker (Fc-"a"-determinant 3xGS), **(B)** 1xG₄S linker (Fc-"a"-determinant 1xGS), **(C)** w/o G₄S linker (Fc-"a"-determinant w/o GS). **(D)** The construct utilizing a 3xG₄S linker was also designed with a glycosylation knockout at N146Q (Fc-"a"-determinant 3xGS (N146Q)). **(E)** The full-length amino-acid sequences is shown for Fc-"a"-determinant 3xGS. The secretion signal (pink) is followed by the antigenic loop of S protein (residues 99-155) (green). The linker (orange) joins the antigenic loop to the hinge and Fc-domain of an IgG (blue). Differences in amino-acid sequences are shown for **(F)** Fc-"a"-determinant 1xGS, **(G)** Fc-"a"-determinant w/o GS and **(H)** Fc-"a"-determinant 3xGS (N146Q).

2.1.2 Structural properties of Fc-“a”-determinant constructs

The Fc-“a”-determinant variants consist of the CH2 and CH3 domains, as well as the hinge region of an IgG antibody, which are fused to the antigenic loop of the HBV S protein (residues 99-169) via a G₄S linker of varying length (Figure 6). The Fc domain allows for a straightforward purification via affinity chromatography using a protein G packed column and serves as a rigid protein scaffold, while the linker grants enough flexibility to enable correct formation of the antigenic loop. Additionally, by working with a dimeric protein scaffold, the putative dimerization of the “a”-determinant is facilitated [Suffner et al. 2018].

2.1.2.1 Fc-“a”-determinant variants

To evaluate the impact of the length of the linker sequence, three different constructs were designed. The Fc-“a”-determinant 3xGS utilizes a 3xG₄S linker (Figure 6A, E), the Fc-“a”-determinant 1xGS a 1xG₄S linker (Figure 6B, F) and the Fc-“a”-determinant w/o GS completely lacks the linker so that the antigenic loop is directly fused to the hinge region of the IgG (Figure 6C, G). Electron microscopy data showed that the antigenic loop is about 10 Å in length and that two protrusions of the HBV S protein are roughly 68 Å apart when forming subviral particles [Cao et al. 2019]. A typical antibody has a diameter at its base of about 30-40 Å [Tang et al. 2007]. Studies showed that the 3xG₄S linker is about 57 Å in length [Chen et al. 2013]. Consequently, in the Fc-“a”-determinant 3xGS construct, the antigenic loop monomers are roughly 144-154 Å apart corresponding to more than twice their natural distance. Shortening the linker lengths to 1xG₄S or deleting the linker sequence thereby reduces the distance between the two antigenic loop monomers to 68-78 Å, corresponding to their natural distance, and 30-40 Å, corresponding to half of their natural distance, respectively.

For the Fc-“a”-determinant 3xGS (N146Q), the antigenic loop of HBsAg was altered by introducing the point mutation N146Q within the “a”-determinant region. This mutation removes the only glycosylation site of the “a”-determinant, thereby ensuring a homogenous solution of non-glycosylated proteins, which in turn was expected to allow for an easier crystallization approach than a heterogeneous mixture of glycosylated and non-glycosylated proteins. However, since no escape mutants of HBV are known in which this amino acid is altered, the biological relevance of this mutation is rather low [Lazarevic et al. 2019]. Accordingly, only the Fc-“a”-determinant 3xGS was altered to serve as proof of concept (Figure 6D, H). The conserved N-glycosylation site present at position N297 in the CH2 domain was kept intact as it is known to be crucial for the structural integrity of monoclonal antibodies, and that deglycosylated antibodies are prone to aggregation [Higel et al. 2016].

2.1.3 Fc-“a”-determinant constructs show pH sensitivity

For the development of a suitable purification method of the Fc-“a”-determinant constructs, the Fc-“a”-determinant 3xGS (N146Q) served as initial candidate. For production of the protein, HEK293T cells were transiently transfected with the corresponding plasmid via lipofection. The supernatant was purified via affinity chromatography and the purification fractions were analyzed via ELISA (Figure 7A). The fractions showing the highest signals were pooled and further concentrated. The concentrated samples were then subjected to concentration determination via Bradford assay and an SDS-PAGE with subsequent Coomassie staining was performed to ensure the integrity of the protein (Figure 7B). Expected bands would have been at 70 and 35 kDa. Here, multiple bands were observed that did not match the expected pattern, which could be due to protein degradation during the purification process. Bands that show a higher molecular weight than expected could point towards protein aggregation or formation of higher oligomers. For further analyses, another ELISA was performed to confirm the specificity of the construct (Figure 7C). For this, a 96-well NUNC plate was coated with Fc-“a”-determinant 3xGS (N146Q) at concentrations ranging from 0.3 nM to 10 μ M. The immobilized protein was detected with two biotinylated antibodies, namely MoMAb and 4D06, both of which have been shown to detect a conformational epitope of the HBVenv protein [Wolff 2020; Zhao et al. 2021]. Here, it was observed that the ELISA signal increased with increasing sample concentration until reaching a Fc-“a”-determinant 3xGS (N146Q) concentration of 30 nM. Then, the signal dropped again. Overall, a very high background signal was observed. These results were obtained for both detection antibodies and support the theory of higher oligomer formation of the protein.

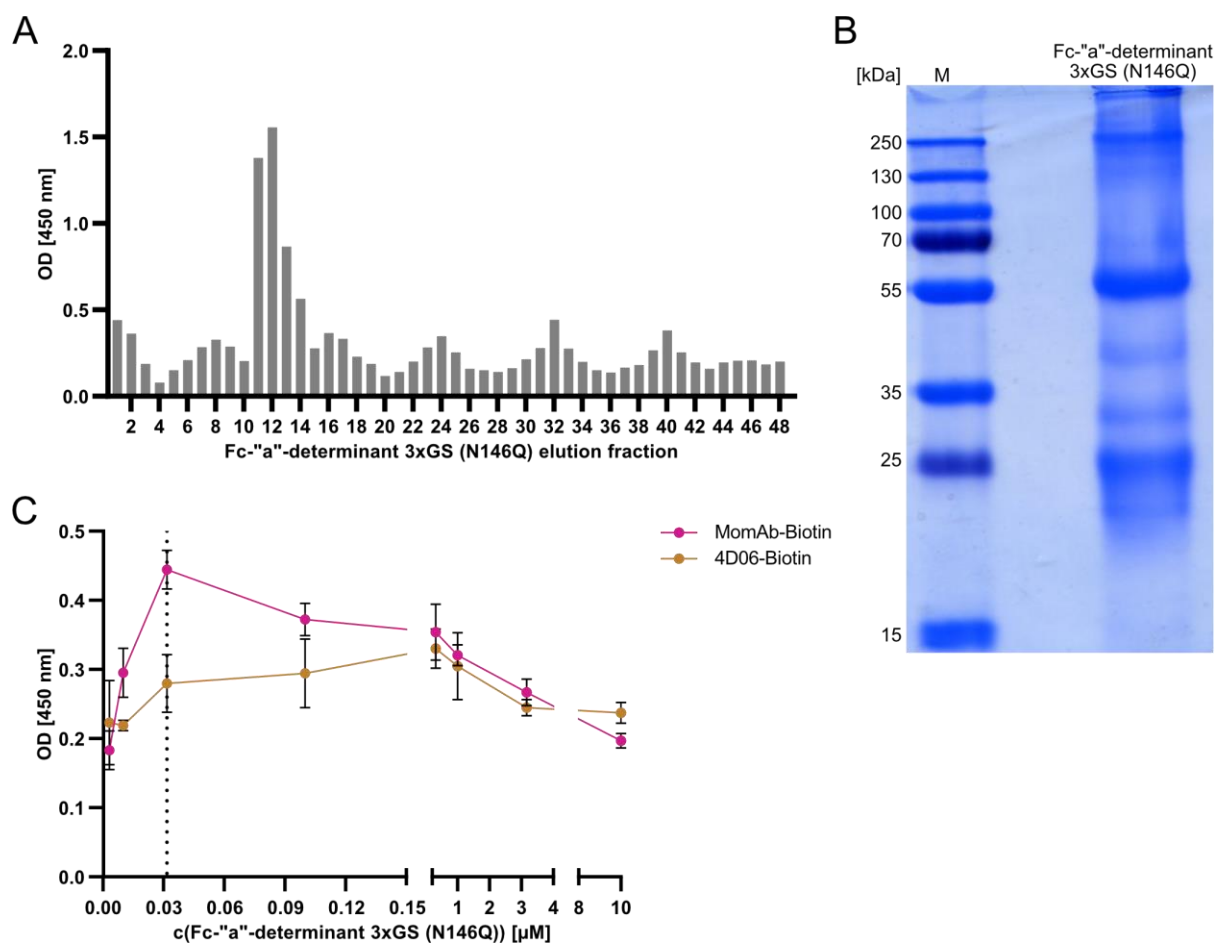


Figure 7 Purification of Fc-"a"-determinant 3xGS (N146Q) via protein G residues using low pH elution conditions. HEK293T cells were transfected with Fc-"a"-determinant 3xGS (N146Q) encoding plasmid, supernatant was collected for one week every second day and subjected to affinity chromatography using a protein G packed column. **(A)** Detection of the Fc-"a"-determinant 3xGS (N146Q) in eluted fractions by ELISA to identify elution peak. The antibody HB1 recognizing a linear epitope of HBsAg was used for detection. **(B)** SDS-PAGE (12.5%) with subsequent Coomassie staining of purified and concentrated Fc-"a"-determinant 3xGS (N146Q) was performed to confirm the identity of the protein. **(C)** Detection of the Fc-"a"-determinant 3xGS (N146Q) in concentrated fractions by ELISA. The antibodies MoMAb and 4D06 recognizing a conformational epitope of HBsAg were used for detection.

As a low pH elution was used, the pH stability of the Fc-"a"-determinant 3xGS (N146Q) was investigated. For this, aliquots of the supernatant of HEK 293T cells that were transiently transfected with the Fc-"a"-determinant 3xGS (N146Q) were adjusted to different pH values. These supernatants were then analyzed via Coomassie stained SDS-PAGE (Figure 8A) and Western blot (Figure 8B). Both, Coomassie and Western blot analysis, showed pronounced bands at roughly 15-20 kDa in samples with a pH of 2-4 and only faint bands at 50 kDa, leading to the conclusion that a low pH disrupts the Fc-"a"-determinant 3xGS (N146Q). At pH ≥ 4.5 , the Western blot displayed strong bands at 50 kDa, which is about 20 kDa lower than expected, while no lower bands were detected. The Coomassie staining supports this finding, pointing towards a protein degradation at pH ≤ 4 .

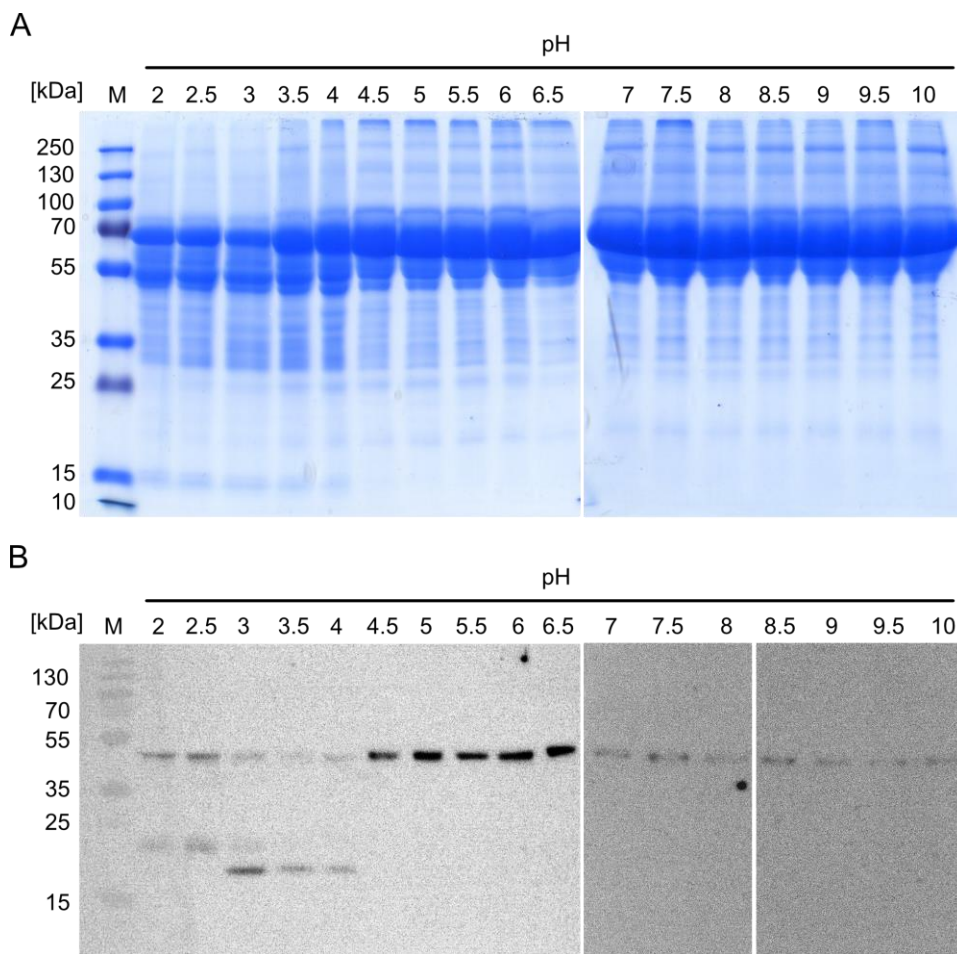


Figure 8 Fc-“a”-determinant 3xGS (N146Q) loses integrity at low pH values. To assess the pH stability of the Fc-“a”-determinant 3xGS (N146Q), the collected supernatant was aliquoted and the pH was adjusted accordingly. **(A)** SDS-PAGE (12.5%) with subsequent Coomassie staining of supernatant from Fc-“a”-determinant 3xGS (N146Q) producer cells at respective pH. **(B)** Western Blot analysis using an anti-HBsAg antibody (HB1) of the samples mentioned in A.

2.1.4 Fc-“a”-determinant folds correctly and forms higher oligomers

To overcome the issue of protein degradation, a protocol using high salt elution under neutral pH conditions was applied. This purification method was performed for two constructs, namely the Fc-“a”-determinant 3xGS (N146Q) and the Fc-“a”-determinant 1xGS. SDS-PAGE and subsequent Coomassie staining of the purified proteins showed pronounced bands at 250 and 55 kDa as well as slight bands at 25 kDa, suggesting that the construct runs slightly different to its expected size of 70 kDa (Figure 9A). Further Western blot analysis utilizing an antibody recognizing a linear epitope (HB1) revealed bands between 130 and 250 kDa as 55 kDa, supporting this suggestion (Figure 9B). Furthermore, the Western blot showed an additional band slightly lower than 55 kDa for both proteins that could point towards a glycosylated isoform.

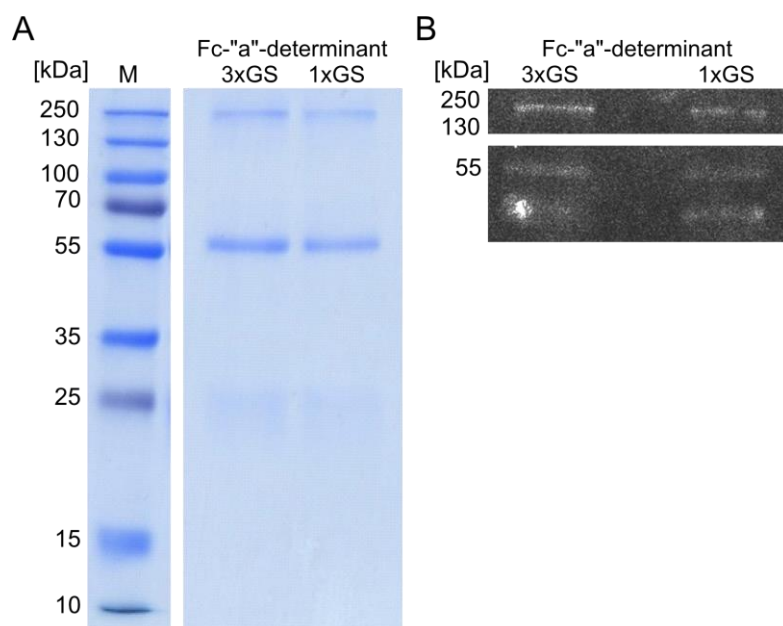


Figure 9 Fc-"a"-determinant constructs run different to expected size in SDS-PAGE. (A) SDS-PAGE (12.5%) of 500 ng purified Fc-"a"-determinant 3xGS and 1xGS and **(B)** Western blot analysis of the same samples detected with an anti-HBsAg antibody (HB1).

While the proteins did not show the expected running behavior, the purity of the proteins could be greatly enhanced with the optimized purification protocol. Therefore, this protocol was applied to purify the Fc-"a"-determinant 3xGS, 1xGS and w/o GS constructs. The purification fractions were collected, and protein concentrations in the elution fractions were determined via spectroscopy (Figure 10A). The fractions with the highest concentration were pooled and concentrated using a spin column, leading to aliquots with 0.9-2 mg/mL for each Fc-"a"-determinant construct. The purified samples were then subjected to PNGase treatment for deglycosylation and analyzed via Coomassie staining (Figure 10B) and Western blot using an anti-HBsAg antibody (HB1) (Figure 10C). SDS-PAGE analysis of glycosylated and deglycosylated proteins showed distinct bands at sizes of 55 and 25 kDa, as well as aggregation artifacts at 250 kDa. The 55 kDa band ran slightly lower in the deglycosylated samples. Furthermore, bands were detected that ran slightly higher than the 55 kDa bands which appeared fainter the shorter the linker between the Fc domain and the antigenic loop. The Western blot verifies the glycosylated nature of the proteins and confirms the presence of the "a"-determinant in the constructs. To further confirm the identity and correct folding of the "a"-determinant, an ELISA with immobilized Fc-"a"-determinant constructs was performed (Figure 10D). Biotinylated MoMAb was used for detection. For the Fc-"a"-determinant 1xGS and w/o GS constructs, the OD_{450} values followed a concentration dependent curve until a coating concentration of 30 nM was reached, suggesting the correct physiological folding of the "a"-determinant. At higher concentrations, the signal slightly diminished in a concentration-dependent manner, pointing towards an oligomerization

of the Fc-“a”-determinant at a quantity above 30 nM. The Fc-“a”-determinant 3xGS showed a different behavior. Here, the ELISA signal also rose until a concentration of 30 nM was reached, dropped slightly and rose again. Despite a high background signal and an overall low signal intensity, the initial peak at 30 nM was reproducibly detected with different batches of Fc-“a”-determinant productions, concluding that these findings are reliable.

To assess the question whether the Fc-“a”-determinant 3xGS, 1xGS and w/o GS constructs form oligomers at higher concentrations, an analytical ultracentrifugation (AUC) was performed in cooperation with Martin Haslbeck from the Department of Biotechnology in Garching. Due to technical issues, no reliable data for the Fc-“a”-determinant 3xGS could be obtained. However, Fc-“a”-determinant 1xGS and w/o GS showed a peak at roughly 140 kDa (data not shown), suggesting that the constructs are not present in their monomeric form but rather form dimers. These findings support the ELISA results that showed a decrease in detection signal with higher sample concentrations which might arise from oligomer formation (Figure 10D).

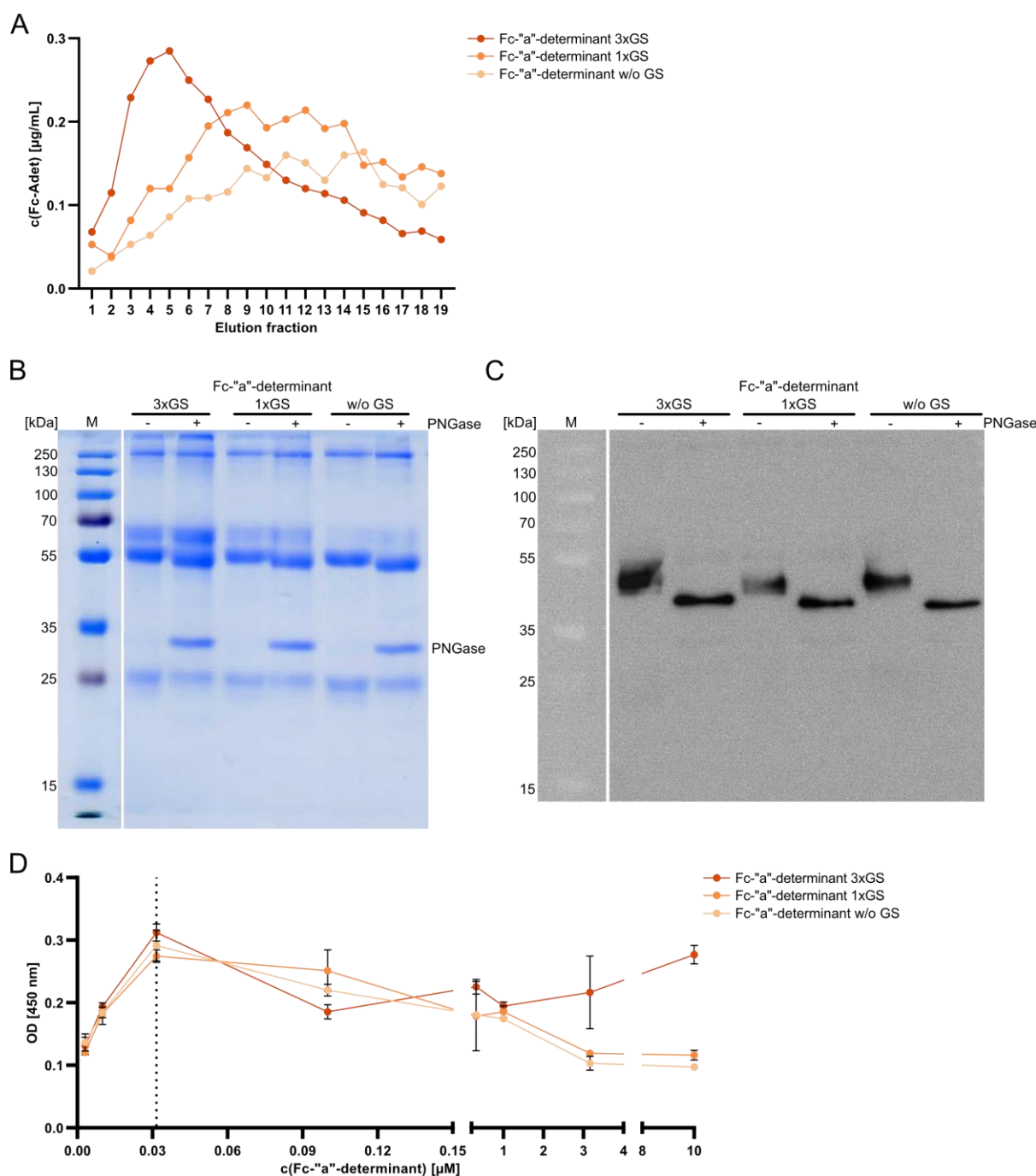


Figure 10 High salt elution results in pure and intact Fc-"a"-determinant proteins. Fc-"a"-determinant constructs were purified utilizing the optimized purification protocol with a high-salt elution step rather than with a low pH. **(A)** The concentration of elution fractions of indicated samples was quantified by spectrometry at 280 nm. **(B)** SDS-PAGE analysis of 2 μg glycosylated and deglycosylated proteins (-/+ PNGase). Bands just underneath the 35 kDa mark correspond to the PNGase. **(C)** Western blot analysis using the HB1 antibody which recognizes the "a"-determinant of HBsAg of 2 μg glycosylated and deglycosylated proteins (-/+ PNGase). **(D)** ELISA analysis with immobilized Fc-"a"-determinant constructs at indicated concentrations. Fc-"a"-determinant constructs were detected by the HBsAg-specific antibody MoMAb. Data is represented as mean \pm SD of technical triplicates (n = 3) (Prism).

2.1.5 Assessment of antibody binding affinities using the Fc-“a”-determinant constructs

While structure determination of the HBsAg via co-crystallization with antibodies remains difficult, the Fc-“a”-determinant constructs provide a promising alternative for affinity measurements via microscale thermophoresis (MST). MST allows for the detection of protein-protein interactions based on the principles of thermophoresis, the directed movement of molecules along a temperature gradient, and temperature-related intensity change (TRIC), which describes the intrinsic property of fluorophores to change their fluorescence intensity as a function of temperature [Mueller et al. 2017]. For the MST measurements, the Monolith NT.115 device of NanoTemper was used. To detect binding and calculate affinities, one binding partner is fluorescently labeled, while the other stays unlabeled. To analyze binding affinities of different antibodies, the Fc-“a”-determinant constructs were labeled with a red fluorophore dye, using the labeling kit of NanoTemper following the provided protocol. MST measurements were performed in triplicates on the same day of labelling and on day 7 after labelling. The sample preparations were stored at 4 °C. For the MoMAb, all measurements with the different Fc-“a”-determinant constructs resulted in K_D values in the lower nanomolar range, varying between 7.8 – 18.4 nM on day 1 (Figure 11A). On day 7 after labelling, the determined K_D values slightly increased for all constructs, resulting in values between and 28.1 – 45.3 nM (Figure 11B). These findings provide evidence that these novel constructs harbor correctly folded immunogenic epitopes that are successfully engaged by an established HBVenv-specific antibody that was shown to detect a conformational epitope [Zhao et al. 2021] and, thus, might provide a suitable lipid-free alternative to solve the structure of the “a”-determinant by co-crystallization in the near future.

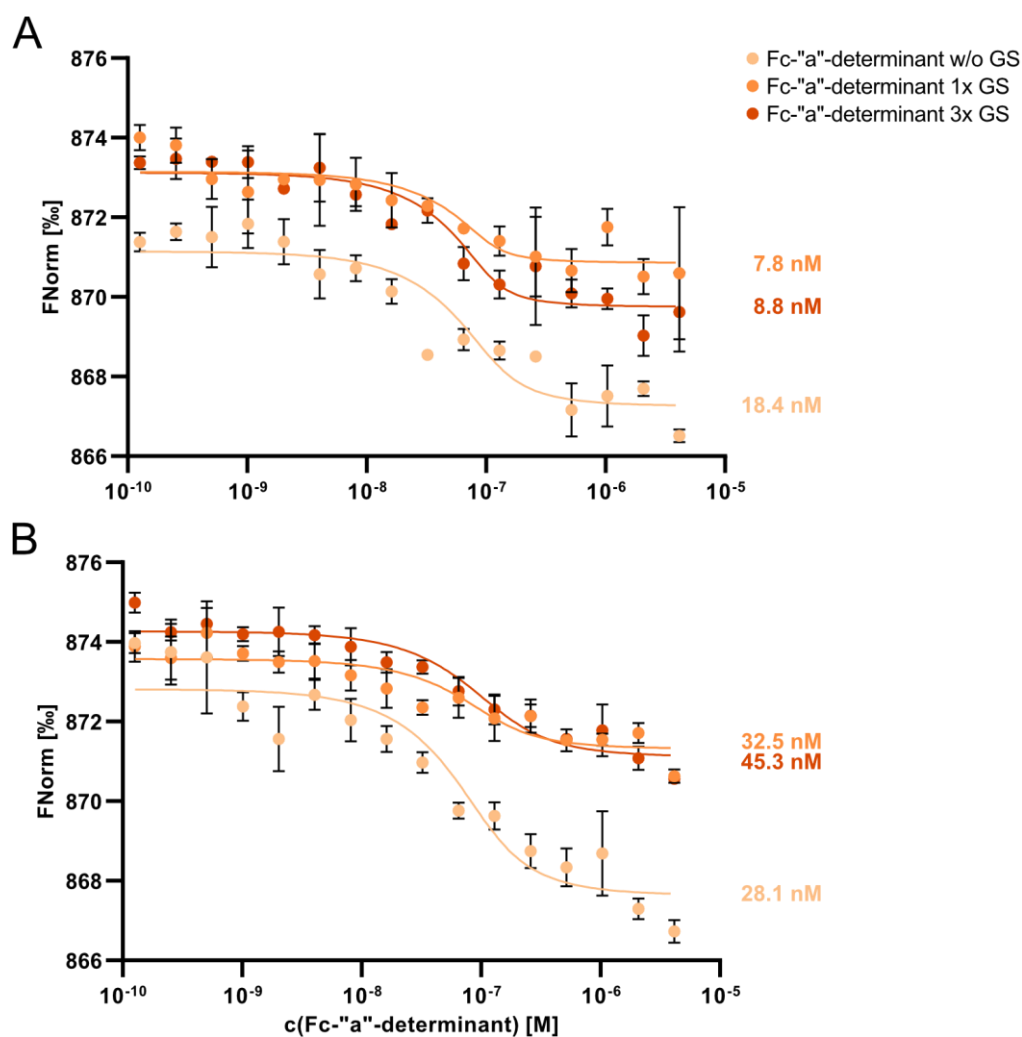


Figure 11 All Fc-"a"-determinant-antibody complexes demonstrate K_D values in the low nanomolar range. MST analysis of Fc-"a"-determinant constructs with MoMAb resulted in binding affinities in the low nanomolar range. **(A)** Binding affinities were measured on the same day as Fc-"a"-determinant constructs were labelled. **(B)** Labelled Fc-"a"-determinant constructs were stored at 4 °C for 7 days and the binding affinity measurement was repeated. Data is represented as mean \pm SD of technical replicates ($n = 3$) (MO.Affinity Control software; NanoTemper).

2.2 Fc-engineered antibodies to enhance antibody dependent cellular cytotoxicity (ADCC)

The mechanism of antibody effector functions, such as antibody dependent cellular cytotoxicity (ADCC), greatly depends on the binding of antibodies to the Fc γ -receptors CD16 and CD32, which are both expressed on human natural killer (NK) cells. Upon antibody binding to CD16, ADCC is initiated, while binding to CD32 inhibits ADCC. During earlier work by *Lisa Wolff*, monoclonal antibodies were generated via single B-cell cloning [Wolff 2020]. These antibodies show a strong and specific binding to HBsAg with EC₅₀ values in the low nanomolar range. However, their ability to induce ADCC was limited and effective activation of NK cells, as well as lysis of HBVenv-positive target cells was not observed [Wolff 2020]. To further develop this antiviral therapy, the antibody displaying the best overall performance in previous work (referred to as 4D06) [Wolff 2020], was subjected to Fc-engineering in order to modulate ADCC characteristics. Therefore, three different antibody constructs were designed by introducing different mutations in the Fc domain that either only enhance the binding to CD16 or additionally decrease the binding to CD32, while HBsAg specificity is preserved. The following chapter will focus on the structural and biological properties of the different antibody constructs that were designed.

2.2.1 Structural properties of Fc-engineered antibodies

2.2.1.1 4D06 wild type

The 4D06 wild type is a monoclonal IgG antibody with HBsAg specificity (Figure 12). Its EC₅₀ has been reported to be 18.5 nM and it showed a high capability to neutralize HBV infection *in vitro* [Wolff 2020]. For detailed information on IgG structure see 1.4.2.3.1.

2.2.1.2 4D06-DLE

The DLE mutant harbors three mutations in the CH2 domain of 4D06, namely S239D/A330L/I332E (Figure 12, Figure 13A), which does not only result in a predicted enhancement of CD16 binding, but also a decrease of CD32 binding, which could drastically enhance ADCC [Lazar et al. 2006; Mimoto et al. 2013].

2.2.1.3 LPLIL

In the LPLIL mutant, five mutations were introduced at residues F243L/R292P/Y300L/V305I/P369L within the CH2 and the CH3 domain of 4D06 (Figure 12, Figure 13B) to enhance the binding to CD16 [Stavenhagen et al. 2007].

2.2.1.4 KH12

The KH12 mutant forms a heterodimer and 4D06 was altered in a knob-into-hole fashion which promotes the formation of heterodimers rather than homodimers (Figure 12, Figure 13C) [Klein et al. 2012]. The “knob” is formed by introducing a big side chain via the mutation T366W in the CH3 region of heavy chain 1. Three mutations were introduced in the CH3 region of heavy chain 2, namely T366S/L368A/Y407V, which results in the formation of the “hole”. Furthermore, the mutations S354C in heavy chain 1 and Y349C in heavy chain 2 give rise to disulfide bonds between the two CH3 domains, which additionally facilitates heterodimerization. Mutations L234Y/L235Q/G236W/S239M/H268D/D270E/S298A in heavy chain 1 and D207E/K326D/A330M/K334E in heavy chain 2, being located in the respective CH2 domains, were introduced to enhance binding to CD16 [Mimoto et al. 2013; Liu et al. 2014].

Results

V_H-hinge 4D06 WT

```
10      20      30      40      50      60      70      80      90      100     110
LVESGGGLAQ PGRSLRLSCT GSGFTFGDFA VNWVVRQAPGR GLEWIGFIRS KTYGGTTEYA ASMKGRVTIS RDDSKSIAYL QMSSLKSEDT AVFYCSRAAG GYFAAPFDNW
120     130     140     150     160     170     180     190     200     210     220
GQGALVTVSS AGPSVFPLAP SSKSTSGGTA ALGCLVKDYF PEPVTVSWNS GALTSGVHTF PAVLQSSGLY SLSSVVTVPS SSLGTQTYIC NVNHKPSNTK VDKKVEPKSC
230     240     250     260     270     280     290     300     310     320     330
DKTHTCPPCP APELLGGPSV FLFPPKPKDT LMISRTPEVT CVVVDVSHED PEVKFNWYVD GVEVHNAKTK PREEQYNSTY RVVSVLTVLH QDWLNGKEYK CKVSNKALPA
340     350     360     370     380     390     400     410     420     430     440
PIEKTISKAK GQPREPQVYT LPPSRDELTK NQVSLTCLVK GFYPSDIAVE WESNGQPENN YKTTTPVLDS DGSFFLYSKL TVDKSRWQQG NVFSCSVMHE ALHNHYTQKS
LSLSPGK
```

V_K (all constructs)

```
10      20      30      40      50      60      70      80      90      100     110
MTQSPSILSA SVGDRVSFTC RASESIDDWL AWYQHKPGKA PKLLIHRASN LHDGVPSRFS GSGSGTEFTL TISSLQPDFD ATYFCQYNE YSLTFGGGTK VEIKRTVAAP
120     130     140     150     160     170     180     190     200     210
SVFIFPPSDE QLKSGTASVV CLLNFPYPRE AKVQWKVDNA LQSGNSQESV TEQDSKDYSTY SLSSTLTLSK ADYEKHKVYA CEVTHQGLSS PVTKSFNRGE C
```

V_H-hinge 4D06 DLE

```
240     250     260     270     280     290     300     310     320     330     340
APELLGGPDV FLFPPKPKDT LMISRTPEVT CVVVDVSHED PEVKFNWYVD GVEVHNAKTK PREEQYNSTY RVVSVLTVLH QDWLNGKEYK CKVSNKALPL PEEKTISKAK
```

V_H-hinge 4D06 LPLIL

```
250     260     270     280     290     300     310     320     330     340     350
FLLLPKPKDT LMISRTPEVT CVVVDVSHED PEVKFNWYVD GVEVHNAKTK PPEEQYNSTL RVVSILTVLH QDWLNGKEYK CKVSNKALPA PIEKTISKAK GQPREPQVYT
360     370     380     390     400
LPPSRDELTK NQVSLTCLVK GFYPSDIAVE WESNGQPENN YKTTPLVLDS
```

V_H-hinge 4D06 KH1 (knob)

```
270     280     290     300     310     320     330     340     350     360     370
CVVVDVSDEE PEVKFNWYVD GVEVHNAKTK PREEQYNATY RVVSVLTVLH QDWLNGKEYK CKVSNKALPA PIEKTISKAK GQPREPQVYT LPPCRDELTK NQVSLWCLVK
```

V_H-hinge 4D06 KH2 (hole)

```
270     280     290     300     310     320     330     340     350     360     370
CVVVDVSEE PEVKFNWYVD GVEVHNAKTK PREEQYNSTY RVVSVLTVLH QDWLNGKEYK CKVSDALPM PIEETISKAK GQPREPQVCT LPPSRDELTK NQVSLSCAVK
380     390     400
GFYPSDIAVE WESNGQPENN YKTTTPVLDS DGSFFLVSKL
```

Figure 12 Amino-acid sequences of Fc-engineered antibodies. The full amino-acid sequences of the heavy and light chains of 4D06 are shown. While the light chain is identical in all Fc-engineered antibody constructs, the heavy chains are altered in the different mutants. Mutations in the respective constructs are highlighted in red.

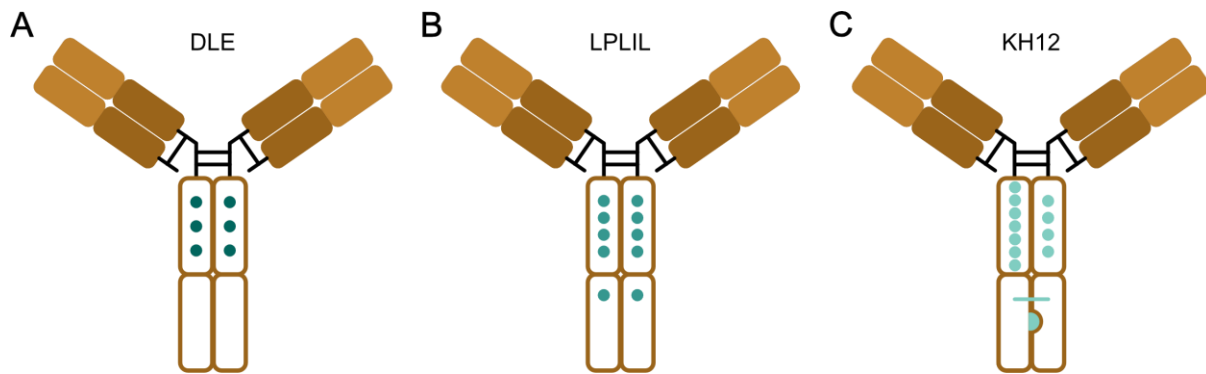


Figure 13 Schematic representation of Fc-engineered antibodies. An HBsAg-specific monoclonal antibody with a high neutralization capacity, namely 4D06 [Wolff 2020], was subjected to Fc-engineering to enhance the capability of inducing ADCC. Three different constructs were designed. **(A)** DLE harbors three mutations, S239D/A330L/I332E, which should not only increase binding strength to CD16, but also decrease binding strength to the ADCC inhibiting FcγR CD32 [Lazar et al. 2006]. **(B)** LPLIL forms a homodimer with mutations F243L/R292P/Y300L/V305I/P369L, all of them being reported to enhance binding to CD16, the ADCC activating FcγR [Stavenhagen et al. 2007]. **(C)** The heterodimerization of KH12 is facilitated by a knob-into-hole approach. The “knob” is formed by the mutation T366W of heavy chain 1. The mutations T366S/L368A/Y407V in heavy chain 2 form the “hole”. Mutations S354C in heavy chain 1 and Y349C in heavy chain 2 enable disulfide bonds between the two CH3 domains. Mutations L234Y/L235Q/G236W/S239M/H268D/D270E/S298A in heavy chain 1 and D207E/K326D/A330M/K334E in heavy chain 2 should enhance binding to CD16 [Mimoto et al. 2013; Liu et al. 2014]. The inclusion of unsymmetrical mutations within the CH2 domain has been shown to increase binding to CD16 [Mimoto et al. 2013; Liu et al. 2014].

2.2.2 Fc-engineered antibodies are successfully produced in HEK293T cells

For expression of the different antibodies, human embryonic kidney (HEK) 293T cells were transiently transfected via lipofection with two plasmids, one encoding the anti-HBEnv-specific light chains and the other encoding the heavy chains, respectively. As the best ratio of heavy:light chain for expression of wild type IgG was previously determined to be 1:1 [Wolff 2020], the same ratio was used for the engineered constructs as well. To ensure successful expression and secretion of the antibodies, the supernatant was subjected to ELISA and SDS-PAGE analyses prior to purification (Figure 14). For ELISA, a 96-well NUNC plate was coated with either recombinant HBsAg, to check for HBEnv-specificity, or with anti-IgG antibodies to ensure the integrity of the antibodies. The antibodies in the supernatant were detected with a goat-anti-human antibody labelled with HRP. PBS served as negative control. For all constructs, positive signals could be observed in both ELISA setups (Figure 14A).

2.2.3 Fc-engineered antibodies are successfully purified

After confirming the presence of antibodies in the supernatant, purification via affinity chromatography with protein G was applied. Antibodies were eluted with low pH and collected in 1 mL aliquots containing a neutralization buffer to ensure neutral storage conditions. ELISA analysis of the elution fractions with immobilized HBsAg showed HBEnv-specificity on a similar level for all antibodies, while analysis with immobilized anti-IgG antibodies proved the presence of intact

antibodies (Figure 14B, C). Elution fractions eliciting the highest signals for HBVenv-specificity were pooled and concentrated using a spin column filter with a molecular weight cutoff (MWCO) of 100 kDa that also allows for elimination of BSA from the cell culture media. During the concentration, the storage buffer was changed to PBS. Aliquots with concentrations ranging from 1-5 mg/mL were successfully produced for all constructs. SDS-PAGE with subsequent Coomassie staining of the purified antibodies showed bands at 25 and 50 kDa, corresponding to the light and heavy chains, respectively (Figure 14D). Even after storage for 6-12 months at 4 °C, no degradation of the antibodies was observed (data not shown).

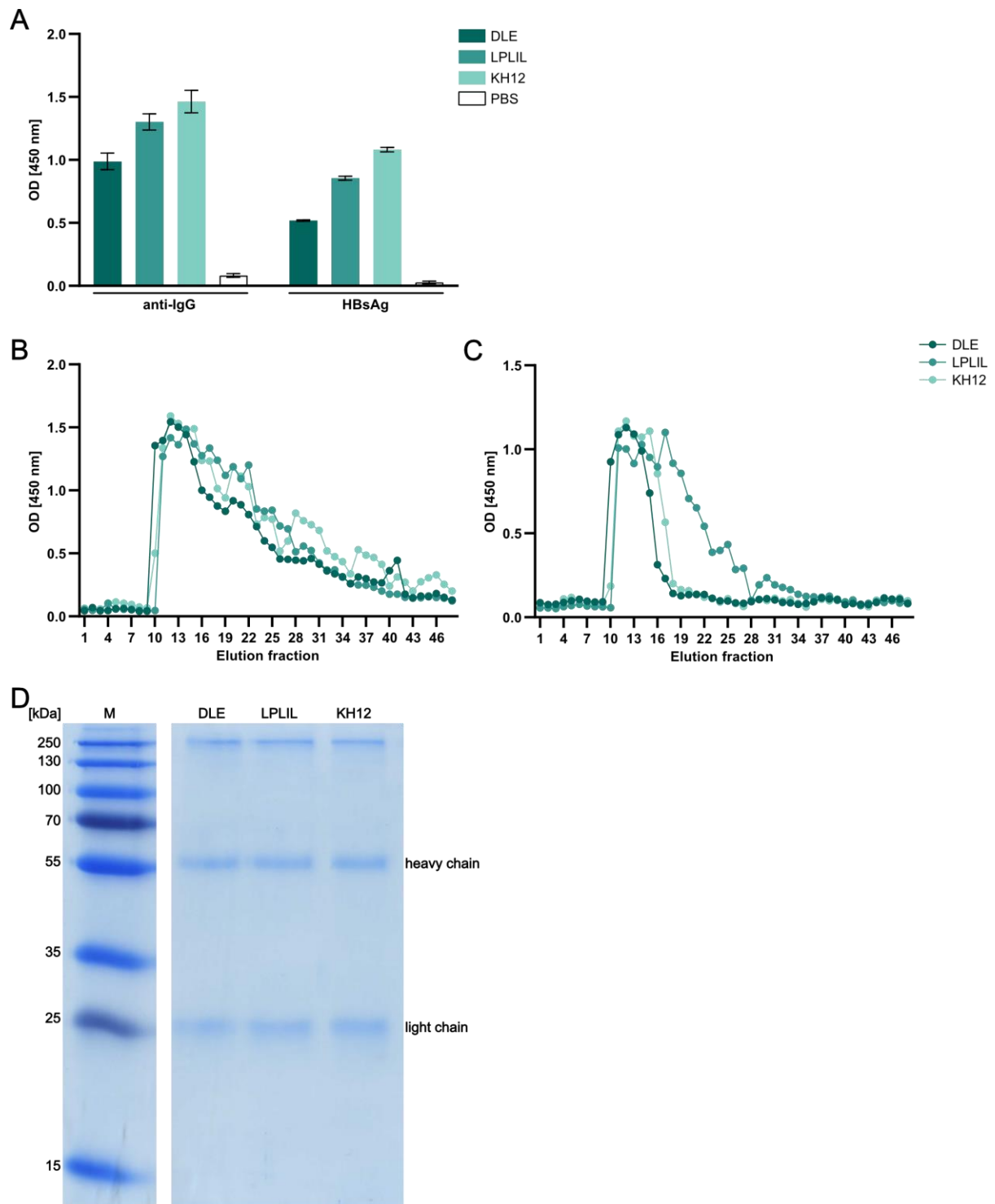


Figure 14 Fc-engineered antibodies are successfully purified via affinity chromatography. Fc-engineered antibodies were purified via affinity chromatography using a protein G packed column and low pH elution conditions. **(A)** ELISA analysis of supernatants of HEK293T cells producing Fc-engineered antibodies (DLE, LPLIL, KH12) using immobilized anti-IgG and HBsAg, respectively. Data is represented as mean \pm SD of technical triplicates ($n = 3$) (Prism). **(B, C)** ELISA analysis of eluted fractions using immobilized **(B)** anti-IgG to certify protein integrity and **(C)** HBsAg to confirm HBsAg-specificity, respectively **(D)** SDS-PAGE (12.5%) of 500 ng of purified Fc-engineered antibodies.

2.2.4 Fc-engineered antibodies recognize HBsAg

After successfully purifying the antibody constructs, ELISAs were performed to compare the total IgG levels in the preparations and to confirm HBsAg specificity (Figure 15A). Total IgG levels in the preparations decreased for the antibody variants in comparison to the wild type, which might be due to lesser binding of the anti-IgG antibody due to the mutations introduced in the Fc domain. HBsAg-ELISA signals varied between the constructs with LPLIL showing the strongest and KH12 the weakest signal among the newly designed antibodies. All mutant versions however, showed a reduced HBsAg specific signal compared to the wild type. These results confirm successful production of the Fc-engineered HBsAg-specific antibodies and propose their subsection to further functional characterization.

2.2.5 Neutralization capacity of Fc-engineered antibodies is impaired

To gain more information about the functional properties of the antibodies, neutralization experiments were performed (Figure 15B-C). For this, decreasing concentrations of antibodies ranging from 10-1000 nM were incubated with HBV for 3 hours at 37 °C to allow for immune complex formation before infection. On days 4 and 8 post infection (pi), the supernatant was collected and HBeAg levels, serving as surrogate marker for HBV infection, were quantified (Figure 15B) to determine the neutralization efficiency (Figure 15C) of the different antibodies. All antibodies showed a neutralizing effect, however, the wild type already neutralizes an HBV infection at concentrations as low as 3-100 nM, while the mutants show reduced neutralization requiring concentrations higher than 100 nM.

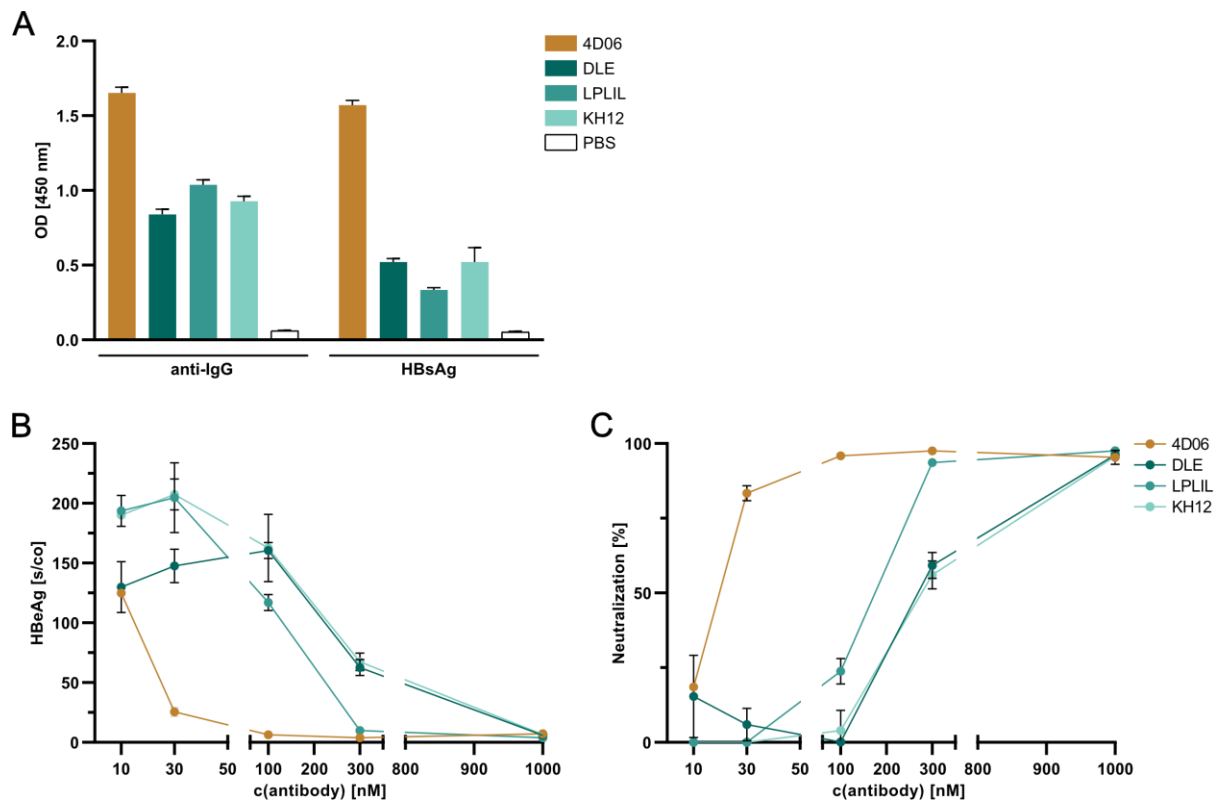


Figure 15 Fc-engineered antibodies show lower antigen-specificity and neutralization capacity than the wild type. (A) ELISA analysis of purified and concentrated antibody samples with immobilized anti-IgG and HBsAg, respectively. PBS served as negative control. Data is represented as mean \pm SD of technical triplicates ($n = 3$) (Prism). (B, C) Different concentrations of antibodies ranging from 10 – 1000 nM were incubated with the virus before infection. On days 4 and 8 post infection (pi), (B) HBeAg levels in the supernatant were quantified and (C) the neutralization efficiency was calculated. Data is represented as mean \pm SD of biological triplicates ($n = 3$) (Prism).

2.2.6 ADCC assessment via reporter cell line

To assess the ability of the Fc-engineered antibodies to induce ADCC, a reporter cell line was established. For this, a Jurkat cell line expressing human CD16 fused to the human CD3 ζ domain, kindly provided by Philipp Kolb (Institute of Virology, Universitätsklinikum Freiburg), were used. To confirm the presence of the transgene on the cell surface, cells were stained with a CD16 specific antibody and analyzed via flow cytometry. After thawing, the percentage of CD16 expressing cells was low (4-5%) (Figure 16B) so that the cells were selected with puromycin for 7 days to increase the expression of the transgene. When the cell line reached a CD16 expression of ~95% (Figure 16B), cells were transiently transfected with a plasmid encoding a moxGFP as transfection marker in sense, and a luciferase under a minimal IL-2 promotor and NFAT transcription factor in antisense direction (Figure 16C). 24 hours post transfection, the 4D06 wild type antibody was added to the cells at different concentrations. Upon binding of antibodies to CD16, the NFAT pathway should be activated and in turn the luciferase should be expressed. After addition of the substrate D-luciferin, the luciferase activity in cell lysate was measured (Figure 16D). Here, a very high background signal was observed. However, a slight trend was visible, which pointed towards higher ADCC activation with high antibody concentration. As the gene of interest was inserted into a lentiviral backbone to facilitate the subsequent lentiviral transduction and is thereby flanked by the 3' and 5' long terminal repeats (LTR), which act as promotor in both, sense and antisense direction, the luciferase was constitutively expressed independent of NFAT signaling, which possibly lead to the high background signal.

2.3 DNA Nanoshells

As alternative approach to develop an antiviral therapy on the basis of the HBV-specific monoclonal antibodies, DNA nanoshells were designed in collaboration with the group of Hendrik Dietz. These molecules are meant to be conjugated with any kind of antibodies, aptamers, or other binding moieties to subsequently engulf viruses, thereby preventing infection. They can be designed in a size range of 43-925 MDa and can therefore be easily adapted to different sizes of target viruses [Sigl et al. 2021]. In this study, HBV-specific antibodies, either binding to HBsAg or HBcAg, were conjugated to the shells. Each shell harbors a total of 900 antibodies that target HBV particles, leading to encapsulation of the viral particle by the DNA nanoshells [Sigl et al. 2021]. To demonstrate the benefit of this novel approach, the neutralization efficacy of these shells was studied and compared to unconjugated antibodies.

2.3.1 Conjugated antibodies still recognize their targets

To ensure that the antibodies conjugated to the DNA nanoshells are still able to recognize their targets, ELISA analyses were performed (Figure 17A, B). For this, recombinant HBsAg and anti-IgG, respectively, were coated to a 96-well NUNC plate, nanoshells conjugated with anti-HBsAg antibodies were added and detected by an HRP-labelled anti-human IgG. Two differently sized nanoshells were used, one being octahedral and one being icosahedral. Antibodies conjugated to the DNA handle and the unconjugated antibodies served as positive controls, while PBS served as negative control. OD₄₅₀ signals show the same intensity for both types of nanoshells in comparison to both positive controls, suggesting that conjugated antibodies are still able to recognize their specific target (Figure 17B).

2.3.2 DNA nanoshells conjugated with anti-HBcAg antibodies efficiently engulf recombinant HBcAg

To prove the concept of virus encapsulation, a different ELISA setup was used. For this, 96-well NUNC plates were coated with anti-HBcAg antibodies and loaded with nanoshells conjugated to a second anti-HBcAg antibody that was previously incubated with HBcAg particles. A third anti-HBcAg antibody, labelled with HRP, was used to detect binding of nanoshell-HBcAg complexes to the plate. Absence of binding provides evidence for successful encapsulation of core particles by the nanoshells (Figure 17C). For this, also two different nanoshell symmetries were used. Untreated HBcAg particles served as positive control, while the storage buffer of the shells served as negative control. The ELISA data shows a drop of the signal in the nanoshell-treated samples, with the icosahedral nanoshell depicting a slightly lower decrease, suggesting successful encapsulation of HBcAg particles (Figure 17D).

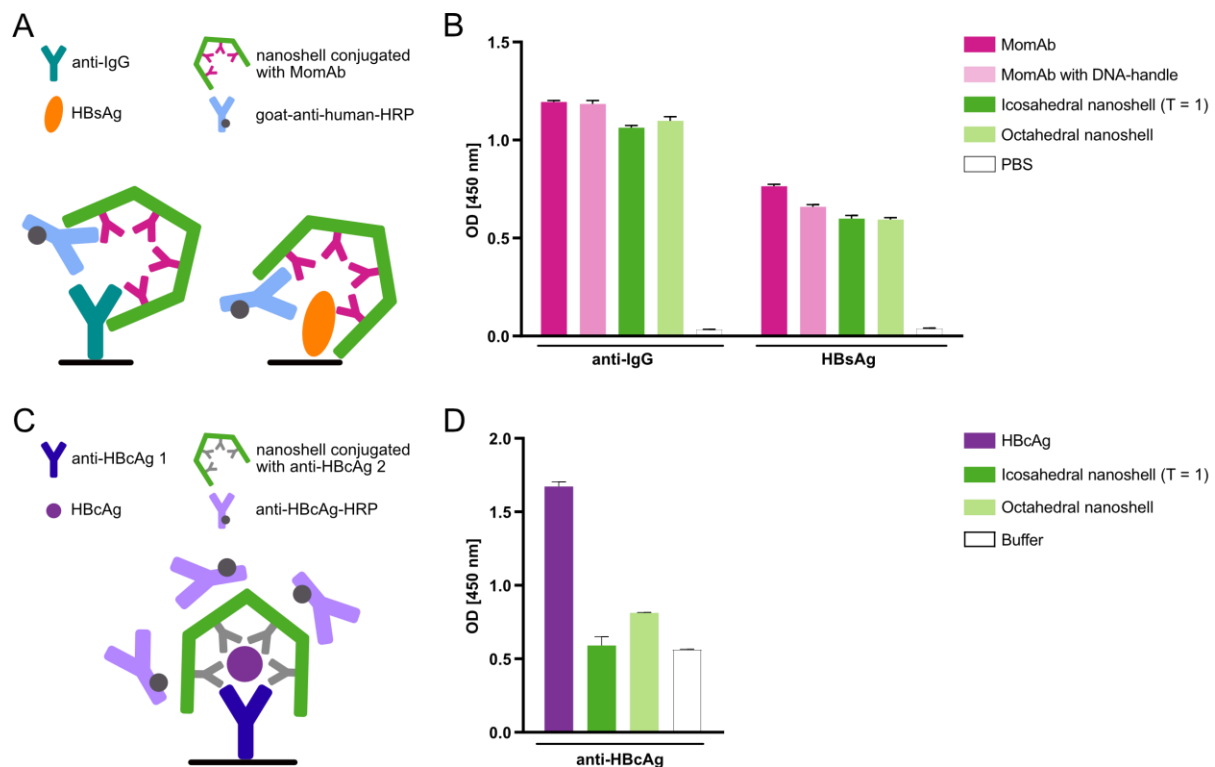


Figure 17 Antibodies conjugated to DNA nanoshells recognize their targets and enable engulfment of HBcAg particles. (A) Schematic representation of different ELISA setups using immobilized anti-IgG and HBsAg, respectively, to confirm integrity and antigen specificity of antibodies conjugated to nanoshells. (B) ELISA analysis with immobilized anti-IgG and HBsAg, respectively, of differently dimensioned nanoshells conjugated with HBsAg antibodies (MoMAb) (green shades) and MoMAb conjugated to the DNA-handle without forming nanoshells (light pink). MoMAb alone (dark pink) served as positive and PBS (white) as negative control. (C) Schematic representation of ELISA setup using immobilized anti-HBcAg to ensure HBcAg-engulfment by nanoshells. (D) ELISA analysis with immobilized anti-HBcAg of differently dimensioned nanoshells conjugated with HBcAg-antibodies, which were preincubated with HBcAg particles (green shades). Recombinant HBcAg (violet) served as positive and nanoshell storage buffer (white) as negative control. Data is represented as mean \pm SD of technical duplicates ($n = 2$) (Prism).

2.3.3 DNA nanoshells conjugated with anti-HBsAg antibodies efficiently neutralize HBV infection *in vitro*

To validate the neutralization capacity of the antibody-conjugated nanoshells *in vitro*, HBV neutralization assays were performed. For assay establishment an antibody with suboptimal neutralization capacity (MoMAb) was applied at different concentrations. Virus was incubated with different concentrations of MoMAb for 3 h at 37 °C and subsequently used to infect HepG2-NTCP cells at an MOI of 100 virus particles/cell. On days 4 and 8 pi, the supernatant was collected and HBeAg levels were quantified. For calculation of the neutralization capacity, the HBeAg levels of the HBV only control served as 0% neutralization data point. Neutralization capacity of unconjugated MoMAb was observed at antibody concentrations of up to 417 nM (Figure 18A). In future experiments, suboptimal

antibody concentrations (0.04-14.4 nM) were used to demonstrate a neutralizing effect promoted solely by the conjugation of MoMAb to the nanoshells. To compare the neutralization capacity of the DNA nanoshells to unconjugated antibodies, icosahedral nanoshells were coupled to MoMAb and neutralization assays were performed (Figure 18B-C). Antibodies conjugated to the DNA handle served as control. Furthermore, a strongly neutralizing antibody (Nabi), nanoshells without antibodies, HBV pre-incubated with nanoshells and a mock control without any treatment served as negative controls. HBeAg levels were used to determine neutralization capacity (Figure 18B). Furthermore, on day 8 pi the cells were lysed and prepared DNA was subjected to qPCR analysis to evaluate cccDNA levels (Figure 18C). While antibodies alone did not show any neutralizing capacity in the setup, nanoshells conjugated with the same antibody were observed to already neutralize HBV infection at antibody concentrations of 10.8 nM *in vitro*. This correlated with the corresponding intracellular cccDNA levels.

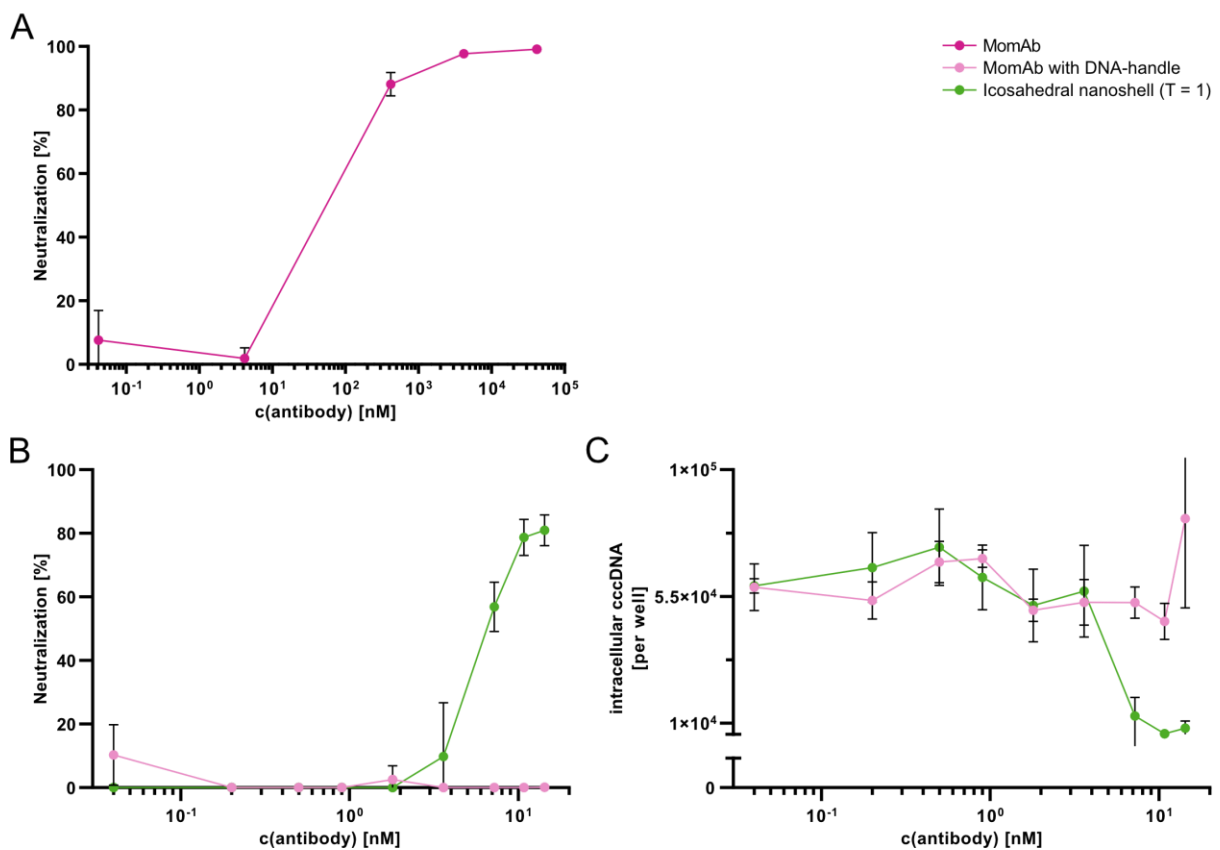


Figure 18 DNA nanoshells conjugated with anti-HBsAg antibodies efficiently neutralize HBV infection *in vitro*. (A) HBV was incubated with indicated concentrations of MoMAb before HepG2-NTCP cells were infected with HBV-antibody complexes (MOI 100 infectious particles/cell). On day 8 pi, HBeAg levels in supernatant were used to determine neutralization efficiency. (B, C) HBV was incubated with indicated concentrations of MoMAb with DNA-handle and nanoshells conjugated with corresponding MoMAb concentrations. HepG2-NTCP cells were infected with HBV-antibody and HBV-nanoshell complexes (MOI 100 infectious particles/cell), respectively. (B) On day 8 pi, HBeAg levels in supernatant were used to determine neutralization efficiency. Data is represented as mean \pm SD of biological triplicates (n = 3) (Prism). (C) Cells were lysed on day 8 pi and lysates were subjected to qPCR to determine intracellular cccDNA levels. Data is represented as mean \pm SEM of biological triplicates (n = 3) (Prism).

2.3.4 DNA nanoshells need to be present at time of infection to facilitate neutralization *in vitro*

In order to evaluate a potential therapeutic as well as prophylactic treatment option of the nanoshells, HepG2-NTCP cells were infected with an rHBV virus expressing luciferase at an MOI of 10 infectious particles/cell and nanoshells were added at different time points before (Figure 19A) and after infection (Figure 19B). Non-infected cells, infected cells without shells, a strongly neutralizing antibody (Nabi) and virus preincubated with nanoshells served as controls (Figure 19C). On day 8 post infection, the cells were lysed, harvested and luciferase levels in the lysates determined. The nanoshells efficiently neutralized HBV infection *in vitro* when added to the media prior to infection at any time point until 8 h after addition of the nanoshells. After 24 h however, no neutralization was observed anymore (Figure 19A). Furthermore, the addition of nanoshells after infection of cells did not result in efficient neutralization (Figure 19B). The controls verified the assay (Figure 19C).

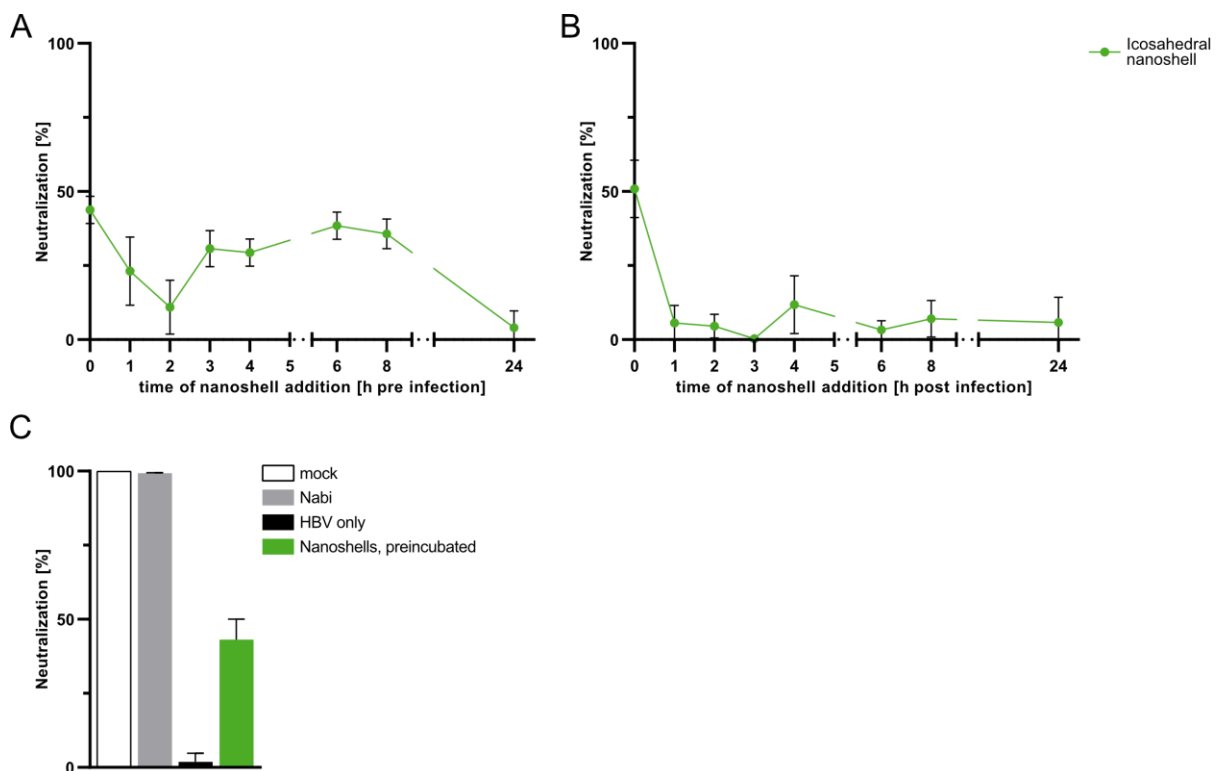


Figure 19 Nanoshells efficiently inhibit HBV infection when present at timepoint of infection. (A) To evaluate the prophylactic applicability of the nanoshells, they were added to HepG2-NTCP cells at indicated time points before they were infected with a nano-Luciferase expressing rHBV (MOI 10 infectious particles/cell). On day 8 pi, luciferase levels in the supernatant were measured and neutralization efficiency was calculated. **(B)** For evaluation of the therapeutic potential of the nanoshells, they were added to HepG2-NTCP cells at indicated time points after they were infected with a nano-Luciferase expressing rHBV (MOI 10 infectious particles/cell). On day 8 pi, luciferase levels in the supernatant were measured and neutralization efficiency was calculated. **(C)** Controls for the neutralization efficiency. Mock (white), the strong neutralizing antibody Nabi (grey) and nanoshells preincubated with the virus (green) served as positive controls, while HBV only (black) served as negative control. Data is represented as mean \pm SD of biological triplicates ($n = 3$) (Prism).

2.3.5 DNA nanoshells seem to be taken up by monocyte derived dendritic cells

To determine whether the nanoshells get taken up by antigen presenting cells (APC), for instance dendritic cells (DC), an uptake assay was performed. For this, human PBMC were isolated and monocyte derived dendritic cells (moDC) were selected via negative magnetic sorting. Upon stimulation of the cells, the isolated monocytes were differentiated into DCs *in vitro*. These cells were then fed with AF647-labelled HBsAg (1 µg/mL and 0.1 µg/mL) and with labelled HBsAg plus nanoshells (0.1 µg/mL), respectively (Figure 20). After 4 hours of incubation at 37 °C, flow cytometry and fluorescence microscopy was performed. Flow cytometry analysis of moDC fed with fluorescently labelled HBsAg at 1 µg/mL revealed roughly 93% of HBsAg-positive cells. Cells fed with either 0.1 µg/mL labelled HBsAg alone or with labelled HBsAg together with nanoshells both depicted frequencies of 70-80% positive cells, while nanoshells alone did not show any positive signal as was expected (Figure 21B). Fluorescence microscopy supported this finding (Figure 21C). Both methods confirm that labelled HBsAg is present in the cells in both samples, with and without nanoshells, suggesting an uptake of HBsAg irrespective of encapsulated into DNA-nanoshells.

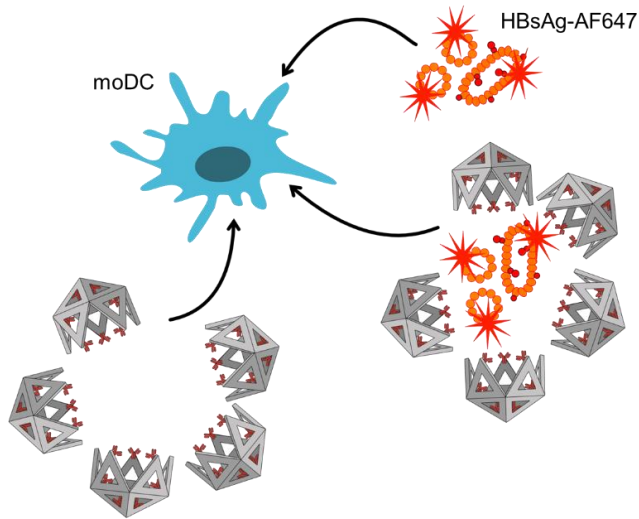


Figure 20 Schematic representation of uptake assay. Monocyte derived dendritic cells were fed with AF647-labelled HBsAg (1 $\mu\text{g}/\text{mL}$ and 0.1 $\mu\text{g}/\text{mL}$), labelled antigen and corresponding nanoshells (0.1 $\mu\text{g}/\text{mL}$), as well as with nanoshells alone, respectively. After incubation for 4 hours at 37 $^{\circ}\text{C}$, cells were subjected to flow cytometry and fluorescence microscopy analysis.

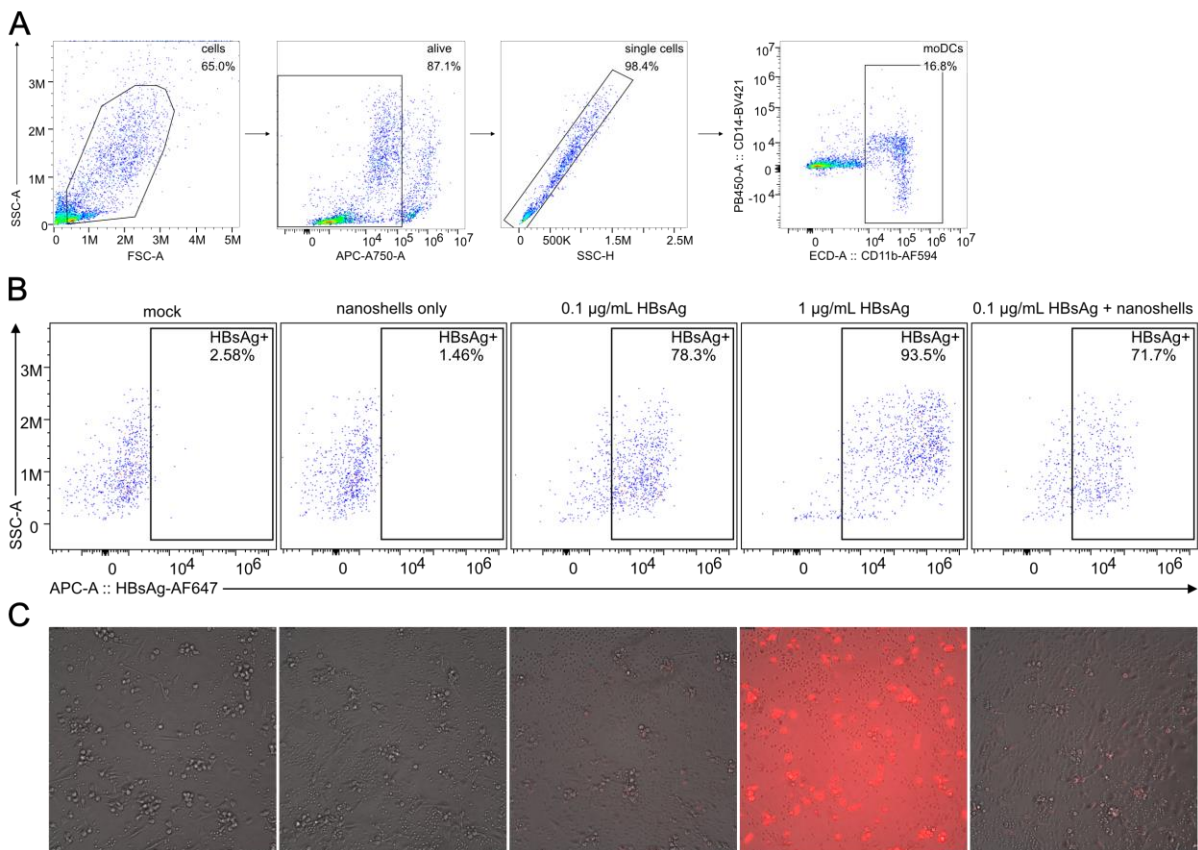


Figure 21 DNA nanoshells seem to be taken up by moDC. (A) Gating strategy of flow cytometry analysis of moDC fed with AF647-labelled HBsAg \pm nanoshells. (B) Flow cytometric analysis of moDC 4 hours post treatment with AF647-labelled HBsAg \pm nanoshells at indicated conditions. (C) Fluorescence microscopy of moDC 4 hours post treatment with AF647-labelled HBsAg \pm nanoshells at indicated conditions.

3 Discussion

Chronic hepatitis B remains a global health problem, leading to up to 880,000 deaths per year due to HBV-related liver cirrhosis or hepatocellular carcinoma [WHO 2022]. So far, no curative treatment is available and patients require life-long antiviral therapy, while still carrying an increased risk for HCC development. Thus, there is a high medical need for novel treatment options that provide viral cure. In the scope of this thesis, monoclonal antibodies against HBsAg were studied and optimized to not only achieve functional cure of patients in the future, but also to improve the understanding of the interaction between antibodies and HBsAg. Furthermore, a novel therapeutic approach utilizing antibody-conjugated DNA nanoshells for efficient neutralization of infectious HBV particles was investigated.

3.1 Fc-“a“-determinant

The main epitope of antibodies directed against HBsAg is located on the so called “a“-determinant within the antigenic loop of the HBV S protein. While the amino acid sequence of the antigen is well described in literature, it was not yet possible to determine the tertiary structure of the protein. One reason for this is the complexity of HBsAg. As it is not a monomeric protein but forms subviral particles and filaments of different sizes, it is challenging to get a homogenous solution of HBsAg and to degrade it to its monomeric form, the S protein, which is needed to determine its structure. Furthermore, the S protein harbors two transmembrane domains which renders crystallization studies in particular and thereby structure determination rather complicated as the protein needs the membrane environment to fold physiologically, which so far can only be provided in NMR studies [Yeh et al. 2020]. While models of the putative S protein structure are available in literature [Suffner et al. 2018], no electron microscopy or similar analysis to confirm the tertiary structure was successfully accomplished. To overcome this challenge, a novel construct was designed which makes the structure determination of the “a“-determinant not only more feasible but which also serves as a tool to determine antibody-antigen binding affinities of HBsAg-specific antibodies. So far, a reliable model for the study of antibody kinetics in the field of HBV research remains elusive. The designed constructs and their applicability in HBV research will be discussed in the following.

3.1.1 Design and production and of Fc-“a“-determinant constructs

The “a“-determinant was fused to the Fc-part of an IgG antibody to allow efficient purification via affinity chromatography using a protein G packed column. Furthermore, the Fc-scaffold provides a rigid and stable scaffold to allow the “a“-determinant to form its physiological structure. Since a dimer formation of two S proteins is predicted [Suffner et al. 2018], the dimeric nature of the antibody

scaffold can facilitate the correct folding. Constructs were designed with different lengths of G₄S linkers between the Fc domain and the antigenic loop to provide enough flexibility for the “a”-determinant to form, referred to as Fc-“a”-determinant 3xGS, 1xGS and w/o GS, respectively (Figure 6A-C, E-G). Furthermore, the Fc-“a”-determinant 3xGS was also designed without the glycosylation site within the “a”-determinant, referred to as Fc-“a”-determinant 3xGS (N146Q) (Figure 6D, H). G₄S linkers are known to be able to couple structurally different proteins while maintaining their individual structure and function [Quitt et al. 2021]. After purification of Fc-“a”-determinant 3xGS (N146Q) with low pH elution, no plausible SDS-PAGE results could be obtained, while the purified protein showed functionality in ELISA (Figure 7B, C). SDS-PAGE neither showed bands at the expected size of 35 kDa for the monomeric proteins, nor at 70 kDa for the dimeric proteins. However, multiple bands were visible at various sizes (~ 23, 25, 30, 40, 55 and 250 kDa). The bands at 55 kDa could correspond to the desired proteins, portraying a different running behavior. This so called “gel shifting” has been shown to be a challenge when analyzing membrane proteins in particular via SDS-PAGE [Rath et al. 2009]. The bands at ~23, 25, 30 and 40 kDa can probably be assigned to degradation products, while the band at ~250 kDa could point towards protein aggregation or higher oligomer formation. Subsequent SEC analysis, which was outsourced to Zahra Harati in Garching, showed a peak at 150 kDa instead of 70 kDa which supports the theory of protein aggregation or oligomer formation (data not shown). To study the purification characteristics in more detail, a Coomassie staining for all flow-through- and elution fractions collected during the purification was performed (data not shown). This analysis confirmed protein degradation during the elution step, leading to the conclusion that the low pH used during elution harms the constructs, which is a well-known complication in protein studies, especially for proteins harboring an Fc domain [Fink et al. 1994; Latypov et al. 2012]. Therefore, the pH stability of the Fc-“a”-determinant 3xGS (N146Q) was evaluated. At low pH (2-4), a characteristic migration pattern in Coomassie staining was observed (Figure 8A). Here, bands at lower molecular sizes were detectable, which were absent at higher pH values. Similar results were obtained by Western blot analysis using an anti-HBsAg antibody that recognizes a linear epitope of the “a”-determinant for detection (Figure 8B). Since the elution was performed at pH 2.9, it was concluded that the protein was partly degraded during this step. These findings underline that the previous purification protocol was harmful for the constructs and explain why no conclusive results could be obtained in neither SDS-PAGE analyses, nor SEC analyses. To overcome this challenge, the purification protocol was optimized, and elution was then achieved by using high salt concentration, which has been described to maintain protein integrity and avoid aggregation [Scheffel and Hober 2021]. Because of the high salt concentration in the elution buffer, the proteins were stored in a phosphate free 0.5 M Tris-HCl buffer with pH 7.5 to avoid precipitation of the protein as was suggested by the manufacturers

[Thermo Scientific 2011]. Both, subsequent SDS-PAGE and Coomassie staining as well as Western blot analysis of purified Fc-“a”-determinant 3xGS and 1xGS confirmed the presence and identity of the constructs (Figure 9). While the bands still do not appear at the expected size of 35 kDa, but rather at 55 kDa, the fact that the bands at the same size are obtained in the Western blot using a specific antibody, suggests that the proteins do not run true to size. As stated above, this has been observed for membrane proteins already, especially hairpin structures that consist of helix-loop-helix structures [Rath et al. 2009]. While the Fc-“a”-determinant proteins do not harbor helical domains, their structure is still similar to the described hairpin with the Fc domain anchoring the loop. Furthermore, it has been shown that the extracellular domains of human E- and N-cadherins bind lesser detergent in SDS-PAGE analysis due to their acidity, consequently showing less mobility and appearing at higher sizes than expected [Tiwari et al. 2019]. Using the online tool “EMBOSS Pepstats” by EMBL-EBI [Madeira et al. 2022; Embl-ebi 2022], the isoelectric point (pI) of the Fc-“a”-determinant proteins was calculated to be ~6.788, portraying a slightly acidic protein. Therefore, the bands at 55 kDa could be assigned to Fc-“a”-determinant protein monomers that bind less detergent due to their structure and acidity, thereby showing an impaired running behavior. Keeping this in mind, the results showed that a protein solution of rather high purity was achieved with the new purification protocol and the constructs were subjected to further functional analyses.

3.1.2 Fc-“a”-determinant constructs take on physiological structure

Functional analyses of Fc-“a”-determinant 3xGS, 1xGS and w/o GS were performed by ELISA with two different detection antibodies, both recognizing a conformational epitope (MoMAb and 4D06, both biotinylated). A conformational change of the epitope due to unphysiological folding would result in reduced binding of the antibodies. Indeed, HBV immune escape mutants are known to utilize mutations within the “a”-determinant which alter its conformation to evade recognition [Lada et al. 2006; Cremer et al. 2018; Lazarevic et al. 2019]. Therefore, only correctly-folded Fc-“a”-determinant constructs harboring their physiological structure should be detected in the ELISA. HRP-conjugated avidin was used to bind the biotinylated antibodies and to start the colorimetric reaction with TMB. Analysis with either antibody showed an expected increase of signal with higher coated protein concentrations until reaching an Fc-“a”-determinant concentration of 0.3 μ M. Upon exceeding this concentration, however, the antibody binding signal dropped in a concentration-dependent manner (Figure 10D). This observation was reproducibly observed for all constructs. One explanation for this finding is the formation of Fc-“a”-determinant oligomers or aggregation at concentrations higher than 0.03 μ M, which can reduce the accessibility to the antibody binding sites, leading to a signal drop. Detrimental ELISA signal loss due to aggregation of amyloid-beta (A β), the characteristic of Alzheimer’s

disease, has been shown before [Janssen et al. 2015], which further supports this assumption. The fact that the decrease in signal also seems to be concentration dependent, promotes this theory.

To gain more insights into the behavior of the protein, an analytical ultracentrifugation (AUC) was performed. For this, samples were prepared at a concentration of 0.8 mg/mL and the analysis was kindly performed by Martin Haslbeck at the institute of Biotechnology in Garching. While the data for the Fc-“a”-determinant 3xGS could not be analyzed due to technical issues, the data for Fc-“a”-determinant 1xGS and w/o GS clearly show a peak at a size of 140 kDa, corresponding to oligomers, rather than the expected dimers (data not shown). While the AUC could only be performed once due to sample limitations and needs to be repeated for each construct to allow for a certain conclusion, the preliminary data further supports the proposition of the Fc-“a”-determinant forming higher oligomers as soon as a concentration of 0.03 μ M is exceeded. Furthermore, also SDS-PAGE analysis showed bands at 250 kDa that could be assigned to oligomer structures (Figure 10B). Similar findings were observed in SEC analysis where molecules with a size of 150 kDa were detected (data not shown). As it is known that HBsAg forms subviral particles comprising multiple S protein monomers under physiological conditions [Bruss 2007], oligomerization of the Fc-“a”-determinant constructs is a reasonable expectation. Initially, these constructs were designed to allow for co-crystallization with antibodies and thereby enabling the structure determination of the “a”-determinant. For crystallization studies, typically a protein concentration of 2-50 mg/mL is required, with 10 mg/mL being the rule of thumb [Dessau and Modis 2011; Wlodawer et al. 2013]. In this study, however, proteins started to precipitate at concentrations \geq 1.5 mg/mL, rendering crystallization unfeasible. To avoid oligomerization, the Fc-“a”-determinant proteins need to be stored at lower concentration and detergents to stabilize its structure need to be added to higher concentrated samples. However, protein crystallization is further complicated by addition of detergents, as they need to be thoroughly screened to avoid protein denaturation during the process [Birch et al. 2018; Kermani 2021]. Another solution could be the incubation of Fc-“a”-determinant constructs and antibodies at low concentrations, followed by crosslinking of the complexes and subsequent concentration. This might help to overcome the oligomerization of the constructs and allow successful crystallization in the next step. However, this would also come with a high percentage of sample loss during further concentration of the samples. While structure determination of the “a”-determinant remains difficult, the Fc-“a”-determinant constructs were successfully designed and purified in a small scale. Furthermore, it was shown that HBVenv-specific antibodies engage Fc-“a”-determinant constructs, confirming their physiological structure.

3.1.3 Fc-“a”-determinant constructs can be used to obtain antibody binding kinetics

Due to the complex structure and the formation of multimeric subviral particles, affinity determination for HBsAg-specific antibodies remains challenging. Since the novel Fc-“a”-determinant constructs show correct folding resulting in the physiological structure of the “a”-determinant, they provide a suitable alternative to determine binding affinities of various anti-HBsAg antibodies with conformational epitopes. Because the gold standard of affinity determination, surface plasmon resonance (SPR), is rather expensive in regards of assay optimization and supply costs, a different approach was followed. Binding affinities were determined by microscale thermophoresis (MST), which is not only cost effective, but also requires reduced sample quantity. While SPR commonly requires at least 100 μL of sample [Drescher et al. 2009], MST analyses utilize a minimum sample amount of 10 μL [NanoTemper Technologies 2022]. Furthermore, MST enables the measurement of K_D values in a pM-mM range [NanoTemper Technologies 2022], thereby offering an efficient method to determine binding affinities which dimensions are unknown. Binding affinities of an HBVenv-antibody (MoMAb) to the Fc-“a”-determinant 3xGS, 1xGS and w/o GS constructs were successfully measured and compared. It was observed, that the calculated binding affinities did not differ majorly between the different Fc-“a”-determinant constructs (Figure 11). Furthermore, calculations were reproducible over a period of multiple days using the same labelled batches stored at 4 °C for 1 week leading to the conclusion that the measurements result in reliable binding affinities (Figure 11B). In general, the curves generated when applying the Fc-“a”-determinant w/o GS showed the most constant course. This proposes that a linker between the rigid Fc-part and the antigenic loop rather destabilizes the complex and does not help to form the correct protein conformation. For future affinity measurements, it would be sufficient to only use this construct, thereby saving time not only during the measurements but also in the purification process, as the other constructs would not need to be expressed anymore.

3.2 Fc-engineered antibodies

3.2.1 Design of Fc-engineered antibodies

Chronic HBV infection is characterized by an exhausted T-cell population, leading to a weak T-cell response. Current treatments like NUCs and IFNs efficiently suppress viral replication but mostly fail in eradicating the virus completely. Many drugs are in development in order to overcome this issue and to achieve a full regeneration of the weakened immune system. All of them aim at achieving a so called functional cure, which is characterized by a seroconversion from HBsAg to anti-HBsAg. One approach is the therapy with monoclonal antibodies directed against HBVenv-proteins. Recently, the mouse monoclonal antibody (mAb) E6F6 [Zhang et al. 2016] which mediated ADCC- and CDC-independent HBV-suppression [Gao et al. 2017] was humanized utilizing structure-guided humanization and *in silico* scanning mutagenesis [Zhou et al. 2020]. First *in vivo* studies showed substantial suppression of serum HBsAg levels for 2 weeks. After 4 weeks, however, the initial HBsAg levels were restored [Zhou et al. 2020]. Previously, administration of a mixture of 2 HBVenv-specific mAbs into HBV chronic carrier chimpanzees resulted in a similar outcome, displaying an initial drop of HBsAg serum levels that rebounded after 72 hours [Eren et al. 2000]. Both studies thereby reinforce that combinational therapy with mAbs lowering serum HBsAg levels, followed by an immune-restoring approach might be a promising option to treat CHB. Utilizing single B-cell cloning, HBVenv-specific antibodies were determined and characterized in this institute [Wolff 2020]. One of these antibodies, 4D06, portrayed a very promising drug candidate due to its high HBVenv-specificity and high neutralization capacity. However, its ability to induce ADCC was not as strong as for comparable antibodies [Wolff 2020]. Especially in the scope of chronic hepatitis B, the major challenge is to permanently eradicate infected cells and thereby the persisting nuclear cccDNA. Antibodies with a strong neutralization capacity do help against reinfection and are able to capture soluble HBsAg, however, they fail to eliminate already infected cells without the induction of potent antibody effector functions, such as ADCC. The human antibody 2H5-A14 directed against the preS1 domain has been shown to not only effectively neutralize HBV infection but also elicit potent ADCC and ADCP, resulting in sustained HBsAg loss without emergence of escape mutants [Li et al. 2017], highlighting the great potential of antibody effector functions in treatment of CHB. For this reason, the isolated and characterized 4D06 was subjected to Fc-engineering, enhancing its ability to induce ADCC. To find the optimal candidate, 3 different mutants were designed. Introduced mutations were chosen based on literature. All variants harbor different mutations that provide enhanced binding to CD16, the ADCC initiating FcγR in humans.

3.2.1.1 4D06-DLE

In the 4D06-DLE variant, the wild type was altered by introducing the following mutations: S239D/A330L/I332E. This triple mutant has previously been shown to induce a stronger ADCC in the context of alemtuzumab, an anti-CD52 antibody [Lazar et al. 2006]. Furthermore, a 255-fold binding affinity after introduction of these substitutions compared to the respective wild type has been reported [Mimoto et al. 2013].

3.2.1.2 4D06-LPLIL

For the 4D06-LPLIL, five mutations were introduced in the heavy chain, namely F243L/R292P/Y300L/V305I/P369L. This mutant has been reported to show a stronger binding to CD16 while sustaining a comparable binding affinity to the wild type, thereby eliciting a strong ADCC with an approximately 100-fold increased lysis rate [Stavenhagen et al. 2007].

3.2.1.3 4D06-KH12

As it has been shown that an asymmetrical Fc-engineering approach greatly enhances ADCC and also antibody stability [Mimoto et al. 2013; Liu et al. 2014], a heterodimeric antibody was designed, which consists of two different heavy chains. These are designed in a “knob-into-hole”-fashion, which is a commonly used approach to insert different alterations in the two heavy chains but to also promote the formation of heterodimers, rather than homodimers [Ridgway et al. 1996]. A large amino acid group is introduced into one of the chains, while the other chain harbors a stoichiometrically fitting notch that allows for the favoring formation of heterodimers. One heavy chain included substitutions L234Y/L235Q/G236W/S239M/H268D/D270E/S298A/S354C/T366W, with T366W forming the “knob”, while the second heavy chain included substitutions D270E/K326D/A330M/K334E/Y349C/T366S/L368A/Y407V with T366S/L368A/Y407V forming the “hole” [Ridgway et al. 1996; Mimoto et al. 2013]. Additionally, disulfide bridges were introduced to further stabilize the heterodimers. The binding affinity of antibodies harboring these mutations to FcγRIIIa has been shown to increase 1000-fold in comparison to the respective wildtype while FcγRIIb binding was comparable [Mimoto et al. 2013]. Correct heterodimerization is achieved in more than 97%, with “hole-hole” homodimers accounting for the rest while “knob-knob” homodimers are typically not observed [Klein et al. 2012].

3.2.2 Production and stability of Fc-engineered antibodies

After successful design and production of the Fc-engineered antibodies in HEK293T cells, they were tested for their stability and integrity. SDS-PAGE analysis with subsequent Coomassie staining showed protein bands at a size of ~250 kDa, which indicated aggregate formation of antibodies (Figure 14D).

These bands have previously been observed in SDS-PAGE analysis of the wildtype antibody as well. However, Western blot analysis did not show bands at 250 kDa [Wolff 2020], leading to the conclusion that they do not arise from antibodies, but can rather be assigned to serum proteins that aggregated during concentration with spin columns as the protein expression was performed in the presence of 10% FCS. When considering the intended use of these antibodies in a clinical context, their purity is of utmost importance and would need improvement. According to the European Medicines Agency (EMA), impurities in antibody preparations that are designated for clinical use should be avoided and need to be identified and characterized in order to ensure product safety [European Medicines Agency 2023]. Adding a size exclusion chromatography after the affinity chromatography step would be a feasible option to improve the purity of the Fc-engineered antibodies. In the context of this thesis, however, the overall purity of the antibodies was satisfactory enough to proceed with their functional characterization. Particular attention was directed to antibody stability, which is not only important for large scale production, but also in the clinical context. Antibodies were stored in PBS at 4 °C and no degradation was observed after 1 year of storage, highlighting their high stability. Consequently, purification was scaled up to a 5 mL column from a 1 mL column, resulting in a batch-dependent 5-10-fold yield of pure antibody for further analyses.

3.2.3 Fc-engineered antibodies show less HBsAg-specificity and neutralization capacity than the wild type

After confirming the integrity of the antibodies, their HBsAg specificity was determined by ELISA analysis. All Fc-engineered antibodies showed similar HBsAg specificity, however, the wild type showed the highest signal in ELISA (Figure 15A). Currently, there is an in-house assay in development, which allows affinity measurements via microscale thermophoresis. This assay was already used to reproducibly quantify the affinity of the HBVenv-specific antibody MoMAb to the Fc-“a“-determinant constructs. As soon as this method is fully established, the Fc-“a“-determinant will be used to determine affinities of anti-HBVenv antibodies in house, including the Fc-engineered constructs. Since the affinity of antibodies to their antigen is largely dependent on the antigen-binding site [Rudnick and Adams 2009], the affinity of the Fc-engineered antibodies should be comparable to the wild type, as all versions harbor the identical Fab domain. In contrast to the affinity, the avidity is also determined by intramolecular interactions and might differ between the constructs [Rudnick and Adams 2009], which suggests that the Fc-engineered antibodies have a weaker avidity due to their Fc-alterations resulting in lower ELISA signals. When examining the neutralization capacity of the Fc-engineered variants, a similar trend was observed. While the wild type shows neutralizing activity at concentrations as low as 30 nM, a 10-fold higher concentration of the Fc-engineered antibodies was

needed in order to reach the same result (Figure 15B, C). This is in line with the theory of decreased avidity in the Fc-engineered variants, as the avidity was shown to have a determining influence on the neutralization capacity of antibodies [Bachmann et al. 1997]. As these mutants were designed to elicit a stronger ADCC than their respective wild types, their impact on neutralization capacity has not been described in literature. While this suggests a deterioration of the wild type antibody through introduction of the mutations, a reduced neutralization capacity does not interfere with their intended therapeutic application. In chronic hepatitis B, the main challenge is the persistence of the virus within infected cells due to the formation of cccDNA. While high neutralization capacity can substantially reduce infection, it has no influence on the persistence of cccDNA. Antibodies eliciting potent ADCC, however, could specifically target and lyse the infected cells, thereby eliminating the cccDNA. In the scope of CHB treatment, it would therefore be desirable to have an antibody with a high capacity to induce ADCC rather than an antibody that only shows neutralization. *In vivo* studies with an antibody eliciting effector functions such as ADCC and antibody dependent cellular phagocytosis (ADCP) not only showed sustained low serum HBsAg levels but also other anti-viral effects that can be attributed to antibody effector functions [Li et al. 2017]. Furthermore, it has been reported that ADCC is strongly impaired in patients with chronic and acute hepatitis B, which might be due to sequestration of effector cells in the liver [Bortolotti et al. 1978], pointing towards an important role of ADCC in the clearance of HBV infection. Accordingly, the Fc-engineered antibody, which would show a higher capacity of inducing ADCC compared to the wild type in future analyses, would be favorable even if its neutralization capacity would be lower. Should none of the antibodies described here portray an enhanced capacity of inducing ADCC, Fc-engineering remains a promising approach and other Fc mutations might be considered.

3.2.4 Comparison of antibody therapy with other therapeutic approaches

Current treatment of chronic HBV infection is limited to nucleos(t)ide analogues (NUCs) and pegylated interferon (PEG-IFN). These induce disease remission, however, they mostly fail in eradicating the virus completely, leading to the necessity of taking the medication lifelong. The goal of a “functional cure”, defined by the loss of serum HBsAg, suppression of serum HBV DNA and seroconversion to anti-HBsAg antibodies is only reached in less than 10% of cases [Bertoletti and Le Bert 2018]. One of the reasons is that NUCs only function as DNA chain terminators when integrated in synthesized DNA strands, thereby stopping the viral DNA polymerase [Papatheodoridis et al. 2002]. They do not, however, interact with the already formed viral cccDNA which remains persistent in infected cells, serving as template for persistent viral replication. Additionally, NUCs are not specified for viral DNA and also affect mitochondrial DNA which has been reported to lead to loss of bone mineral density in tenofovir treated HIV patients [Gafni et al. 2006]. Moreover, NUCs do not affect viral protein

translation, leading to a maintenance of high HBsAg serum levels, which was shown to be crucial for the impairment of B- and T-cell responses in chronic HBV infection [Bensch et al. 2014; Burton et al. 2018; Salimzadeh et al. 2018]. PEG-IFN also interferes with virus dissemination by indirectly mediating antiviral and immune-modulating effects. The PEG prolongs the durability of the interferon [Abuchowski et al. 1977; Caliceti 2004]. PEG-IFN is commonly administered once weekly during the course of 48 weeks [Ye and Chen 2021]. It resulted in sustained loss of serum HBsAg and undetectable HBV DNA levels in 30% of patients [Perrillo 2006], highlighting the advantage of a finite treatment and option of sustained viral clearance in comparison to NUC treatment. Furthermore, the risk of developing HCC is less in PEG-IFN- than in NUC-treated patients [Liang et al. 2016]. However, IFN-treatment is accompanied by severe side effects which include, but are not limited to, depression, heart damage and high blood pressure, emphasizing the need of a different medication approach [Khakoo et al. 2005; Lotrich 2009; Dhillon et al. 2010; Somers et al. 2012; Chiu et al. 2017].

As pointed out, it is of great importance to consider limitations and side effects when developing potentially new treatment options for chronic HBV infection. When it comes to eliminating infected liver cells by introducing ADCC-inducing antibodies, the potential liver toxicity needs to be contemplated. In a 2003 study with 20 CHB patients 1-35% of hepatocytes were infected [Rodríguez-Iñigo et al. 2003], highlighting the large variance between patients. Eliminating all of the infected hepatocytes too fast so that the turnover of healthy cells cannot keep up, might result in complete liver damage rather than in a cure of the disease. Therefore, the individual cell count of infected hepatocytes would need to be analyzed from liver biopsies before including patients for the antibody therapy. Furthermore, it would be important to consider the time frame to give the drug and the dose in order to achieve a clearance of infected cells. In the ongoing randomized phase I clinical trial of Cetrelimab, a monoclonal antibody with high PD-1 specificity, a single antibody dose will be administered, followed by a 24-week follow-up phase [Janssen Research & Development, LLC 2022]. While the fate of cccDNA during cell division was unknown for a long period of time, recently it was shown that cccDNA levels greatly decline during mitosis [Tu et al. 2022]. These findings suggest that once all infected cells are eliminated, only healthy cells will arise leading to healthy tissue replenishment after treatment. While neutralizing antibodies alone will probably not be sufficient to achieve complete clearance, a co-therapy with other treatments such as NUCs or PEG-IFN is possible. Antibodies would help to decrease serum levels of HBsAg and prevent reinfection by neutralizing the virus, while the NUCs/IFN would prevent the virus to spread further. First clinical studies have been deducted in this direction where CHB patients who were receiving long-term NUC treatment and showed low HBsAg levels as well as undetectable titers of HBV DNA were given monthly injections of Hepatitis B immunoglobulins (HBIG), which prevent virus entry. 4 out of 8 patients showed significantly

reduced levels of HBsAg serum levels and three patients even became anti-HBs positive after one year of treatment. During this study no side effects were detected [Tsuge et al. 2016]. HBIg is isolated from plasma of donors with high anti-HBs titers and is administered to unvaccinated people as well as infants born from HBV infected mothers to achieve fast antigen loss and prevent vertical transmission. However, a subsequent prophylactic vaccination is necessary as the antigen loss is not sustained [Terrault et al. 2018]. It is further applied as postexposure immunoprophylaxis which can also be administered to unvaccinated individuals within 24 hours of exposure to HBV via bites, needles or sexual contacts [Terrault et al. 2018]. Overall, HBIg can only be applied in specific cases and does therefore not portray a broadly applicable treatment option. This further emphasizes the need of an effective treatment option and antibodies eliciting strong effector functions such as ADCC might be able to provide an efficient therapy for CHB.

While antibody and also NUC or IFN treatment focusses on reduction of viral DNAs and antigen levels, therapeutic vaccination also addresses the challenge of inducing strong and specific B- and T-cell responses. A therapeutic vaccination administering a protein prime followed by an MVA boost, TherVacB, has been shown to efficiently restore CD8+ T cells and induce the production of HBsAg-specific antibodies *in vivo* when HBV antigen levels were low at time point of vaccination. In contrast, mice with a high HBsAg titer did not show an increased number of effector T cells and were unable clear the virus [Michler et al. 2020]. To overcome this challenge, a combination therapy is conceivable. Administering antibodies to reduce HBsAg levels followed by therapeutic vaccination might not only accomplish a functional cure, but also a restoration of the patients B- and T-cell responses. Furthermore, therapeutic vaccination has been shown to induce production of anti-HBsAg antibodies which further helps to overcome the chronic infection [Kosinska et al. 2021].

As alternative to antibodies, small-interfering RNA (siRNA) can be used to lower HBsAg levels in the circulation. While antibodies interact with the HBsAg directly, siRNA targets viral DNA transcripts, thereby preventing the expression of the viral proteins. Different targets for siRNAs have been studied in combination with therapeutic vaccination, many of them showing a sustained control of the HBV infection, ultimately leading to the conclusion that combinational therapy with siRNA and therapeutic vaccination is a promising approach to cure chronic Hepatitis B [Michler et al. 2020; Bunse et al. 2022]. While siRNA delivery portrayed a challenge for a long time, as they do not easily cross cell membranes due to their negative net charge, siRNAs conjugated with *N*-acetylgalactosamine (GalNAc) which binds the asialoglycoprotein receptor on hepatocytes can now be successfully delivered to the liver [Debacker et al. 2020]. While these studies seem promising, there is a major downside for the usage of siRNA in therapeutics as they are prone to enzymatic degradation and renal filtration.

A different approach is T-cell therapy. As pointed out in 1.4.2, functional T cells are crucial for the clearance of HBV [Thimme et al. 2003]. By utilizing adoptive transfer of T cells that are equipped with HBV-specific receptors, T-cell responses can be restored. The T cells are transduced with either HBV-specific T-cell receptors (TCR) or chimeric antigen receptors (S-CAR). It has been shown that these cells are capable of eliciting a virus specific immune response, thereby promoting the elimination of infected hepatocytes and controlling the viral infection [Krebs et al. 2013]. A potential drawback of this approach is the high number of target cells and in turn excessive activation of transferred effector cells, which may lead to side effects such as cytokine release syndrome (CRS) [Stern and Stern 2021]. Studies already focused on overcoming this issue by introducing safeguard mechanisms. One of these is the addition of an inducible caspase 9 (iC9) in the transgene, which can induce rapid elimination of effector cells *in vivo* upon administration of a dimerizer, highlighting a promising concept to tackle CRS or fatal liver damage in adoptive T-cell therapy of chronic HBV infection [Klopp et al. 2021]. A main advantage of CARs in comparison to HBV-specific TCRs is that they do not need to be HLA matched for every individual patient as they target native protein on the cell membrane independent of MHC. In general, T cell products require individual engineering for each patient, which is a major disadvantage when comparing them to antibodies that allow of-the-shelf application. This suggests a supportive role of antibodies in adoptive CHB therapy. A combination therapy could include antibodies to lower antigen load and prevent reinfection, and adoptively transferred T-cells to restore T-cell function to promote a complete cure [Fiscaro et al. 2020].

Another approach which showed first successful results in clinical studies are nucleic acid polymers (NAP). They act as inhibitors for the assembly and production of subviral particles. Latest studies showed clearance of HBsAg during NAP treatment in both, HBV monoinfected and HBV/HDV coinfecting patients [Bazinet et al. 2022]. Another randomized phase 2 clinical trial investigated the tolerability of NAPs in a co-treatment with tenofovir disoproxil fumarate (TDF), a reverse transcriptase inhibitor, and pegIFN [Bazinet et al. 2020]. This study showed a significant reduction of HBsAg levels in the circulation and subsequent seroconversion to anti-HBsAg antibodies in comparison to treatment without NAPs, resulting in functional cure which persisted in 14 out of 40 patients during the 48 week treatment free follow up phase. Furthermore, addition of NAP did not hamper the tolerability of the treatment, paving the way for a promising co-therapeutic approach against chronic HBV infection [Bazinet et al. 2020]. Further phase 2 clinical trials in Europe, USA and Asia are soon to follow [Replicor 2020].

3.3 DNA nanoshells

The EU-funded Virofight project focuses on a novel approach to catch virus particles and virions to prevent infection of cells. For this, the group of Hendrik Dietz designed and produced DNA nanoshells [Sigl et al. 2021]. These shells consist of DNA arranged in triangles that can then be conjugated to virus-specific binders, like antibodies or aptamers. These triangles are then driven to form shells. Different quantity of triangles are used to obtain different sizes of shells [Sigl et al. 2021]. This innovative approach illustrates a unique drug candidate that provides the possibility to rapidly react to new emerging viruses. As the SARS-CoV-2 pandemic showed, new pharmaceuticals are always in need and a rapid production and distribution is of the essence. With this approach, nearly every virus of any size can be captured and neutralized. The virus-specific binders, such as antibodies or aptamers, do not need to harbor any neutralization capacity on their own, as the neutralization would be achieved by engulfing the virus with the DNA nanoshell. While there are neutralizing antibodies available against HBV, this is not the case for every viral disease. At the beginning of the SARS-CoV-2 pandemic for example, mostly non-neutralizing antibodies were identified in COVID-19 patients [Seydoux et al. 2020], therefore not serving as potential drug targets at that time. Another advantage of the nanoshells over classical antibody therapy is that the DNA is completely inert and should not induce any kind of adverse effects like antibody dependent enhancement (ADE), which has been described to be a concern with antibodies against SARS-CoV-2 [Lee et al. 2020]. As a proof of concept, DNA nanoshells were designed and conjugated with anti-HBsAg and anti-HBcAg antibodies, respectively, to capture and inactivate HBV virions. These shells consist of 10 triangles, each of them binding 90 antibodies, that form a half shell and their functional properties as well as their potential applicability as future drug will be discussed in the following.

3.3.1 DNA nanoshells efficiently inactivate HBV *in vitro* when present at time of infection

After confirming that antibodies conjugated to DNA nanoshells still recognize their antigen targets, neutralization assays were performed with HepG2-NTCP cells as target. Cells were infected with HBV and DNA nanoshells were added at different concentrations to achieve virus neutralization. As a control, the same amount of antibodies was administered without being conjugated to DNA. The data clearly show a higher neutralization capacity of the shells in comparison to unconjugated antibodies (Figure 18). To evaluate the applicability of the shells as therapeutic or preventive treatment, the nanoshells were added at different time points before and after HBV infection. Neutralization was only achieved as long as nanoshells were present at time of infection. This goes in line with previous data showing the presence of HBV DNA in the cytoplasm 1 hour after infection and in the nuclear

fraction 3 hours after infection [Chakraborty et al. 2020]. Recent data in our research group point towards even faster infection kinetics, showing the presence of HBV DNA in nuclear fractions within 30 minutes post infection [personal communication with Lea Hansen-Palmus]. Delayed administration of the nanoshells as well as infection 24 h post nanoshell addition impaired the neutralization capacity (Figure 19A, B). This leads to the conclusion that the stability of the nanoshells is rather low *in vitro*, which was already shown in mouse sera where the half-life was detected to be 24 hours [Sigl et al. 2021]. In general, a neutralization of 50%-80% could be observed in nanoshell treated cells (Figure 18, Figure 19C). This variance can be attributed to different nanoshell batches as well as different HBV stocks. Overall, during the course of this thesis, a neutralization of 80% was detected repeatedly, highlighting the efficacy of the nanoshells. The short half-life limits the applicability of the nanoshells in clinical studies, as they need to be applied as preventive therapy and have no effect on previously established infections (Figure 19). To overcome this, coating of the DNA with different inhibitors is conceivable to prevent DNases from degrading it. Furthermore, there are several different drug delivery systems that could be applied in order to not only help the nanoshells to get taken up so they could function within the cell, but also to include a tissue specific marker to avoid potential side effects when targeting too many cells at once. Many drug delivery systems are commercially available which might be helpful for this application [Vargason et al. 2021]. As the nanoshells are already quite large to capture the respective viruses, an approach that does not further enlarge them would be favorable. Furthermore, nanoshells need to be conjugated to a specific virus-binder in order to target the virus and achieve neutralization. This in turn weakens their strong advantage, as specific binders might not be available for newly emerging viral threats. Studies with heparin-sulfate modified nanoshells demonstrated their ability to neutralize a large variety of viruses, including adeno, adeno-associated, chikungunya, dengue, human papilloma, noro, polio, rubella, and SARS-CoV-2 viruses or VLPs [Monferrer et al. 2022]. However, utilizing heparin-sulfate as binder increases the risk of off-target effects in comparison to specific binders which needs to be considered in future studies. Recently, severe acute hepatitis cases in children were linked to common AAV2 infection [Grand 2022]. To study this finding in more detail, shells are currently designed to capture AAV2 particles. These nanoshell preparations are produced with an additional step to eliminate endotoxins allowing their administration to mice, which enables *in vivo* studies in the future. These shells will be tested *in vitro* and, when showing neutralizing capacity, will be administered to mice infected with AAV2 carrying an HBsAg-encoding gene as surrogate marker for infection. These data will greatly enhance the knowledge about the mode of action of the nanoshells and illustrate further potential for clinical application.

A question that has not been sufficiently answered is what happens to nanoshells and virus upon complex formation. Preliminary data suggest that the complexes are taken up by antigen-presenting cells (Figure 21). Assumingly, after being taken up by antigen-presenting cells, the DNA is degraded by DNases and the virus is digested and presented on MHC molecules [van Montfoort et al. 2014]. This in turn would induce T-cell responses. First attempts of a flow cytometry analysis of T cells added to PBMC as well as macrophages fed with conjugated and unconjugated nanoshells to strengthen this theory, however, did not show differences in cytokine secretion levels which would point towards T-cell activation (data not shown). As the T-cell activation was also not pronounced in the respective positive controls, this was likely due to an unfavorable experimental setup which needs refinement, rather than a contrary result. Another potential advantage of the nanoshells, namely the absence of raising side effects such as ADE, is currently under investigation. For this, a Jurkat cell line that expresses an artificial CD16-CD3 ζ fusion protein, established and kindly provided by Philipp Kolb (Institute of Virology, Universitätsklinikum Freiburg), will be used. The cells will be transiently transfected to express NFAT-dependent nano-Luciferase (nano-Luc). After binding of antibodies to CD16, NFAT will be activated, leading to the expression of the transgenic nano-Luc which in turn will be secreted and luciferase activity could be measured in the supernatant. ADE occurs when an antibody binds virus and Fc γ receptors on a cell, followed by an uptake of the virus antibody complex by the cell [Xu et al. 2015]. The virus then replicates in the cell and the infection is promoted. Since the nanoshells are coupled to the antibodies via their Fc-domain, binding to Fc receptors should be sterically impaired and ADE should be prevented. Absence of luciferase activity after treatment with antibody conjugated nanoshells singly or in complex with the viral particle would support this argument. Data to confirm this theory will be generated in the near future.

3.3.2 Effective neutralization with Nanoshells requires less antibody

All experiments showed that a much smaller amount of antibodies is needed in order to neutralize an HBV infection when conjugated to DNA nanoshells in comparison to unconjugated antibodies. While the same amount of antibodies conjugated to the nanoshells was applied in the unconjugated control, neutralization was only observed in the nanoshells samples (Figure 18). This outlines one major advantage of the nanoshells. The production of antibodies is costly, while the production and assembly of the DNA nanoshells is comparatively fast and inexpensive. If the nanoshells could be designed in a way that they not only persist for a longer time but could also function within an infected cell, the lesser needed amount of antibodies would further push this novel treatment.

3.3.3 Potential other fields of application of DNA nanoshells

The discovery and development of a new drug is a long, costly process and often not successful. In total, only 10% of potential drug candidates, which successfully entered phase I clinical trials, will get the approval and a lot of money may be lost on the way [Sun et al. 2022]. The DNA nanoshells are still at a very early stage in pre-clinical development. Because of this, it is important to consider other possibilities for their application. The data generated in this study suggest that in regard to antiviral therapy, DNA nanoshells are not feasible for therapeutic but rather preventive treatment and their short half-life might limit clinical application. Nonetheless, their antiviral properties can be explored in water or air filtering. As the shells can be designed in different shapes and sizes, they are able to engulf and neutralize a broad variety of viruses. One approach to exploit the antiviral properties is the combination of shells conjugated with various different virus-binders followed by immobilization on a filter. Then, contaminated water could be filtered and the shells would capture the viruses rendering the water clean and consumable. While this approach might come at a higher cost than the gold-standard method of UV irradiation, depending on the sizes of the filter, it might be more feasible to transport them in low-developed countries. Furthermore, filters would not need any kind of electricity, which might also be hard to come by in the affected countries.

4 Final evaluation and outlook

Even though prophylactic vaccines exist, curative treatment for chronic hepatitis B remains elusive. Current treatment options suppress viral replication but fail to eradicate the virus completely from the infected cells due to its persistence form, the cccDNA. While these treatments have been shown to improve the outcome of CHB in general, the risk of developing liver cirrhosis and HCC remains high in CHB patients. Therefore, eradicating cccDNA from infected cells is still the major goal in future therapeutic approaches. Currently, there are several therapies in development, including therapeutic vaccination and adoptive T-cell transfer. While both approaches show promising results, it became clear that a single therapy might not be sufficient to clear chronic HBV infection. Co-therapy with HBVenv-specific antibodies provides a promising solution. In order to design specific and potent antibodies, structural knowledge about their antigen is of utmost importance. This study provides a novel protein construct that can help to crystallize and analyze the antigenic loop of the HBV S protein, one of the major antigens of HBV. While structural determination was not feasible in the scope of this study, the protein was successfully used to measure affinity of HBVenv-specific antibodies in a simple, reproducible, and cost efficient way. Furthermore, it was shown that an alteration of the Fc domain of HBVenv-specific antibodies modifies the antigen-specificity which is important to keep in mind when it comes to antibody design.

Finally, a novel therapeutic approach has been proposed with nanoshells designed via DNA origami that can be conjugated to a variety of virus binders, such as antibodies and aptamers. First results in this study show a significantly higher neutralization of HBV infection *in vitro* in comparison to unconjugated antibodies. While the fate of the administered nanoshells is still under evaluation, they portray a versatile therapy that can be used for a variety of viral infections. Coupled with broadband virus-specific binders, nanoshells provide a promising treatment option for newly emerging viruses. Therefore, more thorough evaluation of the nanoshells and their potential applicability need to be examined in further studies. These need to include further characterization *in vitro* as well as *in vivo* to confirm their applicability and rule out potential side effects. Taken together, this study not only provides a novel protein to facilitate HBsAg structure determination, but also presents an innovative therapeutic approach with high potential for emerging viruses and pathogens that cannot be eradicated by neutralizing antibodies.

5 Materials and Methods

5.1 Materials

5.1.1 Devices

Product	Supplier
Agarose Gel Chambers	PeqLab
Architect™ platform	Abbot Laboratories
BEP III platform	Siemens Healthcare
Centrifuge 5920R	Eppendorf
CytoFLEX S	Beckmann Coulter
ELISA-Reader infinite F200	Tecan
Fluorescence microscope FluoView FV10i	Olympus
Freezing device	Nalgene / Biocision Coolcell
Incubator Heracell 150	Heraeus Holding GmbH
Intas Chemostar M6	Intas Science imaging
Invitrogen™ Dynal DynaMag™-15	Thermo Fisher Scientific™
Light Cycler® 480 II	Roche Diagnostics
Mini Trans-Blot® cell	Bio-Rad
Monolith NT.115	NanoTemper
Multi-channel Pipettes	Ergo One
NanoDrop One	Thermo Fisher Scientific™
Neubauer improved hemocytometer	Brand
NucleoCounter NC250	Chemometric
PCR Cycler TOptical Gradient 96	Biometra
Peristaltic Pump MasterFlex L/S	Cole Parmer
Pipettes	Eppendorf
Pipette 'Accu-jet pro'	Brand

Shaker and incubator for bacteria	INFORS AG; Heraeus Holding GmbH
Sterile Hood HERA Safe	Thermo Fisher Scientific™
T professional Trio Thermocycler	Analytik Jena

5.1.2 Consumables

Product	Supplier
Amicon Ultra Centrifugal Filters, 30K, 2 mL	Merck
Cell culture flasks, dishes, plates	TTP
Cryo vials	Grainer Bio One
ELISA 96-well plates Nunc MaxiSorb	Thermo Fisher Scientific™
FACS plate 96-well, V-bottom	Roth
Falcon tubes 15 mL/50 mL	Grainer Bio One
Filter tips	Greiner Bio One
HiTrab Protein G HP column, 1mL/5mL	GE Life sciences
Immobilon-P, PVDF membrane, 0.45 µm	Merck
MasterFlex Tubing, L/S 16	Cole Parmer
PCR Tubes	Thermo Fisher Scientific™
Pipette Tips 10 µL – 1 mL	Biozym / Greiner Bio One / Gilson
Pipettes (disposable) 2 mL, 5 mL, 10 mL, 50 mL	Greiner Bio One
Protein Lo Bind Tubes 1.5 mL	Eppendorf
Reaction Tubes 1.5 mL, 2 mL	Greiner Bio One, Eppendorf
Reagent reservoirs, sterile	Corning
Sterile Filters, 0.45 µm, 0.2 µm	Sarstedt
Surgical Disposable Scalpels	Braun
Syringes	Braun
Zeba™ Spin desalting columns, 7K MWCO, 5ml	Invitrogen

5.1.3 Chemicals and Reagents

Products	Supplier
2-Phenoxyethanol	Roth®
Acetic acid	Roth®
Agarose	PeqLab
Ammonium persulfate (APS)	Roth®
Ampicillin	Roth®
Acrylamide/Bisacrylamide, Rotiphorese Gel 40	Roth®
Biocoll separating solution (density 1.077 g/mL)	Biochrom
Blasticidin S HCl 50 mg	Invitrogen
Bovine Gamma Globulin Standard	Pierce
Bovine serum albumin (BSA)	Roth®
Bradford Reagent	Thermo Fisher Scientific™
Brefeldin A (BFA)	Sigma
Collagen R	Serva
Coomassie Brilliant blue G-250	Roth®
Dapi Fluorochrome G	Southern Biotech
Dimethyl sulfoxide (DMSO)	Sigma
Disodium phosphate (Na ₂ HPO ₄)	Roth®
D-Luciferin	p.j.k
Smart Ladder, 200 bp - 10kb	Eurogentech
Dulbecco's Modified Eagle's Medium (DMEM)	Gibco®
ECL solution	GE Healthcare Amersham
EDTA disodium salt (Na ₂ EDTA)	Roth
Fetal calf serum (FCS)	Gibco®

Fugene® HD Transfection reagent	Promega
Glycine	Roth®
Glycine-HCl	Roth®
Heparin-Natrium 25000	Ratiopharm
HEPES 1M	Gibco®
Hydrochloric acid (HCl)	Roth®
Isopropanol	Roth®
L-Glutamine, 200 mM	Gibco®
Laemmli-Buffer (4X)	Bio-Rad
Live/Dead™ fixable Aqua dead cell stain	Invitrogen
Live/Dead™ fixable Near-IR dead cell stain	Invitrogen
Magnesium chloride (MgCl ₂)	Sigma
Pierce™ Gentle Ag/Ab Binding Buffer, pH 8.0	Thermo Fisher Scientific™
Pierce™ Gentle Ag/Ab Elution Buffer, pH 6.6	Thermo Fisher Scientific™
Powdered Milk (milk)	Roth®
Non-essential amino acids (NEAA), 100X	Gibco®
OptiMEM	Gibco®
PageRuler™ plus pre-stained protein ladder 10 – 250 kDa	Thermo Fisher Scientific™
Paraformaldehyde (PFA), 4%	ChemCruz
PEG6000	Merck
Penicillin Streptomycin, 10,000 U/mL (100X)	Gibco®
Phorbol 12-myristate 13-acetate (PMA)	Sigma
Phosphate-buffered saline (PBS) 10X	Gibco®
Polyethylenimine (PEI)	Polyscience
Potassium chloride (KCl)	Roth®
Potassium hydrogen carbonate (KHCO ₃)	Roth®

RNAasin (RNase Inhibitor), 40 U/ μ L	Promega
Roti [®] -Safe Gel Stain	Roth [®]
RPMI 1640	Gibco [®]
Sodium bicarbonate (NaHCO ₃)	Roth [®]
Sodium carbonate (Na ₂ CO ₃)	Roth [®]
Sodium dihydrogen phosphate (NaH ₂ PO ₄)	Roth [®]
Sodium hydroxide (NaOH)	Roth [®]
Sodium pyruvate, 100 mM	Gibco [®]
Sulfuric acid, (H ₂ SO ₄), 2N	Roth [®]
TEMED, N,N,N',N'-Tetramethyl ethylenediamine	Roth [®]
TMB, stabilized chromagen for ELISA	Invitrogen
Tris Base	Roth [®]
Trypan blue	Gibco [®]
Trypsin-EDTA	Gibco [®]
Tryptone	Roth [®]
Tween 20	Roth [®]
Yeast extract	Roth [®]
β -Mercaptoethanol, 50 mM	Gibco [®]

5.1.4 Solutions and Buffers

Buffer	Ingredients
Binding buffer	0.02 M sodium phosphate in Milli-Q® H ₂ O, pH 7.0
Blocking and assay buffer for Western blot	5% (w/w) milk in TBS-T buffer
Carbonate buffer (0.1M)	5.76 g Sodium bicarbonate 3.31 g Sodium carbonate in 1L H ₂ O, pH 9.6
Coomassie destain solution	10% (v/v) Acetic acid 50% (v/v) Methanol 40% (v/v) H ₂ O
ELISA blocking solution	5% BSA in PBS
ELISA wash	0.05% Tween-20 in PBS
Elution buffer	0.1 M Glycine-HCl in MilliQ H ₂ O, pH 2.7
FACS buffer	0.1% BSA in PBS
Lower buffer (SDS-PAGE)	0.5 M Tris-HCl 10% SDS (w/w) in H ₂ O, pH 6.8
Lysis buffer	25 mM HEPES 100 mM NaCl 2 mM MgCl ₂ 0.5% Triton X-100 1x protease inhibitor
Neutralization buffer	1 M Tris-HCl in MilliQ H ₂ O, pH 9.0
SDS-Running buffer (10X)	30 g Tris Base 144 g Glycine 10 g SDS in 1L H ₂ O, pH 8.3

TAE Buffer (50X)	2M Tris Base 2M Acetic acid 50 mM EDTA 50 mM in H ₂ O, pH 8.0
TBS-T buffer (10X)	24 g Tris base 88 g NaCl 0.1% Tween-20 in 1L H ₂ O, pH 7.6
Transfer buffer (10X)	30.8 g Tris base 144.1 g glycine in 1L H ₂ O
Transfer buffer working solution (1X)	100 mL Transfer buffer (10X) 200 mL Methanol 700 mL H ₂ O
Upper buffer (SDS-PAGE)	1.5 M Tris-HCl 10% SDS (w/w) in H ₂ O, pH 8.8

5.1.5 Kits

Product

Enzygnost HBeAg test

EZ-Link™ Micro Sulfo-NHS-Biotinylation Kit

Fixation/Permeabilization Solution Kit

GeneJet Gel extraction Kit

GeneJet Plasmid Miniprep Kit

High pure PCR Purification Kit

LightCycler 480 SYBR green master mix

NuceloBond® Xtra Midi

NucleoSpin Tissue DNA Kit

Supplier

Siemens Healthcare Diagnostics

Thermo Fisher Scientific™

BD Biosciences

Thermo Fisher Scientific™

Thermo Fisher Scientific™

Roche®

Roche®

Macherey-Nagel

Macherey-Nagel

5.1.6 Enzymes

Enzyme	Supplier
FastAP	Thermo Fisher Scientific™
FastDigest restriction enzymes including FastDigest Green Buffer (10X)	Thermo Fisher Scientific™
Phusion Hot Start Flex 2x Master Mix	New England Biolabs®
PNGase F	New England Biolabs®
T4 DNA Ligase including T4 Ligase buffer	Thermo Fisher Scientific™
T5 Exonuclease including NEB 4 buffer	New England Biolabs®

5.1.7 Primers

Primers were purchased from Microsynth AG, Balgach, Switzerland.

Primer name	Sequence	Application
HBVcccDNA (2760) fwd	GACTCTCTCGTCCCCTTCTC	qPCR cccDNA
HBVcccDNA (156) rev	ATGGTGAGGTGAACAATGCT	qPCR cccDNA
Prp_fwd	TGCTGGGAAGTGCCATGAG	qPCR <i>PRNP</i>
Prp_rev	CGGTGCATGTTTTACGATAGTA	qPCR <i>PRNP</i>
rcDNA_fwd	GTTGCCCGTTTGCCTCTAATTC	qPCR rcDNA
rcDNA_rev	GGAGGGATACATAGAGGTTCTTGA	qPCR rcDNA

5.1.8 Plasmids

Plasmid name	Transgene	Source
pA1k3A (plasmid bank #1255)	human IgG1 heavy chain constant, including cloning site for Ig variable region and human leader sequence	L. Wolff

pA1k3A_DLE (plasmid bank #1554)	human IgG1 heavy chain constant with mutations S239D/A330L/I332E, including cloning site for Ig variable region and human leader sequence	F. Kolbe
pA1k3A_FcAdet0 (plasmid bank #1559)	human IgG1 CH2, CH3 and hinge fused to HBV S protein luminal loop without linker	F. Kolbe
pA1k3A_FcAdet1 (plasmid bank #1560)	human IgG1 CH2, CH3 and hinge fused to HBV S protein luminal loop with 1xG ₄ S linker	F. Kolbe
pA1k3A_FcAdet3 (plasmid bank #1561)	human IgG1 CH2, CH3 and hinge fused to HBV S protein luminal loop with 3xG ₄ S linker	F. Kolbe
pA1k3A_FcAdet3N146Q (plasmid bank #1562)	human IgG1 CH2, CH3 and hinge fused to HBV S protein luminal loop, including mutations N146Q, with 3xG ₄ S linker	F. Kolbe
pA1k3A_KH1 (plasmid bank #1555)	human IgG1 heavy chain constant with mutations L234Y/L235Q/G236W/S239M/H268D/D270E/S298A/T366W, including cloning site for Ig variable region and human leader sequence	F. Kolbe
pA1k3A_KH2 (plasmid bank #1556)	human IgG1 heavy chain constant with mutations D207E/K326D/A330M/K334E/T366S/L368A/Y407V, including cloning site for Ig variable region and human leader sequence	F. Kolbe
pA1k3A_LPLIL (plasmid bank #1557)	human IgG1 heavy chain constant with mutations F243L/R292P/Y300L/V305I/P369L, including cloning site for Ig variable region and human leader sequence	F. Kolbe
pB1k1A (plasmid bank #1254)	human Ig kappa light chain constant, including cloning site for Ig kappa variable region and human leader sequence	L. Wolff
p524_moxGFP_NFAT-nLuc antisense (plasmid bank #1558)	Sense moxGFP as transfection control and antisense NFAT binding motif followed by minimal IL2 promoter and nLuc for generation of Jurkat reporter cellline	F. Kolbe

5.1.9 Cell lines, bacterial and viral strains

Cell line, bacterial strain, viral strain	Description	Supplier
HEK 293T	Human embryonic kidney cell line; transformed with fragments of adenovirus type 5 DNA	AG Protzer
HepG2-NTCP	HepG2 cells expressing NTCP, Clone K7; enabling infection of HBV	generated by D. Stadler
JKK CD16-CD3 ζ	Jurkat cells expressing human CD16-CD3 ζ	generated by P. Kolb (Institute of Virology, Universitätsklinikum Freiburg)
<i>E. coli</i> STBL3	Chemical competent <i>Escherichia coli</i> cells	Invitrogen
<i>E. coli</i> TOP10	Chemical competent <i>Escherichia coli</i> cells	Invitrogen
HBV (genotype D, <i>adw</i>)	Virus purified from stable transfected HepAD38 cell culture supernatant	AG Protzer, generated and purified by J. Wettengel

5.1.10 Media

Medium	Ingredients	
RPMI wash medium	RPMI 1640	500 mL
	Pen/Strep, 10,000 U/ml	5.5 mL
RPMI complete medium	RPMI 1640	500 mL
	Pen/Strep, 10,000 U/mL	5.5 mL
	FCS	50 mL
	L-Glutamine, 200 mM	5.5 mL
	NEAA, 100X	5.5 mL
	Sodium pyruvate, 100 mM	5.5 mL
	HEPES, 1 M	12.5 mL

DMEM complete medium	DMEM	500 mL
	Pen/Strep, 10,000 U/mL	5.5 mL
	FCS	50 mL
	L-Glutamine, 200 mM	5.5 mL
	NEAA, 100X	5.5 mL
	Sodium pyruvate, 100 mM	5.5 mL
Differentiation medium	DMEM	500 mL
	Pen/Strep, 10,000 U/mL	5.5 mL
	FCS	50 mL
	L-Glutamine, 200 mM	5.5 mL
	NEAA, 100X	5.5 mL
	Sodium pyruvate, 100 mM	5.5 mL
	DMSO	13.75 mL
Freezing medium	FCS	90% (v/v)
	DMSO	10% (v/v)
LB medium (for 1 L, pH 7.0)	Tryptone	10 g
	Yeast extract	5 g
	NaCl	10 g

5.1.11 Antigen

Antigen	Application	Supplier
HBcAg (genotype D)	ELISA	Dr. Dišlers, APP Latvijas Biomedicīnas (Rīga, Latvia)
HBsAg, (ad), serum purified	ELISA	Roche®
HBsAg, genotype A	ELISA	Biovac (South Africa)

5.1.12 Antibodies

Antibody	Dilution	Article number	Supplier
Avidin HRP	1:500	18-4100-51	eBioscience
CD11b-AF594	1:50	301340	Biolegend®
CD14-BV421	1:50	AB_2744289	BD Biosciences
CD16-BV605	1:50	302039	Biolegend®
goat anti-human IgG (H+L)	1:500	A18807	Invitrogen
goat anti-human IgG HRP	1:1000 1:10,000	A8667	Sigma
goat anti-mouse IgG HRP	1:1000 1:10,000	A21235	Sigma
HB-1 monoclonal antibody	0.5 µg/mL		Dieter Glebe
human BD Fc Block	2.5 µg/well	564219	BD Biosciences
Nabi-HB	0.1 IU/mL		Nabi Biopharmaceuticals

5.1.13 Software

Software	Supplier
FlowJo 10.4	BD Biosciences
CytExpert	Beckman Coulter
Graph Pad Prism 9	Graph Pad Software Inc.
i-control™ software	Tecan Group
Lightcycler 480 Software	Roche®
MO.Affinity Analysis	NanoTemper
MO.Control	NanoTemper
Serial Cloner	Serial Basics
Windows 7/8/10, MS Office	Windows

5.2 Methods

5.2.1 Cell culture and transfection of mammalian cells

5.2.1.1 Maintenance of cell lines

HEK283T and HepG2-NTCP cells were kept in T25, T75 or T150 tissue culture flasks (TPP®) in Dulbecco's Modified Eagle Medium (DMEM) (Gibco®) (supplemented with 10% fetal bovine serum (FCS), 50 U/ml penicillin/streptomycin, 2 mM L-glutamine, 1% sodium pyruvate and 1% non-essential amino acids (NEAA), all from Gibco®, referred to as DMEM full medium). Upon reaching a confluency of 80-100%, media was discarded and the cells were detached using trypsin. Following trypsinization, cells were resuspended in pre-warmed media, supplemented with the appropriate antibiotics and split accordingly to start at a new confluency level of about 8-10%. For HepG2-NTCP cells, cell culture flasks were collagenized using 10% collagen diluted in ddH₂O to enable a better attachment to the plate surface. Jurkat cells (JKK) were kept in Roswell Park Memorial Institute (RPMI) 1640 Medium (Gibco®) (supplemented with 10% fetal bovine serum (FCS), 50 U/ml penicillin/streptomycin, 2 mM L-glutamine, 1% sodium pyruvate and 0.1 mM β-mercaptoethanol, all from Gibco®, referred to as JKK medium) until reaching a density of about 1-2·10⁶ cells/mL. Then, they were split to start at a density of 3-5·10⁵ cells/mL by taking out the appropriate amount of cell suspension and adding fresh JKK medium.

5.2.1.2 Freezing and thawing of cells

Cells were frozen by resuspending desired cell number in 90% FCS and 10% DMSO (v/v), referred to as freezing medium. Aliquots of 500 μL were pipetted into cryo tubes and transferred into freezing devices filled with isopropanol before transferring them to -80 °C to ensure a slow freezing rate of -1 °C/minute.

To thaw cells, media was prewarmed to 37 °C and cells were resuspended in 20 mL of warm media directly after taking out of the freezer to ensure fast thawing and thereby preventing formation of crystals which would disturb the cells. Afterwards, the cell suspension was centrifuged for 10 minutes at 450 rpm at room temperature. The supernatant was discarded and the cells were resuspended in the desired amount of medium before being plated out and cultured at 37 °C and 5% CO₂.

5.2.1.3 Cell counting

To determine the cell number, either a Neubauer cell counting chamber or the NucleoCounter® NC-250™ (chemometec) was used. After harvesting, cells were resuspended in medium to obtain a single cell solution. For the counting with the Neubauer cell counting chamber, the cell suspension

was diluted 1:1 with trypan blue stain (Gibco®) and single cells were counted utilizing an optical microscope. For automated counting, 20 µL of cell suspension were mixed with 1 µL AO•DAPI Staining Reagent (chemometec) and counted using the NucleoCounter®.

5.2.1.4 Isolation of human PBMC

All centrifugation steps described here were performed at room temperature in a 5920R centrifuge (Eppendorf). For the isolation of human PBMC, fresh blood was mixed with heparin to avoid coagulation and pre-warmed RPMI wash medium (50 U/ml penicillin/streptomycin) was added in a 1:1 ratio. Then, 25 mL of this mixture were carefully layered onto 12.5 mL Bicol (density 1.077 g/mL), without mixing the two phases. These preparations were centrifuged for 25 min at 1200 xg without break. The lymphocyte rings of two falcons were pooled in a fresh 50 mL falcon tube and the volume was adjusted to 40 mL with RPMI wash medium. After centrifugation for 10 min at 700 xg, the supernatant was discarded and the pellet was resuspended in 40 mL RPMI wash medium before being centrifuged for 20 min at 80 xg with the break set to 5. Two pellets were pooled, resuspended in 40 mL RPMI wash medium and centrifuged for 5 min at 350 xg. The concentration of the PBMC suspension was adjusted to $2 \cdot 10^6$ cells/mL and the cells were either frozen at -80 °C or rested overnight at 37 °C and 5% CO₂ before being employed in further experiments.

5.2.1.5 Transfection of cells

For transfection of HEK293T cells, cells were seeded in T150 flasks (TPP®) to reach 80% confluence after two days of culture. Per T150 flask, 12.5 µg total DNA was diluted in 1200 µL OptiMEM (Gibco®) before carefully adding 37 µL FuGENE® 4K Transfection Reagent (Promega™). The FuGENE®/DNA mixture was incubated at room temperature for 10-15 minutes. After removing media from the cells, the mixture was added drop-by-drop before adding 25 mL DMEM full medium. Supernatant was collected and filtered utilizing a 0.2 µm syringe filter every second day for a week for further protein purification. Collected supernatant was replaced with fresh DMEM full media.

5.2.2 HBV infection, neutralization and quantification of viral replication

5.2.2.1 HBV infection and neutralization assay

HepG2-NTCP cells were differentiated for 3 days in collagen-coated 24-well plates (TPP®) at a density of $3 \cdot 10^5$ cells/well in DMEM full medium (supplemented with 2.5% DMSO (Sigma-Aldrich®), referred to as differentiation medium). For neutralization assays, different concentrations of antibodies or nanoshells were mixed 1:1 with HBV. This mixture was incubated at 37 °C for 3 hours. Cells were then infected with HBV alone or with the HBV-antibody/nanoshell mixture in the presence of 4% polyethylene glycol (PEG). After 18 hours, the inoculum was removed, the cells were washed twice

with PBS and 1 mL differentiation media was added to the cells. On day 4 and 8 post infection, the supernatant was collected and HBeAg levels were determined (BEP III, DiaSorin). On day 8 post infection, cells were lysed, collected and subjected to qPCR to determine intracellular cccDNA.

5.2.2.2 Quantitative PCR (qPCR) of viral cccDNA

Intracellular rcDNA and cccDNA levels were quantified by quantitative real time PCR. Cell lysates of HBV infected cells were subjected to DNA extraction using the NucleoSpin® tissue kit (Macherey-Nagel), following the manufacturers' instructions. For cccDNA analysis, extracted DNA was digested with a T5 exonuclease (New England Biolabs®) according to the manufacturers' protocol. For this, 8.5 µL of extracted DNA were mixed with 0.5 µL T5 exonuclease and 1 µL of the corresponding buffer (New England Biolabs®). After incubation at 37 °C for 30 minutes and subsequent heat inactivation at 99 °C for 5 minutes, the samples were diluted 1:4 with H₂O and subjected to qPCR. *PRNP* served as reference gene. 4 µL of T5 digested DNA were mixed with 0.5 µL forward and reverse primer (HBVcccDNA (2760) fwd, HBVcccDNA (156) rev, Prp_fwd, Prp_rev, rcDNA_fwd, rcDNA_rev 20 µM) and 5 µL LightCycler 480 SYBR Green I Master mix (Roche®). The qPCRs were performed in FrameStar® 96 Well Semi-Skirted PCR plates (4Titude) on a LightCycler 480 (Roche®). The following programs were used:

Table 1 qPCR conditions for the amplification of cccDNA.

	Temperature [°C]	Time [sec]	Ramp [°C/sec]	Acquisition mode	Cycles
Denaturation	95	600	4.4		1
Amplification	95	15	4.4		50
	60	5	2.2		
	72	45	4.4		
	88	2	4.4	single	
Melting	95	1	4.4		1
	65	15	2.2		
	95		0.11	Continuous: 5/°C	
Cooling	40	30	2.2		1

Table 2 qPCR conditions for the amplification of HBV rcDNA and *PRNP*.

	Temperature [°C]	Time [sec]	Ramp [°C/sec]	Acquisition mode	Cycles
Denaturation	95	300	4.4		1
Amplification	95	25	4.4		40
	60	10	2.2		
	72	30	4.4	single	
Melting	95	1	4.4		1
	65	60	2.2		
	95		0.11	Continuous: 5/°C	
Cooling	40	30	2.2		1

5.2.3 Molecular cloning methods

5.2.3.1 Transformation of bacteria

For the amplification of a specific plasmid, One Shot® TOP10 and STBL3™ chemically competent *E. coli* cells were used, respectively. For re-transformations, 0.5-1 µg DNA was added to 90 µL of freshly thawed bacteria and mixed gently. For transformations, 10-20 µL ligation product was used. The bacteria-DNA mixture was incubated on ice for 30 minutes (min) before being subjected to a heat shock at 42 °C for 45 seconds (sec). After incubation on ice for 2 min, 1 mL super optimal broth with catabolite repression (S.O.C. media) was added and bacteria were incubated for 1 hour at 37 °C and 250 rounds per minute (rpm). Following centrifugation in a table-top centrifuge (Eppendorf Centrifuge 5417 R; 5 min, 600xg), the pellet was resuspended in 200 µL and plated on LB-agar plates containing the respective antibiotics for selection. After incubation at 37 °C overnight, clones were picked and transferred to 3 mL LB media supplemented with the appropriate antibiotic. Working concentrations of Ampicillin (Amp) and Kanamycin (Kan) were 50 µg/mL. Suspensions were incubated overnight at 37 °C and 300 rpm before being subjected to DNA extraction using the NucleoSpin™ Plasmid Mini kit (Macherey-Nagel™) or used to inoculate 100 mL of LB media to proceed with DNA extraction using the NucleoBond™ Xtra Midi kit (Macherey-Nagel™).

5.2.3.2 Agarose gel electrophoresis and gel extraction

To either check for the correct bands after a control digest of ligated plasmids or to purify amplified vectors and insert, agarose gels were run. For this, 1% agarose (w/v) was dissolved in TAE buffer using a microwave. The liquid agarose was poured into a gel chamber and appropriate amounts of 20,000x ROTI® GelStain (Carl Roth®) were to allow for DNA detection. DNA samples were mixed with 6x agarose gel loading dye (Thermo Scientific™), loaded on the gel, and run for 45-60 minutes at 120 V. Afterwards, the VWR® Imager2 and its corresponding software were used to detect DNA bands. In case of control digests, samples showing the expected pattern were further sent to Eurofins for sequence confirmation. For DNA extraction and purification, the corresponding bands were cut out of the gel and the DNA was extracted and purified using the NucleoSpin® Gel and PCR Clean-up Mini kit (Macherey-Nagel™), following the manufacturer's instructions. The purified DNA was either used for ligation directly or stored at -20 °C.

5.2.3.3 Restriction digest

For any restriction digests, the fast restriction enzymes by Thermo Scientific™ were used. They were mixed with the respective DNA and 10x fast digest buffer for 15 min at 37 °C. When the restricted DNA was used for subsequent ligation, the vector backbone was also incubated with a FastAP thermosensitive alkaline phosphatase (Thermo Scientific™) during the digest to inhibit recirculation of the vector.

5.2.3.4 Ligation

For DNA ligation, the T4 ligase and the corresponding buffer from NEB® were used. Ligation was performed overnight at 4 °C in a total reaction volume of 50 µL with an insert:vector ratio of 3:1.

5.2.3.5 Isolation of plasmid DNA

Plasmid DNA produced by *E. coli* was isolated using the the NucleoSpin™ Plasmid Mini or the NucleoBond™ Xtra Midi kit (Macherey-Nagel™), following the manufacturer's instructions.

5.2.3.6 Polymerase chain reaction (PCR)

PCR was performed using the Phusion™ Flash High-Fidelity PCR Master Mix of Thermo Scientific™ with 20 pmol/µL of each primer and 0.2-2 µg of target DNA, depending on the source of DNA. All primers were ordered from Microsynth and are listed in 5.1.7. Annealing temperatures were applied specifically for the used primers based on T_m calculations by the T_m -calculator software of New England Biolabs® (NEB) (<https://tmcalculator.neb.com/#!/main>). Amplification was performed in an Applied Biosciences™ ProFlex™ PCR System by Thermo Fisher. PCR efficiency was verified by running an 1%

agarose gel. The amplified PCR product was purified using the High Pure PCR Purification Kit by Roche®, following the manufacturer's instructions.

5.2.4 Protein production and purity as well as functional analysis

5.2.4.1 Protein purification via affinity chromatography

Proteins of interest that were expressed and secreted by HEK293T cells were purified via affinity chromatography. A protein G column was used to purify Fc-engineered IgG antibodies as well as the Fc-“a”-determinant constructs. The column was first washed with 5 column volumes (CV) milli-Q® purified water. After that, it was equilibrated with 3 CV binding buffer. For IgG purification, a sodium phosphate buffer (0.2 M) was used, while the gentle binding buffer by Thermo Scientific™ was used for the Fc-“a”-determinant constructs. After equilibration, the collected and filtered supernatant was loaded onto the column. After washing the column with 10 CV of binding buffer again, the sample was eluted with elution buffer. For IgG purification a glycine-HCl buffer (pH 2.7) was used, whereas the gentle elution buffer by Thermo Scientific™ was used for the Fc-“a”-determinant constructs. The protein was eluted in 1 mL fractions. For the IgG purification, the protein was eluted in 75 µL of neutralization buffer (1 M Tris-HCl, pH 9) per 1 mL of elution fraction. The column was then re-equilibrated with 5 CV of binding buffer and rinsed with 10 CV of 20% ethanol. The column was stored in 20% ethanol at 4 °C.

5.2.4.2 Bradford Assay

To determine the protein concentration in different samples, a Bradford assay was performed in addition to measurements on the NanoDrop™ (Thermo Scientific™). A serial dilution of BSA or BGA with concentrations ranging from 0 mg/mL to 2 mg/mL served as standard. 10 µL of sample was pipetted into a well of a 96-well plate and 300 µL of Bradford agent was added. The plate was shaken for 30 seconds at 750 rpm before being incubated at room temperature for 10 minutes in the dark. Finally, the optical density (OD) at 595 nm was measured using the Infinite® F Plex plate reader (Tecan GmbH) and the standard was used to calculate the concentrations of the samples.

5.2.4.3 SDS-polyacrylamide gel electrophoresis and Western blot analysis

To analyze the purity and integrity of different proteins, an SDS-polyacrylamide gel electrophoresis (SDS-PAGE) was performed. The separation gel consisted of 12.5 % acrylamide, while the stacking gel consisted of 5% acrylamide. Samples were mixed with 4x Laemmli Buffer (Biorad) and boiled at 95-99 °C for 10-20 minutes, depending on the complexity of the sample. The gel electrophoresis was performed at a constant voltage of 85 V for 3 hours. The gels were subsequently stained with Brilliant Blue G 250 (Carl Roth™). For Western blot analysis, unstained gels were used. All Western blots were

performed as wet blots. For this, the SDS gel was placed onto two Whatman® papers, that were soaked in Western blot running buffer. Then, a nitrocellulose membrane, activated in methanol, was placed on top of the gel, followed by two more soaked Whatman® papers. This sandwich was placed between two sponges which were also soaked in the running buffer. Remaining air between the different layers was released and the whole setup was placed into the Western blot chamber which was equipped with cooling packs, filled up with running buffer and surrounded by ice to keep the setup cool for the whole run. For two blots, a constant current of 300 mA was applied for 1.5 hours, while for one blot only 200 mA were used. After blotting, the membrane was washed 2 times with TBS-T before blocking with 5% milk in TBS-T to avoid unspecific bindings. Afterwards, the membrane was washed 3 times for 15 minutes with TBS-T before applying the primary antibody in its specific dilution in milk TBS-T. The primary antibody was incubated overnight at 4 °C while shaking. After washing again 3 times for 15 minutes, the secondary HRP-labelled antibody, diluted in 5% TBS-T, was applied and incubated for 2-4 hours at room temperature. Subsequently, the membrane was washed with TBS-T again and ECL™ Prime Western Blotting Detection Reagent (Cytiva Amersham™) was used for detection of bands, which were evaluated using the ECL Chemocam and Chemostar software by Intas.

5.2.4.4 Biotinylation of proteins

For the biotinylation of proteins, the EZ-Link® Micro Sulfo-NHS-Biotinylation Kit (Thermo Scientific™) was used, following the manufacturer's instructions. Subsequently, the Pierce Biotin Quantitation Kit (Thermo Scientific™) was used to determine the degree of biotinylation.

5.2.4.5 HBsAg ELISA

To determine the specificity of antibodies and nanoshells conjugated to HBsAg-specific antibodies to HBsAg, an enzyme-linked immunosorbent assay (ELISA) was performed. For this, HBsAg isolated from patient serum (kindly provided by Roche®) was diluted in PBS and coated to a 96-well MicroWell™ MaxiSorp™ plate (Thermo Scientific™) at a concentration of 1 µg/mL (50 µL/well) for 30 minutes at 37 °C, shaking at 350 rpm or at 4 °C overnight. The wells were washed 5 times with 0.5% tween in PBS (PBS-T) and blocked with 5% BSA in PBS for 1 hour at room temperature, shaking at 350 rpm. Plates were washed 5 times with PBS-T again before 50 µL of samples and controls (diluted in PBS) were added and incubated at room temperature for 2 hours, shaking at 350 rpm. After another washing step, 50 µL of the detection antibody (goat-anti-human IgG-HRP (Sigma®), 1 µg/mL in PBS) was added and incubated at room temperature for 1 hour, shaking at 350 rpm. Subsequently, wells were washed again and signal was detected by adding 50 µL/well of TMB solution (Thermo Scientific™). The reaction was stopped with 50 µL/well 2 N sulfuric acid (Carl Roth®) and the OD was measured using the Infinite® F Plex plate reader (Tecan GmbH) at 450 nm with subtraction of the background at 560 nm.

5.2.4.6 *Anti-human IgG ELISA*

To determine the specificity of antibodies and nanoshells conjugated to HBsAg-specific antibodies to anti-human IgG, an ELISA was performed. For this, a goat-anti-human IgG (Invitrogen) was diluted in PBS (5 µg/mL) and coated to a 96-well MicroWell™ MaxiSorp™ plate (Thermo Scientific™) at a concentration of 1 µg/mL (50 µL/well) for 30 minutes at 37 °C, shaking at 350 rpm or at 4 °C overnight. The wells were washed 5 times with PBS-T and blocked with 5% BSA in PBS for 1 hour at room temperature, shaking at 350 rpm. Plates were washed 5 times with PBS-T again before 50 µL of samples and controls (diluted in PBS) were added and incubated at room temperature for 2 hours, shaking at 350 rpm. After another washing step, 50 µL of the detection antibody (goat-anti-human IgG-HRP (Sigma®), 1 µg/mL in PBS) was added and incubated at room temperature for 1 hour, shaking at 350 rpm. Subsequently, wells were washed again and signal was detected by adding 50 µL/well of TMB solution (Thermo Scientific™). The reaction was stopped with 50 µL/well 2 N sulfuric acid (Carl Roth®) and the OD was measured using the Infinite® F Plex plate reader (Tecan GmbH) at 450 nm with subtraction of the background at 560 nm.

5.2.4.7 *Fc-“a”-determinant ELISA*

After purification of the Fc-“a”-determinant constructs, the different purification fractions were analyzed with an ELISA to determine the elution peak. An antibody recognizing a linear epitope of the “a”-determinant (HB1, kindly provided by Dieter Glebe) was diluted in carbonate buffer (pH 9.6) and coated to a 96-well MicroWell™ MaxiSorp™ plate (Thermo Scientific™) at a concentration of 0.5 µg/mL (50 µL/well) at 4 °C overnight. After washing and blocking with 5% BSA in PBS for 1 hour the next day, the different purification fractions were added (50 µL/well) for 2 hours at room temperature, shaking at 350 rpm. After another washing step, the constructs were detected using an HRP-conjugated anti-human Fc antibody (Sigma®). TMB solution (Thermo Scientific™) was added (50 µL/well) and the reaction was stopped using 2 N sulfuric acid (50 µL/well; Carl Roth®). The OD was measured using the Infinite® F Plex plate reader (Tecan GmbH) at 450 nm with subtraction of the background at 560 nm and the elution fractions showing the highest signals were pooled and further concentrated using a spin column with a molecular weight cut off (MWCO) of 10 kDa.

To ensure the correct folding of the purified and concentrated Fc-“a”-determinant constructs, a different ELISA setup was performed. For this, the Fc-“a”-determinant constructs were diluted in coating buffer and coated to a 96-well MicroWell™ MaxiSorp™ plate (Thermo Scientific™) at different concentrations (0, 0.003, 0.01, 0.03, 0.1, 0.3, 1, 3.1, 10 µM; 50 µL/well) at 4 °C overnight. After washing and blocking with 5% BSA in PBS for 1 hour, a biotinylated antibody recognizing a conformational epitope of the “a”-determinant was added (4D06, produced in house or MoMAb,

production outsourced to InVivo) at a concentration of 10 µg/mL (for biotinylation method refer to 5.2.4.4). HRP-labelled avidin (1:500, 50 µL/well; eBioscience™) was used to detect the binding. TMB solution (Thermo Scientific™) was added (50 µL/well) and the reaction was stopped using 2 N sulfuric acid (50 µL/well; Carl Roth®). The OD was measured using the Infinite® F Plex plate reader (Tecan GmbH) at 450 nm with subtraction of the background at 560 nm.

5.2.5 Flow cytometry

For flow cytometry analyses, different antibody panels were used. In general, for the analysis around $2.5 \cdot 10^5$ cells/well were added to a V-bottom 96-well plate (Corning®) and centrifuged at 450xg for 2.5 minutes. After washing the cells twice with FACS buffer (0.1% BSA in PBS), the extracellular staining was applied to the cells with 50 µL per well. For the extracellular staining of moDC the following antibodies were used: CD11b-AF594 (1:50, Biolegend®), CD14-BV421 (1:50, BD Biosciences) and Live/Dead™ fixable Near-IR dead cell stain (1:1000, Invitrogen). The Jurkat cells were stained with CD16-BV605 (1:50, Biolegend®) and Live/Dead™ fixable Near-IR dead cell stain (1:1000, Invitrogen). The staining was incubated on the cells on ice for 30 minutes in the dark. Cells were washed thrice with FACS buffer. For the analysis of intracellular AF647-labelled HBsAg in moDC, cells were fixed using 100 µL/well Cytofix/Cytoperm™ (BD Biosciences). Following thorough washing with Perm/Wash™ (BD Biosciences) or FACS Buffer (for non-fixed samples), cells were resuspended in 250 µL corresponding buffer and subjected to flow cytometry analysis using a Cytoflex S (Beckman Coulter).

5.2.6 Affinity measurements

5.2.6.1 Labeling of proteins with red dye

To be able to determine the dissociation constants of different protein-protein interactions via microscale thermophoresis, one binding partner has to be labeled with a fluorophore. For this, the Protein Labeling Kit RED-NHS (NanoTemper) was used. Labeling, as well as determination of degree of labeling (DOL), were performed following the manufacturer's instructions.

5.2.6.2 *kD measurements of Fc-“a”-determinant constructs and MoMAb via microscale thermophoresis (MST)*

Microscale thermophoresis (MST) is a method to assess protein-protein interactions. To evaluate the *kD* of certain antibody-antigen interactions, one of the binding partners is labelled with a fluorophore (for labeling method refer to 5.2.6.1). The concentration of the labelled interaction partner is kept constant, while the concentration of the unlabeled partner is titrated. The fluorescence of the labelled protein changes due to an applied temperature change. These changes in fluorescence can then be used to calculate binding affinities and relevant values for binding events such as the *kD* or *EC*₅₀. The

MST measurements were conducted using the Monolith NT.115 (NanoTemper). Directly before MST measurements, different amounts of labelled Fc-“a”-determinant were added to a constant concentration of antibody, calculated by the MO.Control software (NanoTemper). These preparations were filled in glass capillaries, provided by NanoTemper and subsequently subjected to MST analysis. Using the MO.Affinity Analysis software (NanoTemper), MST data were used to calculate K_D values of the different Fc-“a”-determinant constructs to MoMAb.

5.2.7 ADCC assessment via NFAT reporter cell line

Jurkat cells stably expressing hCD16-CD3 ζ (kindly provided by Philipp Kolb; Institute of Virology, Universitätsklinikum Freiburg) were transiently transfected with a plasmid coding for NFAT-dependent luciferase expression, seeded into a 24-well cell culture plate (10^5 cells/well, 500 μ L/well; TPP[®]) and cultured at 37 °C and 5% CO₂. 24 hours post transfection, 4D06 (produced in house) was added to the cells at different final concentrations (0, 10, 100, 1000 nM) and cells were incubated again for 24 hours at 37 °C and 5% CO₂. Then, cells were lysed using a HEPES lysis buffer (25 mM HEPES, 100 mM NaCl, 2 mM MgCl₂, 0.5% Triton X-100, 1x protease inhibitor). 10 μ L of lysate was transferred to a well of a white, flat bottom 96-well plate (XXX) and the Infinite[®] F Plex plate reader (Tecan GmbH) was utilized to add luciferin (100 μ L/well, 200 μ M; p.j.k.) directly before measuring the luminescence.

6 List of figures

Figure 1. Structural properties of HBV.....	11
Figure 2. Proposed structure of HBsAg.....	12
Figure 3. Genomic organization of HBV.....	13
Figure 4. Replication cycle of HBV.	15
Figure 5 Structural properties of an IgG1 molecule.....	26
Figure 6 Schematic representation of Fc-“a”-determinant constructs.	32
Figure 7 Purification of Fc-“a”-determinant 3xGS (N146Q) via protein G residues using low pH elution conditions.....	35
Figure 8 Fc-“a”-determinant 3xGS (N146Q) loses integrity at low pH values.	36
Figure 9 Fc-“a”-determinant constructs run different to expected size in SDS-PAGE.....	37
Figure 10 High salt elution results in pure and intact Fc-“a”-determinant proteins.	39
Figure 11 All Fc-“a”-determinant-antibody complexes demonstrate K_D values in the low nanomolar range.	41
Figure 12 Amino-acid sequences of Fc-engineered antibodies.	44
Figure 13 Schematic representation of Fc-engineered antibodies.....	45
Figure 14 Fc-engineered antibodies are successfully purified via affinity chromatography.	47
Figure 15 Fc-engineered antibodies show lower antigen-specificity and neutralization capacity than the wild type.	49
Figure 16 Reporter cell line can be used to assess ADCC induction.	51
Figure 17 Antibodies conjugated to DNA nanoshells recognize their targets and enable engulfment of HBcAg particles.	53
Figure 18 DNA nanoshells conjugated with anti-HBsAg antibodies efficiently neutralize HBV infection <i>in vitro</i>	54
Figure 19 Nanoshells efficiently inhibit HBV infection when present at timepoint of infection.....	55
Figure 20 Schematic representation of uptake assay.....	57
Figure 21 DNA nanoshells seem to be taken up by moDC	57

7 List of tables

Table 1 qPCR conditions for the amplification of cccDNA.	89
Table 2 qPCR conditions for the amplification of HBV rcDNA and <i>PRNP</i>	90

8 Bibliography

- ABUCHOWSKI, A., VAN ES, T., PALCZUK, N.C., AND DAVIS, F.F. 1977. Alteration of immunological properties of bovine serum albumin by covalent attachment of polyethylene glycol. *The Journal of biological chemistry* 252, 11, 3578–3581. <https://pubmed.ncbi.nlm.nih.gov/405385/>.
- ARANKALLE, V.A., GANDHE, S.S., BORKAKOTY, B.J., WALIMBE, A.M., BISWAS, D., AND MAHANTA, J. 2010. A novel HBV recombinant (genotype I) similar to Vietnam/Laos in a primitive tribe in eastern India. *Journal of viral hepatitis* 17, 7, 501–510.
- ARAUZ-RUIZ, P., NORDER, H., ROBERTSON, B.H., AND MAGNIUS, L.O. 2002. Genotype H: a new Amerindian genotype of hepatitis B virus revealed in Central America. *The Journal of general virology* 83, Pt 8, 2059–2073. <https://pubmed.ncbi.nlm.nih.gov/12124470/>.
- BACHMANN, M.F., KALINKE, U., ALTHAGE, A., FREER, G., BURKHART, C., ROOST, H., AGUET, M., HENGARTNER, H., AND ZINKERNAGEL, R.M. 1997. The role of antibody concentration and avidity in antiviral protection. *Science (New York, N.Y.)* 276, 5321, 2024–2027. <https://pubmed.ncbi.nlm.nih.gov/9197261/>.
- BACKES, S., JÄGER, C., DEMBEK, C.J., KOSINSKA, A.D., BAUER, T., STEPHAN, A.-S., DIŠLERS, A., MUTWIRI, G., BUSCH, D.H., BABIUK, L.A., GASTEIGER, G., AND PROTZER, U. 2016. Protein-prime/modified vaccinia virus Ankara vector-boost vaccination overcomes tolerance in high-antigenemic HBV-transgenic mice. *Vaccine* 34, 7, 923–932. <https://pubmed.ncbi.nlm.nih.gov/26776470/>.
- BANCROFT, W.H., MUNDON, F.K., AND RUSSELL, P.K. 1972. Detection of additional antigenic determinants of hepatitis B antigen. *Journal of immunology (Baltimore, Md. : 1950)* 109, 4, 842–848. <https://pubmed.ncbi.nlm.nih.gov/4116360/>.
- BAZINET, M., ANDERSON, M., PÂNTEA, V., PLACINTA, G., MOSCALU, I., CEBOTARESCU, V., COJUHARI, L., JIMBEI, P., IAROVIOI, L., SMESNOI, V., MUSTEATA, T., JUCOV, A., DITTMER, U., GERSCH, J., HOLZMAYER, V., KUHNS, M., CLOHERTY, G., AND VAILLANT, A. 2022. HBsAg isoform dynamics during NAP-based therapy of HBeAg-negative chronic HBV and HBV/HDV infection. *Hepatology Communications* 6, 8, 1870–1880. <https://aasldpubs.onlinelibrary.wiley.com/doi/10.1002/hep4.1951>.
- BAZINET, M., PÂNTEA, V., PLACINTA, G., MOSCALU, I., CEBOTARESCU, V., COJUHARI, L., JIMBEI, P., IAROVIOI, L., SMESNOI, V., MUSTEATA, T., JUCOV, A., DITTMER, U., KRAWCZYK, A., AND VAILLANT, A. 2020. Safety and Efficacy of 48 Weeks REP 2139 or REP 2165, Tenofovir Disoproxil, and Pegylated Interferon Alfa-2a in Patients With Chronic HBV Infection Naïve to Nucleos(t)ide Therapy. *Gastroenterology* 158, 8, 2180–2194. [https://www.gastrojournal.org/article/S0016-5085\(20\)30320-6/fulltext](https://www.gastrojournal.org/article/S0016-5085(20)30320-6/fulltext).
- BENGSCHE, B., MARTIN, B., AND THIMME, R. 2014. Restoration of HBV-specific CD8+ T cell function by PD-1 blockade in inactive carrier patients is linked to T cell differentiation. *Journal of Hepatology* 61, 6, 1212–1219. <https://pubmed.ncbi.nlm.nih.gov/25016223/>.
- BENSON, E., MOHAMMED, A., GARDELL, J., MASICH, S., CZEIZLER, E., ORPONEN, P., AND HÖGBERG, B. 2015. DNA rendering of polyhedral meshes at the nanoscale. *Nature* 523, 7561, 441–444. <https://www.nature.com/articles/nature14586>.
- BERGMAN, L.W., AND KUEHL, W.M. 1979. Formation of an intrachain disulfide bond on nascent immunoglobulin light chains. *The Journal of biological chemistry* 254, 18, 8869–8876. <https://pubmed.ncbi.nlm.nih.gov/113402/>.
- BERTOLETTI, A., AND GEHRING, A.J. 2006. The immune response during hepatitis B virus infection. *The Journal of general virology* 87, Pt 6, 1439–1449. <https://pubmed.ncbi.nlm.nih.gov/16690908/>.
- BERTOLETTI, A., AND LE BERT, N. 2018. Immunotherapy for Chronic Hepatitis B Virus Infection. *Gut and liver* 12, 5, 497–507. <https://pubmed.ncbi.nlm.nih.gov/29316747/>.

- BIRCH, J., AXFORD, D., FOADI, J., MEYER, A., ECKHARDT, A., THIELMANN, Y., AND MORAES, I. 2018. The fine art of integral membrane protein crystallisation. *Methods* 147, 150–162. <https://www.sciencedirect.com/science/article/pii/S1046202317303766>.
- BLUMBERG, B.S., ALTER, H.J., AND VISNICH, S. 1965. A "new" antigen in leukemia sera. *JAMA* 191, 541–546.
- BORTOLOTTI, F., REALDI, G., DIODATI, G., AND FATTOVICH, G. 1978. Antibody dependent cellular cytotoxicity (ADCC) in acute hepatitis B and in chronic active hepatitis. *Clinical and Experimental Immunology* 33, 2, 211–216. <https://www.ncbi.nlm.nih.gov/pmc/articles/PMC1537570/>.
- BRUNETTO, M.R., AND BONINO, F. 2014. Interferon therapy of chronic hepatitis B. *Intervirology* 57, 3-4, 163–170. <https://pubmed.ncbi.nlm.nih.gov/25034484/>.
- BRUSS, V. 2007. Hepatitis B virus morphogenesis. *World journal of gastroenterology* 13, 1, 65–73.
- BUCCI, M. 2020. First recombinant DNA vaccine for HBV. <https://www.nature.com/articles/d42859-020-00016-5>.
- BUNSE, T., KOSINSKA, A.D., MICHLER, T., AND PROTZER, U. 2022. PD-L1 Silencing in Liver Using siRNAs Enhances Efficacy of Therapeutic Vaccination for Chronic Hepatitis B. *Biomolecules* 12, 3. <https://pubmed.ncbi.nlm.nih.gov/35327662/>.
- BURTON, A.R., PALLETT, L.J., MCCOY, L.E., SUVEIZDYTE, K., AMIN, O.E., SWADLING, L., ALBERTS, E., DAVIDSON, B.R., KENNEDY, P.T., GILL, U.S., MAURI, C., BLAIR, P.A., PELLETIER, N., AND MAINI, M.K. 2018. Circulating and intrahepatic antiviral B cells are defective in hepatitis B. *The Journal of clinical investigation* 128, 10, 4588–4603. <https://pubmed.ncbi.nlm.nih.gov/30091725/>.
- BUSCHOW, S.I., AND JANSEN, DIAHANN T. S. L. 2021. CD4+ T Cells in Chronic Hepatitis B and T Cell-Directed Immunotherapy. *Cells* 10, 5, 1114. <https://www.ncbi.nlm.nih.gov/pmc/articles/PMC8148211/>.
- CALICETI, P. 2004. Pharmacokinetics of pegylated interferons: what is misleading? *Digestive and liver disease : official journal of the Italian Society of Gastroenterology and the Italian Association for the Study of the Liver* 36 Suppl 3, S334-9. <https://pubmed.ncbi.nlm.nih.gov/15645663/>.
- CAO, J., ZHANG, J., LU, Y., LUO, S., ZHANG, J., AND ZHU, P. 2019. Cryo-EM structure of native spherical subviral particles isolated from HBV carriers. *Virus research* 259, 90–96. <https://www.sciencedirect.com/science/article/pii/S0168170218303721>.
- CHAKRABORTY, A., KO, C., HENNING, C., LUCKO, A., HARRIS, J.M., CHEN, F., ZHUANG, X., WETTENGEL, J.M., ROESSLER, S., PROTZER, U., AND MCKEATING, J.A. 2020. Synchronised infection identifies early rate-limiting steps in the hepatitis B virus life cycle. *Cellular Microbiology* 22, 12, e13250. <https://onlinelibrary.wiley.com/doi/full/10.1111/cmi.13250>.
- CHEN, M.T., BILLAUD, J.-N., SÄLLBERG, M., GUIDOTTI, L.G., CHISARI, F.V., JONES, J., HUGHES, J., AND MILICH, D.R. 2004. A function of the hepatitis B virus precore protein is to regulate the immune response to the core antigen. *Proceedings of the National Academy of Sciences of the United States of America* 101, 41, 14913–14918. <https://www.pnas.org/doi/10.1073/pnas.0406282101>.
- CHEN, X., ZARO, J.L., AND SHEN, W.-C. 2013. Fusion protein linkers: property, design and functionality. *Advanced drug delivery reviews* 65, 10, 1357–1369. <https://www.ncbi.nlm.nih.gov/pmc/articles/PMC3726540/>.
- CHIEN, R.-N., AND LIAW, Y.-F. 2022. Current Trend in Antiviral Therapy for Chronic Hepatitis B. *Viruses* 14, 2. <https://pubmed.ncbi.nlm.nih.gov/35216027/>.
- CHIOU, H.L., LEE, T.S., KUO, J., MAU, Y.C., AND HO, M.S. 1997. Altered antigenicity of 'a' determinant variants of hepatitis B virus. *The Journal of general virology* 78 (Pt 10), 2639–2645. <https://pubmed.ncbi.nlm.nih.gov/9349486/>.

- CHISARI, F.V., ISOGAWA, M., AND WIELAND, S.F. 2010. Pathogenesis of hepatitis B virus infection. *Pathologie-biologie* 58, 4, 258–266. <https://www.ncbi.nlm.nih.gov/pmc/articles/PMC2888709/>.
- CHIU, W.-C., SU, Y.-P., SU, K.-P., AND CHEN, P.-C. 2017. Recurrence of depressive disorders after interferon-induced depression. *Transl Psychiatry* 7, 2, e1026. <https://www.nature.com/articles/tp2016274>.
- CREMER, J., HOFSTRAAT, S.H.I., VAN HEININGEN, F., VELDHUIJZEN, I.K., VAN BENTHEM, B.H.B., AND BENSCHOP, K.S.M. 2018. Genetic variation of hepatitis B surface antigen among acute and chronic hepatitis B virus infections in The Netherlands. *Journal of medical virology* 90, 10, 1576–1585. <https://pubmed.ncbi.nlm.nih.gov/29797607/>.
- DANE, D.S., CAMERON, C.H., AND BRIGGS, M. 1970. Virus-like particles in serum of patients with Australia-antigen-associated hepatitis. *Lancet (London, England)* 1, 7649, 695–698. <https://pubmed.ncbi.nlm.nih.gov/4190997/>.
- DEBACKER, A.J., VOUTILA, J., CATLEY, M., BLAKEY, D., AND HABIB, N. 2020. Delivery of Oligonucleotides to the Liver with GalNac: From Research to Registered Therapeutic Drug. *Molecular therapy : the journal of the American Society of Gene Therapy* 28, 8, 1759–1771. <https://www.sciencedirect.com/science/article/pii/S1525001620303051>.
- DEJEAN, A., SONIGO, P., WAIN-HOBSON, S., AND TIOLLAIS, P. 1984. Specific hepatitis B virus integration in hepatocellular carcinoma DNA through a viral 11-base-pair direct repeat. *Proceedings of the National Academy of Sciences of the United States of America* 81, 17, 5350–5354.
- DESSAU, M.A., AND MODIS, Y. 2011. Protein crystallization for X-ray crystallography. *Journal of Visualized Experiments : JoVE*, 47. <https://www.ncbi.nlm.nih.gov/pmc/articles/PMC3182643/>.
- DEY, S., FAN, C., GOTHELF, K.V., LI, J., LIN, C., LIU, L., LIU, N., NIJENHUIS, M.A.D., SACCÀ, B., SIMMEL, F.C., YAN, H., AND ZHAN, P. 2021. DNA origami. *Nat Rev Methods Primers* 1, 1, 1–24. <https://www.nature.com/articles/s43586-020-00009-8>.
- DHILLON, S., KAKER, A., DOSANJH, A., JAPRA, D., AND VANTHIEL, D.H. 2010. Irreversible pulmonary hypertension associated with the use of interferon alpha for chronic hepatitis C. *Digestive Diseases and Sciences* 55, 6, 1785–1790. <https://www.ncbi.nlm.nih.gov/pmc/articles/PMC2882564/>.
- DONG, Y., LI, X., ZHANG, L., ZHU, Q., CHEN, C., BAO, J., AND CHEN, Y. 2019. CD4+ T cell exhaustion revealed by high PD-1 and LAG-3 expression and the loss of helper T cell function in chronic hepatitis B. *BMC Immunology* 20, 1, 27. <https://www.ncbi.nlm.nih.gov/pmc/articles/PMC6686459/>.
- DRESCHER, D.G., RAMAKRISHNAN, N.A., AND DRESCHER, M.J. 2009. Surface plasmon resonance (SPR) analysis of binding interactions of proteins in inner-ear sensory epithelia. *Methods in molecular biology (Clifton, N.J.)* 493, 323–343.
- DU, H., YI, Z., WANG, L., LI, Z., NIU, B., AND REN, G. 2020. The co-expression characteristics of LAG3 and PD-1 on the T cells of patients with breast cancer reveal a new therapeutic strategy. *International Immunopharmacology* 78, 106113. <https://www.sciencedirect.com/science/article/pii/S1567576919323100>.
- EBLE, B.E., LINGAPPA, V.R., AND GANEM, D. 1986. Hepatitis B surface antigen: an unusual secreted protein initially synthesized as a transmembrane polypeptide. *Molecular and cellular biology* 6, 5, 1454–1463. <https://pubmed.ncbi.nlm.nih.gov/3023891/>.
- EBLE, B.E., MACRAE, D.R., LINGAPPA, V.R., AND GANEM, D. 1987. Multiple topogenic sequences determine the transmembrane orientation of the hepatitis B surface antigen. *Molecular and cellular biology* 7, 10, 3591–3601. <https://pubmed.ncbi.nlm.nih.gov/3683395/>.

- EMBL-EBI. 2022. *EMBOSS Pepstats < Sequence Statistics < EMBL-EBI*.
https://www.ebi.ac.uk/Tools/seqstats/emboss_pepstats/. Accessed 11 January 2023.
- ENCYCLOPEDIA BRITANNICA. 2022. *immune system - Classes of immunoglobulins*.
<https://www.britannica.com/science/immune-system/Classes-of-immunoglobulins>. Accessed 7 December 2022.
- EREN, R., ILAN, E., NUSSBAUM, O., LUBIN, I., TERKIELTAUB, D., ARAZI, Y., BEN-MOSHE, O., KITCHINZKY, A., BERR, S., GOPHER, J., ZAUBERMAN, A., GALUN, E., SHOVAL, D., DAUDI, N., EID, A., JURIM, O., MAGNIUS, L.O., HAMMAS, B., REISNER, Y., AND DAGAN, S. 2000. Preclinical evaluation of two human anti-hepatitis B virus (HBV) monoclonal antibodies in the HBV-trimera mouse model and in HBV chronic carrier chimpanzees. *Hepatology (Baltimore, Md.)* 32, 3, 588–596.
<https://pubmed.ncbi.nlm.nih.gov/10960454/>.
- ETIENNE, S., VOSBECK, J., BERNISMEIER, C., AND OSTHOFF, M. 2022. Prevention of Hepatitis B Reactivation in Patients Receiving Immunosuppressive Therapy: a Case Series and Appraisal of Society Guidelines. *J GEN INTERN MED*, 1–12. <https://link.springer.com/article/10.1007/s11606-022-07806-9>.
- EUROPEAN MEDICINES AGENCY. 2023. *Development, production, characterisation and specifications for monoclonal antibodies and related products - Scientific guideline | European Medicines Agency*.
<https://www.ema.europa.eu/en/development-production-characterisation-specifications-monoclonal-antibodies-related-products>. Accessed 7 March 2023.
- FDA. 04.24.2019. Recombivax HB. *FDA (04.24.2019)*.
- FDA. 2019. ENGERIX-B. *FDA (Mar.)*.
- FEIGE, M.J., HENDERSHOT, L.M., AND BUCHNER, J. 2010. How antibodies fold. *Trends in biochemical sciences* 35, 4, 189–198. <https://pubmed.ncbi.nlm.nih.gov/20022755/>.
- FINK, A.L., CALCIANO, L.J., GOTO, Y., KUROTSU, T., AND PALLEROS, D.R. 1994. Classification of acid denaturation of proteins: intermediates and unfolded states. *Biochemistry* 33, 41, 12504–12511.
<https://pubmed.ncbi.nlm.nih.gov/7918473/>.
- FISICARO, P., BARILI, V., ROSSI, M., MONTALI, I., VECCHI, A., ACERBI, G., LACCABUE, D., ZECCA, A., PENNA, A., MISSALE, G., FERRARI, C., AND BONI, C. 2020. Pathogenetic Mechanisms of T Cell Dysfunction in Chronic HBV Infection and Related Therapeutic Approaches. *Front. Immunol.* 11, 849.
<https://www.frontiersin.org/articles/10.3389/fimmu.2020.00849/full>.
- FOOD AND DRUG ADMINISTRATION. 1987. *Summary for basis of approval*. <https://wayback.archive-it.org/7993/20170723025131/https://www.fda.gov/downloads/BiologicsBloodVaccines/Vaccines/ApprovedProducts/UCM244544.pdf>.
- FOOD AND DRUG ADMINISTRATION. 1988. *Summary for basis of approval*. <https://wayback.archive-it.org/7993/20170404184231/https://www.fda.gov/downloads/BiologicsBloodVaccines/Vaccines/ApprovedProducts/UCM110155.pdf>.
- FOOD AND DRUG ADMINISTRATION. 2017. *BLA Clinical Review Memorandum*.
<https://www.fda.gov/media/109802/download>.
- FORNER, A., LLOVET, J.M., AND BRUIX, J. 2012. Hepatocellular carcinoma. *Lancet (London, England)* 379, 9822, 1245–1255. <https://pubmed.ncbi.nlm.nih.gov/22353262/>.
- FUNG, J., LAI, C.-L., SETO, W.-K., AND YUEN, M.-F. 2011. Nucleoside/nucleotide analogues in the treatment of chronic hepatitis B. *The Journal of antimicrobial chemotherapy* 66, 12, 2715–2725.
- GABBUTI, A., ROMANÒ, L., BLANC, P., MEACCI, F., AMENDOLA, A., MELE, A., MAZZOTTA, F., AND ZANETTI, A.R. 2007. Long-term immunogenicity of hepatitis B vaccination in a cohort of Italian healthy adolescents. *Vaccine* 25, 16, 3129–3132. <https://pubmed.ncbi.nlm.nih.gov/17291637/>.

- GAFNI, R.I., HAZRA, R., REYNOLDS, J.C., MALDARELLI, F., TULLIO, A.N., DECARLO, E., WORRELL, C.J., FLAHERTY, J.F., YALE, K., KEARNEY, B.P., AND ZEICHNER, S.L. 2006. Tenofovir disoproxil fumarate and an optimized background regimen of antiretroviral agents as salvage therapy: impact on bone mineral density in HIV-infected children. *Pediatrics* 118, 3, e711-8. <https://pubmed.ncbi.nlm.nih.gov/16923923/>.
- GALON, J., ROBERTSON, M.W., GALINHA, A., MAZIÈRES, N., SPAGNOLI, R., FRIDMAN, W.H., AND SAUTÈS, C. 1997. Affinity of the interaction between Fc gamma receptor type III (Fc gammaRIII) and monomeric human IgG subclasses. Role of Fc gammaRIII glycosylation. *European journal of immunology* 27, 8, 1928–1932. <https://pubmed.ncbi.nlm.nih.gov/9295028/>.
- GANEM, D., AND PRINCE, A.M. 2004. Hepatitis B virus infection--natural history and clinical consequences. *The New England journal of medicine* 350, 11, 1118–1129. <https://pubmed.ncbi.nlm.nih.gov/15014185/>.
- GAO, Y., ZHANG, T.-Y., YUAN, Q., AND XIA, N.-S. 2017. Antibody-mediated immunotherapy against chronic hepatitis B virus infection. *Human Vaccines & Immunotherapeutics* 13, 8, 1768–1773.
- GEHRING, A.J., AND PROTZER, U. 2019. Targeting Innate and Adaptive Immune Responses to Cure Chronic HBV Infection. *Gastroenterology* 156, 2, 325–337. <https://pubmed.ncbi.nlm.nih.gov/30367834/>.
- GERLING, T., WAGENBAUER, K.F., NEUNER, A.M., AND DIETZ, H. 2015. Dynamic DNA devices and assemblies formed by shape-complementary, non-base pairing 3D components. *Science (New York, N.Y.)* 347, 6229, 1446–1452. <https://pubmed.ncbi.nlm.nih.gov/25814577/>.
- GILBERT, R.J.C., BEALES, L., BLOND, D., SIMON, M.N., LIN, B.Y., CHISARI, F.V., STUART, D.I., AND ROWLANDS, D.J. 2005. Hepatitis B small surface antigen particles are octahedral. *Proceedings of the National Academy of Sciences of the United States of America* 102, 41, 14783–14788. <https://www.ncbi.nlm.nih.gov/pmc/articles/PMC1253561/>.
- GORSHTAIN, G. 2022. Structure and Function of Antibodies. *Rapid Novor* (Aug.).
- GOWANS, J.L., AND KNIGHT, E.J. 1964. The route of re-circulation of lymphocytes in the rat. *Proc. R. Soc. Lond. B.* 159, 975, 257–282. <https://pubmed.ncbi.nlm.nih.gov/14114163/>.
- GRAND, R.J. 2022. A link between severe hepatitis in children and adenovirus 41 and adeno-associated virus 2 infections. *The Journal of general virology* 103, 11. <https://pubmed.ncbi.nlm.nih.gov/36367762/>.
- GRIFFIN, L., AND LAWSON, A. 2011. Antibody fragments as tools in crystallography. *Clinical and Experimental Immunology* 165, 3, 285–291. <https://www.ncbi.nlm.nih.gov/pmc/articles/PMC3170977/>.
- GUY, C.S., VIGNALI, K.M., TEMIROV, J., BETTINI, M.L., OVERACRE, A.E., SMELTZER, M., ZHANG, H., HUPPA, J.B., TSAI, Y.-H., LOBRY, C., XIE, J., DEMPSEY, P.J., CRAWFORD, H.C., AIFANTIS, I., DAVIS, M.M., AND VIGNALI, D.A.A. 2013. Distinct TCR signaling pathways drive proliferation and cytokine production in T cells. *Nat Immunol* 14, 3, 262–270. <https://www.nature.com/articles/ni.2538>.
- HAWKES, R.A., AND LAFFERTY, K.J. 1967. The enhancement of virus infectivity by antibody. *Virology* 33, 2, 250–261. <https://www.sciencedirect.com/science/article/pii/0042682267901444>.
- HIGEL, F., SEIDL, A., SÖRGEL, F., AND FRIESS, W. 2016. N-glycosylation heterogeneity and the influence on structure, function and pharmacokinetics of monoclonal antibodies and Fc fusion proteins. *European journal of pharmaceuticals and biopharmaceutics : official journal of Arbeitsgemeinschaft für Pharmazeutische Verfahrenstechnik e.V* 100, 94–100. <https://www.sciencedirect.com/science/article/pii/S0939641116000163>.
- HOHDATSU, T., TOKUNAGA, J., AND KOYAMA, H. 1994. The role of IgG subclass of mouse monoclonal antibodies in antibody-dependent enhancement of feline infectious peritonitis virus infection of

- feline macrophages. *Archives of virology* 139, 3-4, 273–285.
<https://pubmed.ncbi.nlm.nih.gov/7832635/>.
- HU, Z., ZHANG, Z., DOO, E., COUX, O., GOLDBERG, A.L., AND LIANG, T.J. 1999. Hepatitis B virus X protein is both a substrate and a potential inhibitor of the proteasome complex. *Journal of virology* 73, 9, 7231–7240. <https://pubmed.ncbi.nlm.nih.gov/10438810/>.
- ILAN, Y., NAGLER, A., ADLER, R., NAPARSTEK, E., OR, R., SLAVIN, S., BRAUTBAR, C., AND SHOUVAL, D. 1993. Adoptive transfer of immunity to hepatitis B virus after T cell-depleted allogeneic bone marrow transplantation. *Hepatology (Baltimore, Md.)* 18, 2, 246–252.
<https://pubmed.ncbi.nlm.nih.gov/8340054/>.
- ILAN, Y., NAGLER, A., ZEIRA, E., ADLER, R., SLAVIN, S., AND SHOUVAL, D. 2000. Maintenance of immune memory to the hepatitis B envelope protein following adoptive transfer of immunity in bone marrow transplant recipients. *Bone marrow transplantation* 26, 6, 633–638.
<https://www.nature.com/articles/1702571>.
- ISOGAWA, M., ROBEK, M.D., FURUICHI, Y., AND CHISARI, F.V. 2005. Toll-like receptor signaling inhibits hepatitis B virus replication in vivo. *Journal of virology* 79, 11, 7269–7272.
- JANSSEN, L., SOBOTT, F., DEYN, P.P. DE, AND VAN DAM, D. 2015. Signal loss due to oligomerization in ELISA analysis of amyloid-beta can be recovered by a novel sample pre-treatment method. *MethodsX* 2, 112–123. <https://www.sciencedirect.com/science/article/pii/S221501611500014X>.
- JANSSEN RESEARCH & DEVELOPMENT, LLC. 2022. *A Randomized, Double-blind, Placebo-controlled Study to Evaluate the Pharmacokinetics, Pharmacodynamics, and Safety of Single Doses of Cetrelimab (JNJ 63723283), an Anti-PD-1 Monoclonal Antibody, in Virologically Suppressed Participants With Chronic Hepatitis B Virus Infection. NCT05242445, CR109158.*
<https://clinicaltrials.gov/ct2/show/NCT05242445>. Accessed 12 January 2023.
- JUN, H., SHEPHERD, T.R., ZHANG, K., BRICKER, W.P., LI, S., CHIU, W., AND BATHE, M. 2019. Automated Sequence Design of 3D Polyhedral Wireframe DNA Origami with Honeycomb Edges. *ACS nano* 13, 2, 2083–2093.
- JUSZCZYK, J. 2000. Clinical course and consequences of hepatitis B infection. *Vaccine* 18, S23-S25.
- KANG, X.-Z., GUO, X.-R., CHEN, B.-B., ZHANG, T.-Y., YUAN, Q., CHEN, P.-J., ZHANG, J., AND XIA, N.-S. 2018. The unique antibody suppresses HBV viremia and reduces hepatocarcinogenesis in HBV-transgenic mice. *Human Vaccines & Immunotherapeutics* 14, 7, 1779–1781.
- KE, Y., BELLOT, G., VOIGT, N.V., FRADKOV, E., AND SHIH, W.M. 2012. Two design strategies for enhancement of multilayer-DNA-origami folding: underwinding for specific intercalator rescue and staple-break positioning. *Chem. Sci.* 3, 8, 2587–2597.
<https://pubs.rsc.org/en/content/articlelanding/2012/sc/c2sc20446k>.
- KERMANI, A.A. 2021. A guide to membrane protein X-ray crystallography. *The FEBS journal* 288, 20, 5788–5804.
- KHAKOO, A.Y., HALUSHKA, M.K., RAME, J.E., RODRIGUEZ, E.R., KASPER, E.K., AND JUDGE, D.P. 2005. Reversible cardiomyopathy caused by administration of interferon alpha. *Nature clinical practice. Cardiovascular medicine* 2, 1, 53–57. <https://www.nature.com/articles/ncpcardio0069>.
- KLEIN, C., SUSTMANN, C., THOMAS, M., STUBENRAUCH, K., CROASDALE, R., SCHANZER, J., BRINKMANN, U., KETTENBERGER, H., REGULA, J.T., AND SCHAEFER, W. 2012. Progress in overcoming the chain association issue in bispecific heterodimeric IgG antibodies. *mAbs* 4, 6, 653–663.
<https://pubmed.ncbi.nlm.nih.gov/22925968/#>.
- KLOPP, A., SCHREIBER, S., KOSINSKA, A.D., PULÉ, M., PROTZER, U., AND WISSKIRCHEN, K. 2021. Depletion of T cells via Inducible Caspase 9 Increases Safety of Adoptive T-Cell Therapy Against Chronic Hepatitis

- B. *Frontiers in immunology* 12, 734246.
<https://www.ncbi.nlm.nih.gov/pmc/articles/PMC8527178/>.
- KO, C., MICHLER, T., AND PROTZER, U. 2017. Novel viral and host targets to cure hepatitis B. *Current opinion in virology* 24, 38–45.
- KOMLA-SOUKHA, I., AND SUREAU, C. 2006. A tryptophan-rich motif in the carboxyl terminus of the small envelope protein of hepatitis B virus is central to the assembly of hepatitis delta virus particles. *Journal of virology* 80, 10, 4648–4655. <https://www.ncbi.nlm.nih.gov/pmc/articles/PMC1472050/>.
- KOSINSKA, A.D., FESTAG, J., MÜCK-HÄUSL, M., FESTAG, M.M., ASEN, T., AND PROTZER, U. 2021. Immunogenicity and Antiviral Response of Therapeutic Hepatitis B Vaccination in a Mouse Model of HBeAg-Negative, Persistent HBV Infection. *Vaccines* 9, 8.
<https://pubmed.ncbi.nlm.nih.gov/34451966/>.
- KOSINSKA, A.D., MOEED, A., KALLIN, N., FESTAG, J., SU, J., STEIGER, K., MICHEL, M.-L., PROTZER, U., AND KNOLLE, P.A. 2019. Synergy of therapeutic heterologous prime-boost hepatitis B vaccination with CpG-application to improve immune control of persistent HBV infection. *Sci Rep* 9, 1.
<https://pubmed.ncbi.nlm.nih.gov/31346211/>.
- KOYAMA, S., ISHII, K.J., COBAN, C., AND AKIRA, S. 2008. Innate immune response to viral infection. *Cytokine* 43, 3, 336–341. <https://www.sciencedirect.com/science/article/pii/S1043466608002214>.
- KRAMVIS, A., AND KEW, M.C. 1999. The core promoter of hepatitis B virus. *Journal of viral hepatitis* 6, 6, 415–427. <https://pubmed.ncbi.nlm.nih.gov/10607259/>.
- KREBS, K., BÖTTINGER, N., HUANG, L.-R., CHMIELEWSKI, M., ARZBERGER, S., GASTEIGER, G., JÄGER, C., SCHMITT, E., BOHNE, F., AICHLER, M., UCKERT, W., ABKEN, H., HEIKENWALDER, M., KNOLLE, P., AND PROTZER, U. 2013. T cells expressing a chimeric antigen receptor that binds hepatitis B virus envelope proteins control virus replication in mice. *Gastroenterology* 145, 2, 456–465.
<https://www.sciencedirect.com/science/article/pii/S0016508513006847>.
- KRUGMAN, S., OVERBY, L.R., MUSHAHWAR, I.K., LING, C.M., FRÖSNER, G.G., AND DEINHARDT, F. 1979. Viral hepatitis, type B. Studies on natural history and prevention re-examined. *The New England journal of medicine* 300, 3, 101–106. <https://pubmed.ncbi.nlm.nih.gov/758598/>.
- LADA, O., BENHAMOU, Y., POYNARD, T., AND THIBAUT, V. 2006. Coexistence of hepatitis B surface antigen (HBs Ag) and anti-HBs antibodies in chronic hepatitis B virus carriers: influence of "a" determinant variants. *Journal of virology* 80, 6, 2968–2975. <https://pubmed.ncbi.nlm.nih.gov/16501106/>.
- LATYPOV, R.F., HOGAN, S., LAU, H., GADGIL, H., AND LIU, D. 2012. Elucidation of acid-induced unfolding and aggregation of human immunoglobulin IgG1 and IgG2 Fc. *The Journal of biological chemistry* 287, 2, 1381–1396.
- LAU, G.K., LOK, A.S., LIANG, R.H., LAI, C.L., CHIU, E.K., LAU, Y.L., AND LAM, S.K. 1997. Clearance of hepatitis B surface antigen after bone marrow transplantation: role of adoptive immunity transfer. *Hepatology (Baltimore, Md.)* 25, 6, 1497–1501.
<https://aasldpubs.onlinelibrary.wiley.com/doi/10.1002/hep.510250631>.
- LAZAR, G.A., DANG, W., KARKI, S., VAFA, O., PENG, J.S., HYUN, L., CHAN, C., CHUNG, H.S., EIVAZI, A., YODER, S.C., VIEMETTER, J., CARMICHAEL, D.F., HAYES, R.J., AND DAHIYAT, B.I. 2006. Engineered antibody Fc variants with enhanced effector function. *Proceedings of the National Academy of Sciences of the United States of America* 103, 11, 4005–4010.
- LAZAREVIC, I., BANKO, A., MILJANOVIC, D., AND CUPIC, M. 2019. Immune-Escape Hepatitis B Virus Mutations Associated with Viral Reactivation upon Immunosuppression. *Viruses* 11, 9.
<https://www.ncbi.nlm.nih.gov/pmc/articles/PMC6784188/#B54-viruses-11-00778>.

- LE BERT, N., SALIMZADEH, L., GILL, U.S., DUTERTRE, C.-A., FACCHETTI, F., TAN, A., HUNG, M., NOVIKOV, N., LAMPERTICO, P., FLETCHER, S.P., KENNEDY, P.T.F., AND BERTOLETTI, A. 2020. Comparative characterization of B cells specific for HBV nucleocapsid and envelope proteins in patients with chronic hepatitis B. *Journal of Hepatology* 72, 1, 34–44. [https://www.journal-of-hepatology.eu/article/S0168-8278\(19\)30424-6/fulltext](https://www.journal-of-hepatology.eu/article/S0168-8278(19)30424-6/fulltext).
- LE BOUVIER, G.L. 1971. The heterogeneity of Australia antigen. *The Journal of infectious diseases* 123, 6, 671–675. <https://pubmed.ncbi.nlm.nih.gov/4106744/>.
- LEBIEN, T.W., AND TEDDER, T.F. 2008. B lymphocytes: how they develop and function. *Blood* 112, 5, 1570–1580. <https://www.ncbi.nlm.nih.gov/pmc/articles/PMC2518873/>.
- LEE, W.S., WHEATLEY, A.K., KENT, S.J., AND DEKOSKY, B.J. 2020. Antibody-dependent enhancement and SARS-CoV-2 vaccines and therapies. *Nat Microbiol* 5, 10, 1185–1191. <https://www.nature.com/articles/s41564-020-00789-5>.
- LI, D., HE, W., LIU, X., ZHENG, S., QI, Y., LI, H., MAO, F., LIU, J., SUN, Y., PAN, L., DU, K., YE, K., LI, W., AND SUI, J. 2017. A potent human neutralizing antibody Fc-dependently reduces established HBV infections. *eLife* 6. <https://www.ncbi.nlm.nih.gov/pmc/articles/PMC5614562/>.
- LIANG, K.-H., HSU, C.-W., CHANG, M.-L., CHEN, Y.-C., LAI, M.-W., AND YEH, C.-T. 2016. Peginterferon Is Superior to Nucleos(t)ide Analogues for Prevention of Hepatocellular Carcinoma in Chronic Hepatitis B. *J Infect Dis* 213, 6, 966–974. <https://academic.oup.com/jid/article/213/6/966/2459472>.
- LIANG, T.J. 2009. Hepatitis B: the virus and disease. *Hepatology* 49, 5 Suppl, S13-21. <https://www.ncbi.nlm.nih.gov/pmc/articles/PMC2809016/>.
- LIANG, T.J., AND GHANY, M. 2002. Hepatitis B e Antigen--the dangerous endgame of hepatitis B. *The New England journal of medicine* 347, 3, 208–210. <https://pubmed.ncbi.nlm.nih.gov/12124411/>.
- LIU, Z., GUNASEKARAN, K., WANG, W., RAZINKOV, V., SEKIROV, L., LENG, E., SWEET, H., FOLTZ, I., HOWARD, M., ROUSSEAU, A.-M., KOZLOSKY, C., FANSLAW, W., AND YAN, W. 2014. Asymmetrical Fc engineering greatly enhances antibody-dependent cellular cytotoxicity (ADCC) effector function and stability of the modified antibodies. *Journal of Biological Chemistry* 289, 6, 3571–3590. [https://www.jbc.org/article/S0021-9258\(19\)74747-4/fulltext](https://www.jbc.org/article/S0021-9258(19)74747-4/fulltext).
- LOK, A.S.F., MCMAHON, B.J., BROWN, R.S., WONG, J.B., AHMED, A.T., FARAH, W., ALMASRI, J., ALAHDAB, F., BENKHADRA, K., MOUCHLI, M.A., SINGH, S., MOHAMED, E.A., ABU DABRH, A.M., PROKOP, L.J., WANG, Z., MURAD, M.H., AND MOHAMMED, K. 2016. Antiviral therapy for chronic hepatitis B viral infection in adults: A systematic review and meta-analysis. *Hepatology* 63, 1, 284–306. <https://pubmed.ncbi.nlm.nih.gov/26566246/>.
- LOTTRICH, F.E. 2009. Major depression during interferon-alpha treatment: vulnerability and prevention. *Dialogues in Clinical Neuroscience* 11, 4, 417–425. <https://www.ncbi.nlm.nih.gov/pmc/articles/PMC3181938/>.
- MADEIRA, F., PEARCE, M., TIVEY, A.R.N., BASUTKAR, P., LEE, J., EDBALI, O., MADHUSOODANAN, N., KOLESNIKOV, A., AND LOPEZ, R. 2022. Search and sequence analysis tools services from EMBL-EBI in 2022. *Nucleic Acids Res* 50, W1, W276-9. <https://academic.oup.com/nar/article/50/W1/W276/6567472?login=false>.
- MADSEN, M., AND GOTHELF, K.V. 2019. Chemistries for DNA Nanotechnology. *Chemical reviews* 119, 10, 6384–6458. <https://pubmed.ncbi.nlm.nih.gov/30714731/>.
- MAGNIUS, L., MASON, W.S., TAYLOR, J., KANN, M., GLEBE, D., DÉNY, P., SUREAU, C., NORDER, H., AND ICTV, R.C. 2020. ICTV Virus Taxonomy Profile: Hepadnaviridae. *The Journal of general virology* 101, 6, 571–572.

- MAINI, M.K., BONI, C., LEE, C.K., LARRUBIA, J.R., REIGNAT, S., OGG, G.S., KING, A.S., HERBERG, J., GILSON, R., ALISA, A., WILLIAMS, R., VERGANI, D., NAOUMOV, N.V., FERRARI, C., AND BERTOLETTI, A. 2000. The role of virus-specific CD8(+) cells in liver damage and viral control during persistent hepatitis B virus infection. *The Journal of experimental medicine* 191, 8, 1269–1280. <https://pubmed.ncbi.nlm.nih.gov/10770795/>.
- MARCHESI, V.T., AND GOWANS, J.L. 1964. THE MIGRATION OF LYMPHOCYTES THROUGH THE ENDOTHELIUM OF VENULES IN LYMPH NODES: AN ELECTRON MICROSCOPE STUDY. *Proceedings of the Royal Society of London. Series B, Biological sciences* 159, 283–290. <https://pubmed.ncbi.nlm.nih.gov/14114164/>.
- MICHLER, T., KOSINSKA, A.D., FESTAG, J., BUNSE, T., SU, J., RINGELHAN, M., IMHOF, H., GRIMM, D., STEIGER, K., MOGLER, C., HEIKENWALDER, M., MICHEL, M.-L., GUZMAN, C.A., MILSTEIN, S., SEPP-LORENZINO, L., KNOLLE, P., AND PROTZER, U. 2020. Knockdown of Virus Antigen Expression Increases Therapeutic Vaccine Efficacy in High-Titer Hepatitis B Virus Carrier Mice. *Gastroenterology* 158, 6, 1762-1775.e9. [https://www.gastrojournal.org/article/S0016-5085\(20\)30125-6/fulltext](https://www.gastrojournal.org/article/S0016-5085(20)30125-6/fulltext).
- MIMOTO, F., IGAWA, T., KURAMOCHI, T., KATADA, H., KADONO, S., KAMIKAWA, T., SHIDA-KAWAZOE, M., AND HATTORI, K. 2013. Novel asymmetrically engineered antibody Fc variant with superior FcγR binding affinity and specificity compared with afucosylated Fc variant. *mAbs* 5, 2, 229–236. <https://www.ncbi.nlm.nih.gov/pmc/articles/PMC3893233/>.
- MONFERRER, A., KRETMANN, J.A., SIGL, C., SAPELZA, P., LIEDL, A., WITTMANN, B., AND DIETZ, H. 2022. Broad-Spectrum Virus Trapping with Heparan Sulfate-Modified DNA Origami Shells. *ACS nano* 16, 12, 20002–20009. <https://pubmed.ncbi.nlm.nih.gov/36323320/>.
- MUELLER, A.M., BREITSPRECHER, D., DUHR, S., BAASKE, P., SCHUBERT, T., AND LÄNGST, G. 2017. MicroScale Thermophoresis: A Rapid and Precise Method to Quantify Protein–Nucleic Acid Interactions in Solution. In *Functional Genomics*. Humana Press, New York, NY, 151–164.
- MURPHY, K., AND WEAVER, C. 2017. *Janeway's immunobiology*. Garland Science, New York.
- NANOTEMPER TECHNOLOGIES. 2022. *Compare Monolith Series*. <https://nanotempertech.com/compare-monolith-systems/>. Accessed 11 January 2023.
- NASSAL, M. 2015. HBV cccDNA: viral persistence reservoir and key obstacle for a cure of chronic hepatitis B. *Gut* 64, 12, 1972–1984. <https://gut.bmj.com/content/64/12/1972>.
- NOORDEEN, F. 2015. Hepatitis B virus infection: An insight into infection outcomes and recent treatment options. *VirusDisease* 26, 1-2, 1–8. <https://www.ncbi.nlm.nih.gov/pmc/articles/PMC4585049/>.
- NORDER, H., HAMMAS, B., LÖFDAHL, S., COUROUCÉ, A.M., AND MAGNIUS, L.O. 1992. Comparison of the amino acid sequences of nine different serotypes of hepatitis B surface antigen and genomic classification of the corresponding hepatitis B virus strains. *The Journal of general virology* 73 (Pt 5), 1201–1208. <https://pubmed.ncbi.nlm.nih.gov/1588323/>.
- OKAMOTO, H., IMAI, M., TSUDA, F., TANAKA, T., MIYAKAWA, Y., AND MAYUMI, M. 1987. Point mutation in the S gene of hepatitis B virus for a d/y or w/r subtypic change in two blood donors carrying a surface antigen of compound subtype adyr or adwr. *Journal of virology* 61, 10, 3030–3034. <https://pubmed.ncbi.nlm.nih.gov/3041023/>.
- OKAMOTO, H., TSUDA, F., SAKUGAWA, H., SASTROSEWIGNJO, R.I., IMAI, M., MIYAKAWA, Y., AND MAYUMI, M. 1988. Typing hepatitis B virus by homology in nucleotide sequence: comparison of surface antigen subtypes. *The Journal of general virology* 69 (Pt 10), 2575–2583. <https://pubmed.ncbi.nlm.nih.gov/3171552/>.

- PAPASTERGIOU, V., LOMBARDI, R., MACDONALD, D., AND TSOCHATZIS, E.A. 2015. Global Epidemiology of Hepatitis B Virus (HBV) Infection. *Curr Hepatology Rep* 14, 3, 171–178. <https://link.springer.com/article/10.1007/s11901-015-0269-3>.
- PAPATHEODORIDIS, G.V., DIMOU, E., AND PAPADIMITROPOULOS, V. 2002. Nucleoside analogues for chronic hepatitis B: antiviral efficacy and viral resistance. *The American journal of gastroenterology* 97, 7, 1618–1628.
- PEERIDOGAHEH, H., MESHKAT, Z., HABIBZADEH, S., ARZANLOU, M., SHAHI, J.M., ROSTAMI, S., GERAYLI, S., AND TEIMOURPOUR, R. 2018. Current concepts on immunopathogenesis of hepatitis B virus infection. *Virus research* 245, 29–43.
- PERRILLO, R.P. 2006. Therapy of hepatitis B -- viral suppression or eradication? *Hepatology (Baltimore, Md.)* 43, 2 Suppl 1, S182-93. <https://aasldpubs.onlinelibrary.wiley.com/doi/10.1002/hep.20970>.
- PERRILLO, R.P., CHAU, K.H., OVERBY, L.R., AND DECKER, R.H. 1983. Anti-hepatitis B core immunoglobulin M in the serologic evaluation of hepatitis B virus infection and simultaneous infection with type B, delta agent, and non-A, non-B viruses. *Gastroenterology* 85, 1, 163–167. <https://pubmed.ncbi.nlm.nih.gov/6406288/>.
- PERUSSIA, B., STARR, S., ABRAHAM, S., FANNING, V., AND TRINCHIERI, G. 1983. Human natural killer cells analyzed by B73.1, a monoclonal antibody blocking Fc receptor functions. I. Characterization of the lymphocyte subset reactive with B73.1. *Journal of immunology (Baltimore, Md. : 1950)* 130, 5, 2133–2141. <https://pubmed.ncbi.nlm.nih.gov/6833758/>.
- QIN, Y., AND LIAO, P. 2018. Hepatitis B virus vaccine breakthrough infection: surveillance of S gene mutants of HBV. *Acta virologica* 62, 2, 115–121. <https://pubmed.ncbi.nlm.nih.gov/29895151/>.
- QUITT, O., LUO, S., MEYER, M., XIE, Z., GOLSABZ-SHIRAZI, F., LOFFREDO-VERDE, E., FESTAG, J., BOCKMANN, J.H., ZHAO, L., STADLER, D., CHOU, W.-M., TEDJOKUSUMO, R., WETTENGEL, J.M., KO, C., NOEBNER, E., BULBUC, N., SHOKRI, F., LÜTTGAU, S., HEIKENWÄLDER, M., BOHNE, F., MOLDENHAUER, G., MOMBURG, F., AND PROTZER, U. 2021. T-cell engager antibodies enable T cells to control HBV infection and to target HBsAg-positive hepatoma in mice. *Journal of Hepatology* 75, 5, 1058–1071. <https://pubmed.ncbi.nlm.nih.gov/34171437/>.
- RATH, A., GLIBOWICKA, M., NADEAU, V.G., CHEN, G., AND DEBER, C.M. 2009. Detergent binding explains anomalous SDS-PAGE migration of membrane proteins. *Proceedings of the National Academy of Sciences of the United States of America* 106, 6, 1760–1765.
- REPLICOR. 2020. *PIPELINE - Replicor*. <https://replicor.com/pipeline/>. Accessed 12 January 2023.
- RIDGWAY, J.B., PRESTA, L.G., AND CARTER, P. 1996. 'Knobs-into-holes' engineering of antibody CH3 domains for heavy chain heterodimerization. *Protein engineering* 9, 7, 617–621. <https://pubmed.ncbi.nlm.nih.gov/8844834/>.
- RODRÍGUEZ-IÑIGO, E., MARISCAL, L., BARTOLOMÉ, J., CASTILLO, I., NAVACERRADA, C., ORTIZ-MOVILLA, N., PARDO, M., AND CARREÑO, V. 2003. Distribution of hepatitis B virus in the liver of chronic hepatitis C patients with occult hepatitis B virus infection. *Journal of medical virology* 70, 4, 571–580. <https://pubmed.ncbi.nlm.nih.gov/12794719/>.
- ROMANI, S., HOSSEINI, S.M., MOHEBBI, S.R., BOONSTRA, A., HOSSEINI RAZAVI, A., AND SHARIFIAN, A. 2018. Characterization of the "a" determinant region of the hepatitis B virus genome in Iranian patients at different clinical phases of chronic infection. *Gastroenterology and hepatology from bed to bench* 11, 2, 131–137. <https://www.ncbi.nlm.nih.gov/pmc/articles/PMC5990914/>.
- ROMANÒ, L., PALADINI, S., GALLI, C., RAIMONDO, G., POLLICINO, T., AND ZANETTI, A.R. 2015. Hepatitis B vaccination. *Human Vaccines & Immunotherapeutics* 11, 1, 53–57. <https://pubmed.ncbi.nlm.nih.gov/25483515/>.

- RUDNICK, S.I., AND ADAMS, G.P. 2009. Affinity and avidity in antibody-based tumor targeting. *Cancer Biotherapy & Radiopharmaceuticals* 24, 2, 155–161.
<https://www.ncbi.nlm.nih.gov/pmc/articles/PMC2902227/>.
- SALIMZADEH, L., LE BERT, N., DUTERTRE, C.-A., GILL, U.S., NEWELL, E.W., FREY, C., HUNG, M., NOVIKOV, N., FLETCHER, S., KENNEDY, P.T., AND BERTOLETTI, A. 2018. PD-1 blockade partially recovers dysfunctional virus-specific B cells in chronic hepatitis B infection. *The Journal of clinical investigation* 128, 10, 4573–4587. <https://pubmed.ncbi.nlm.nih.gov/30084841/>.
- SCHAEFER, S. 2007. Hepatitis B virus taxonomy and hepatitis B virus genotypes. *World journal of gastroenterology* 13, 1, 14–21. <https://pubmed.ncbi.nlm.nih.gov/17206751/>.
- SCHEFFEL, J., AND HOBBER, S. 2021. Highly selective Protein A resin allows for mild sodium chloride-mediated elution of antibodies. *Journal of chromatography. A* 1637, 461843.
<https://www.sciencedirect.com/science/article/pii/S0021967320311171>.
- SEEMAN, N.C. 1982. Nucleic acid junctions and lattices. *Journal of Theoretical Biology* 99, 2, 237–247.
<https://www.sciencedirect.com/science/article/pii/0022519382900029>.
- SEYDOUX, E., HOMAD, L.J., MACCAMY, A.J., PARKS, K.R., HURLBURT, N.K., JENNEWAIN, M.F., AKINS, N.R., STUART, A.B., WAN, Y.-H., FENG, J., WHALEY, R.E., SINGH, S., BOECKH, M., COHEN, K.W., McELRATH, M.J., ENGLUND, J.A., CHU, H.Y., PANCERA, M., MCGUIRE, A.T., AND STAMATATOS, L. 2020. Analysis of a SARS-CoV-2-Infected Individual Reveals Development of Potent Neutralizing Antibodies with Limited Somatic Mutation. *Immunity* 53, 1, 98-105.e5.
<https://www.sciencedirect.com/science/article/pii/S1074761320302314>.
- SIGL, C., WILLNER, E.M., ENGELEN, W., KRETZMANN, J.A., SACHENBACHER, K., LIEDL, A., KOLBE, F., WILSCH, F., AGHVAMI, S.A., PROTZER, U., HAGAN, M.F., FRADEN, S., AND DIETZ, H. 2021. Programmable icosahedral shell system for virus trapping. *Nat. Mater.* 20, 9, 1281–1289.
<https://www.nature.com/articles/s41563-021-01020-4>.
- SOMERS, E.C., ZHAO, W., LEWIS, E.E., WANG, L., WING, J.J., SUNDARAM, B., KAZEROONI, E.A., McCUNE, W.J., AND KAPLAN, M.J. 2012. Type I interferons are associated with subclinical markers of cardiovascular disease in a cohort of systemic lupus erythematosus patients. *PLOS ONE* 7, 5, e37000.
<https://journals.plos.org/plosone/article?id=10.1371/journal.pone.0037000>.
- STAVENHAGEN, J.B., GORLATOV, S., TUAILLON, N., RANKIN, C.T., LI, H., BURKE, S., HUANG, L., VIJH, S., JOHNSON, S., BONVINI, E., AND KOENIG, S. 2007. Fc optimization of therapeutic antibodies enhances their ability to kill tumor cells in vitro and controls tumor expansion in vivo via low-affinity activating Fcγ receptors. *Cancer research* 67, 18, 8882–8890. <https://pubmed.ncbi.nlm.nih.gov/17875730/>.
- STERNER, R.C., AND STERNER, R.M. 2021. CAR-T cell therapy: current limitations and potential strategies. *Blood Cancer Journal* 11, 4, 69. <https://www.ncbi.nlm.nih.gov/pmc/articles/PMC8024391/>.
- STUYVER, L., GENDT, S. DE, VAN GEYT, C., ZOULIM, F., FRIED, M., SCHINAZI, R.F., AND ROSSAU, R. 2000. A new genotype of hepatitis B virus: complete genome and phylogenetic relatedness. *The Journal of general virology* 81, Pt 1, 67–74. <https://pubmed.ncbi.nlm.nih.gov/10640543/>.
- SU, Q., SCHRÖDER, C.H., HOFMANN, W.J., OTTO, G., PICHLMAYR, R., AND BANNASCH, P. 1998. Expression of hepatitis B virus X protein in HBV-infected human livers and hepatocellular carcinomas. *Hepatology (Baltimore, Md.)* 27, 4, 1109–1120.
- SUFFNER, S., GERSTENBERG, N., PATRA, M., RUIBAL, P., ORABI, A., SCHINDLER, M., AND BRUSS, V. 2018. Domains of the Hepatitis B Virus Small Surface Protein S Mediating Oligomerization. *Journal of virology* 92, 11. <https://www.ncbi.nlm.nih.gov/pmc/articles/PMC5952150/>.
- SUN, D., GAO, W., HU, H., AND ZHOU, S. 2022. Why 90% of clinical drug development fails and how to improve it? *Acta Pharmaceutica Sinica B* 12, 7, 3049–3062.
<https://www.sciencedirect.com/science/article/pii/S2211383522000521>.

- SUNG, H., FERLAY, J., SIEGEL, R.L., LAVERSANNE, M., SOERJOMATARAM, I., JEMAL, A., AND BRAY, F. 2021. Global Cancer Statistics 2020: GLOBOCAN Estimates of Incidence and Mortality Worldwide for 36 Cancers in 185 Countries. *CA: a cancer journal for clinicians* 71, 3, 209–249. <https://pubmed.ncbi.nlm.nih.gov/33538338/>.
- SUREAU, C. 2016. A unique monoclonal antibody for therapeutic use against chronic hepatitis B: not all antibodies are created equal. *Gut* 65, 4, 546–547. <https://gut.bmj.com/content/65/4/546>.
- TABOR, E., HOOFNAGLE, J.H., BARKER, L.F., PINEDA-TAMONDONG, G., NATH, N., SMALLWOOD, L.A., AND GERETY, R.J. 1981. Antibody to hepatitis B core antigen in blood donors with a history of hepatitis. *Transfusion* 21, 3, 366–371. <https://pubmed.ncbi.nlm.nih.gov/7233523/>.
- TAKAHASHI, K., MACHIDA, A., FUNATSU, G., NOMURA, M., USUDA, S., AOYAGI, S., TACHIBANA, K., MIYAMOTO, H., IMAI, M., NAKAMURA, T., MIYAKAWA, Y., AND MAYUMI, M. 1983. Immunochemical structure of hepatitis B e antigen in the serum. *Journal of immunology (Baltimore, Md. : 1950)* 130, 6, 2903–2907. <https://pubmed.ncbi.nlm.nih.gov/6189903/>.
- TANG, X.-R., ZHANG, J.-S., ZHAO, H., GONG, Y.-H., WANG, Y.-Z., AND ZHAO, J.-L. 2007. Detection of hepatitis B virus genotypes using oligonucleotide chip among hepatitis B virus carriers in Eastern China. *World journal of gastroenterology* 13, 13, 1975–1979. <https://www.ncbi.nlm.nih.gov/pmc/articles/PMC4146976/>.
- TARAFDAR, S., VIRATA, M.L., YAN, H., ZHONG, L., DENG, L., XU, Y., HE, Y., STRUBLE, E., AND ZHANG, P. 2022. Multiple epitopes of hepatitis B virus surface antigen targeted by human plasma-derived immunoglobulins coincide with clinically observed escape mutations. *Journal of medical virology* 94, 2, 649–658. <https://pubmed.ncbi.nlm.nih.gov/34406663/>.
- TARAO, K., NOZAKI, A., IKEDA, T., SATO, A., KOMATSU, H., KOMATSU, T., TAGURI, M., AND TANAKA, K. 2019. Real impact of liver cirrhosis on the development of hepatocellular carcinoma in various liver diseases—meta-analytic assessment. *Cancer Medicine* 8, 3, 1054–1065. <https://www.ncbi.nlm.nih.gov/pmc/articles/PMC6434205/>.
- TATEMATSU, K., TANAKA, Y., KURBANOV, F., SUGAUCHI, F., MANO, S., MAESHIRO, T., NAKAYOSHI, T., WAKUTA, M., MIYAKAWA, Y., AND MIZOKAMI, M. 2009. A genetic variant of hepatitis B virus divergent from known human and ape genotypes isolated from a Japanese patient and provisionally assigned to new genotype J. *Journal of virology* 83, 20, 10538–10547. <https://www.ncbi.nlm.nih.gov/pmc/articles/PMC2753143/>.
- TERRAULT, N.A., LOK, A.S.F., MCMAHON, B.J., CHANG, K.-M., HWANG, J.P., JONAS, M.M., BROWN, R.S., BZOWEJ, N.H., AND WONG, J.B. 2018. Update on prevention, diagnosis, and treatment of chronic hepatitis B: AASLD 2018 hepatitis B guidance. *Hepatology* 67, 4, 1560–1599.
- THERMO SCIENTIFIC. 2011. *Gentle Ag/Ab Binding and Elution Buffers*. https://www.thermofisher.com/document-connect/document-connect.html?url=https://assets.thermofisher.com/TFS-Assets%2FMSG%2Fmanuals%2FMAN0011176_Gentle_AgAb_Bind_Elution_Buff_UG.pdf. Accessed 11 January 2023.
- THIMME, R., WIELAND, S., STEIGER, C., GHRAYEB, J., REIMANN, K.A., PURCELL, R.H., AND CHISARI, F.V. 2003. CD8(+) T cells mediate viral clearance and disease pathogenesis during acute hepatitis B virus infection. *Journal of virology* 77, 1, 68–76.
- TIWARI, P., KAILA, P., AND GUPTASARMA, P. 2019. Understanding anomalous mobility of proteins on SDS-PAGE with special reference to the highly acidic extracellular domains of human E- and N-cadherins. *ELECTROPHORESIS* 40, 9, 1273–1281. <https://analyticalsciencejournals.onlinelibrary.wiley.com/doi/10.1002/elps.201800219>.

- TONG, S., AND REVILL, P. 2016. Overview of hepatitis B viral replication and genetic variability. *Journal of Hepatology* 64, 1 Suppl, S4-S16. <https://pubmed.ncbi.nlm.nih.gov/27084035/>.
- TSENG, T.-C., KAO, J.-H., AND CHEN, D.-S. 2014. Peginterferon α in the treatment of chronic hepatitis B. *Expert opinion on biological therapy* 14, 7, 995–1006.
- TSUGE, M., HIRAGA, N., UCHIDA, T., KAN, H., MIYAKI, E., MASAKI, K., ONO, A., NAKAHARA, T., ABE-CHAYAMA, H., ZHANG, Y., NASWA, M.G., KAWAOKA, T., MIKI, D., IMAMURA, M., KAWAKAMI, Y., AIKATA, H., OCHI, H., HAYES, C.N., AND CHAYAMA, K. 2016. Antiviral effects of anti-HBs immunoglobulin and vaccine on HBs antigen seroclearance for chronic hepatitis B infection. *J Gastroenterol* 51, 11, 1073–1080. <https://link.springer.com/article/10.1007/s00535-016-1189-x>.
- TU, T., ZEHNDER, B., WETTENGEL, J.M., ZHANG, H., COULTER, S., HO, V., DOUGLAS, M.W., PROTZER, U., GEORGE, J., AND URBAN, S. 2022. Mitosis of hepatitis B virus-infected cells in vitro results in uninfected daughter cells. *JHEP Reports* 4, 9, 100514.
- TU, T., ZHANG, H., AND URBAN, S. 2021. Hepatitis B Virus DNA Integration: In Vitro Models for Investigating Viral Pathogenesis and Persistence. *Viruses* 13, 2.
- VAN MONTFOORT, N., VAN DER AA, E., AND WOLTMAN, A.M. 2014. Understanding MHC class I presentation of viral antigens by human dendritic cells as a basis for rational design of therapeutic vaccines. *Front. Immunol.* 5, 182. <https://www.frontiersin.org/articles/10.3389/fimmu.2014.00182/full>.
- VARGASON, A.M., ANSELMO, A.C., AND MITRAGOTRI, S. 2021. The evolution of commercial drug delivery technologies. *Nat Biomed Eng* 5, 9, 951–967. <https://www.nature.com/articles/s41551-021-00698-w>.
- VELKOV, S., OTT, J.J., PROTZER, U., AND MICHLER, T. 2018. The Global Hepatitis B Virus Genotype Distribution Approximated from Available Genotyping Data. *Genes* 9, 10. <https://pubmed.ncbi.nlm.nih.gov/30326600/>.
- VENEZIANO, R., RATANALERT, S., ZHANG, K., ZHANG, F., YAN, H., CHIU, W., AND BATHE, M. 2016. Designer nanoscale DNA assemblies programmed from the top down. *Science (New York, N.Y.)* 352, 6293, 1534. <https://pubmed.ncbi.nlm.nih.gov/27229143/>.
- VERRIER, E.R., COLPITTS, C.C., BACH, C., HEYDMANN, L., WEISS, A., RENAUD, M., DURAND, S.C., HABERSETZER, F., DURANTEL, D., ABOU-JAOUDE, G., LÓPEZ LEDESMA, M.M., FELMLEE, D.J., SOUMILLON, M., CROONENBORGH, T., POCHE, N., NASSAL, M., SCHUSTER, C., BRINO, L., SUREAU, C., ZEISEL, M.B., AND BAUMERT, T.F. 2016. A targeted functional RNA interference screen uncovers glypican 5 as an entry factor for hepatitis B and D viruses. *Hepatology* 63, 1, 35–48. <https://aasldpubs.onlinelibrary.wiley.com/doi/10.1002/hep.28013>.
- WAN, Y.Y., AND FLAVELL, R.A. 2009. How diverse--CD4 effector T cells and their functions. *Journal of molecular cell biology* 1, 1, 20–36. <https://www.ncbi.nlm.nih.gov/pmc/articles/PMC2841031/#:~:text=CD4%20effector%20T%20cells%2C%20also,and%20function%20of%20Th%20cells>.
- WEBSTER, G.J.M., REIGNAT, S., BROWN, D., OGG, G.S., JONES, L., SENEVIRATNE, S.L., WILLIAMS, R., DUSHEIKO, G., AND BERTOLETTI, A. 2004. Longitudinal analysis of CD8+ T cells specific for structural and nonstructural hepatitis B virus proteins in patients with chronic hepatitis B: implications for immunotherapy. *Journal of virology* 78, 11, 5707–5719. <https://pubmed.ncbi.nlm.nih.gov/15140968/>.
- WHO. 2022. *Hepatitis B*. <https://www.who.int/news-room/fact-sheets/detail/hepatitis-b>. Accessed 2 December 2022.
- WIECZOREK, M., ABUALROUS, E.T., STICHT, J., ÁLVARO-BENITO, M., STOLZENBERG, S., NOÉ, F., AND FREUND, C. 2017. Major Histocompatibility Complex (MHC) Class I and MHC Class II Proteins: Conformational

- Plasticity in Antigen Presentation. *Front. Immunol.* 8, 292. <https://www.frontiersin.org/articles/10.3389/fimmu.2017.00292/full>.
- WISSKIRCHEN, K., KAH, J., MALO, A., ASEN, T., VOLZ, T., ALLWEISS, L., WETTENGEL, J.M., LÜTGEHETMANN, M., URBAN, S., BAUER, T., DANDRI, M., AND PROTZER, U. 2019. T cell receptor grafting allows virological control of Hepatitis B virus infection. *The Journal of clinical investigation* 129, 7, 2932–2945. <https://www.jci.org/articles/view/120228>.
- WLODAWER, A., MINOR, W., DAUTER, Z., AND JASKOLSKI, M. 2013. Protein crystallography for aspiring crystallographers or how to avoid pitfalls and traps in macromolecular structure determination. *The FEBS journal* 280, 22, 5705–5736. <https://www.ncbi.nlm.nih.gov/pmc/articles/PMC4080831/>.
- WOLFF, L.S. 2020. *Generation and characterization of novel human monoclonal antibodies directed against the hepatitis B virus*. Dissertation, Technische Universität München.
- WOUNDERLICH, G., AND BRUSS, V. 1996. Characterization of early hepatitis B virus surface protein oligomers. *Archives of virology* 141, 7, 1191–1205. <https://pubmed.ncbi.nlm.nih.gov/8774681/>.
- WU, J., MENG, Z., JIANG, M., PEI, R., TRIPPLER, M., BROERING, R., BUCCHI, A., SOWA, J.-P., DITTMER, U., YANG, D., ROGGENDORF, M., GERKEN, G., LU, M., AND SCHLAAK, J.F. 2009. Hepatitis B virus suppresses toll-like receptor-mediated innate immune responses in murine parenchymal and nonparenchymal liver cells. *Hepatology* 49, 4, 1132–1140. <https://aasldpubs.onlinelibrary.wiley.com/doi/10.1002/hep.22751>.
- WUCHERPFENNIG, K.W., GAGNON, E., CALL, M.J., HUSEBY, E.S., AND CALL, M.E. 2010. Structural biology of the T-cell receptor: insights into receptor assembly, ligand recognition, and initiation of signaling. *Cold Spring Harbor perspectives in biology* 2, 4, a005140. <https://pubmed.ncbi.nlm.nih.gov/20452950/>.
- XU, C., CHEN, J., AND CHEN, X. 2021. Host Innate Immunity Against Hepatitis Viruses and Viral Immune Evasion. *Frontiers in microbiology* 12, 740464.
- XU, Y., LEE, J., TRAN, C., HEIBECK, T.H., WANG, W.D., YANG, J., STAFFORD, R.L., STEINER, A.R., SATO, A.K., HALLAM, T.J., AND YIN, G. 2015. Production of bispecific antibodies in "knobs-into-holes" using a cell-free expression system. *mAbs* 7, 1, 231–242.
- YAN, H., ZHONG, G., XU, G., HE, W., JING, Z., GAO, Z., HUANG, Y., QI, Y., PENG, B., WANG, H., FU, L., SONG, M., CHEN, P., GAO, W., REN, B., SUN, Y., CAI, T., FENG, X., SUI, J., AND LI, W. 2012. Sodium taurocholate cotransporting polypeptide is a functional receptor for human hepatitis B and D virus. *eLife Sciences Publications, Ltd* (Nov.).
- YANG, H.-I., LU, S.-N., LIAW, Y.-F., YOU, S.-L., SUN, C.-A., WANG, L.-Y., HSIAO, C.K., CHEN, P.-J., CHEN, D.-S., AND CHEN, C.-J. 2002. Hepatitis B e antigen and the risk of hepatocellular carcinoma. *The New England journal of medicine* 347, 3, 168–174. <https://pubmed.ncbi.nlm.nih.gov/12124405/>.
- YE, J., AND CHEN, J. 2021. Interferon and Hepatitis B: Current and Future Perspectives. *Front. Immunol.* 12, 733364. <https://www.ncbi.nlm.nih.gov/pmc/articles/PMC8452902/>.
- YEH, V., GOODE, A., AND BONEV, B.B. 2020. Membrane Protein Structure Determination and Characterisation by Solution and Solid-State NMR. *Biology* 9, 11. <https://www.ncbi.nlm.nih.gov/pmc/articles/PMC7697852/>.
- YU, X., LAN, P., HOU, X., HAN, Q., LU, N., LI, T., JIAO, C., ZHANG, J., ZHANG, C., AND TIAN, Z. 2017. HBV inhibits LPS-induced NLRP3 inflammasome activation and IL-1 β production via suppressing the NF- κ B pathway and ROS production. *Journal of Hepatology* 66, 4, 693–702. [https://www.journal-of-hepatology.eu/article/S0168-8278\(16\)30751-6/fulltext](https://www.journal-of-hepatology.eu/article/S0168-8278(16)30751-6/fulltext).
- ZAHAVI, D., AND WEINER, L. 2020. Monoclonal Antibodies in Cancer Therapy. *Antibodies (Basel, Switzerland)* 9, 3. <https://www.ncbi.nlm.nih.gov/pmc/articles/PMC7551545/>.

- ZHANG, T.-Y., YUAN, Q., ZHAO, J.-H., ZHANG, Y.-L., YUAN, L.-Z., LAN, Y., LO, Y.-C., SUN, C.-P., WU, C.-R., ZHANG, J.-F., ZHANG, Y., CAO, J.-L., GUO, X.-R., LIU, X., MO, X.-B., LUO, W.-X., CHENG, T., CHEN, Y.-X., TAO, M.-H., SHIH, J.W., ZHAO, Q.-J., ZHANG, J., CHEN, P.-J., YUAN, Y.A., AND XIA, N.-S. 2016. Prolonged suppression of HBV in mice by a novel antibody that targets a unique epitope on hepatitis B surface antigen. *Gut* 65, 4, 658–671. <https://pubmed.ncbi.nlm.nih.gov/26423112/>.
- ZHANG, Z.-H., LI, L., ZHAO, X.-P., GLEBE, D., BREMER, C.M., ZHANG, Z.-M., TIAN, Y.-J., WANG, B.-J., YANG, Y., GERLICH, W., ROGGENDORF, M., LI, X., LU, M., AND YANG, D.-L. 2011. Elimination of hepatitis B virus surface antigen and appearance of neutralizing antibodies in chronically infected patients without viral clearance. *Journal of viral hepatitis* 18, 6, 424–433. <https://onlinelibrary.wiley.com/doi/10.1111/j.1365-2893.2010.01322.x>.
- ZHAO, L., CHEN, F., QUITT, O., FESTAG, M., RINGELHAN, M., WISSKIRCHEN, K., FESTAG, J., YAKOVLEVA, L., SUREAU, C., BOHNE, F., AICHLER, M., BRUSS, V., SHEVTSOV, M., VAN DE KLUNDERT, M., MOMBURG, F., MÖHL, B.S., AND PROTZER, U. 2021. Hepatitis B virus envelope proteins can serve as therapeutic targets embedded in the host cell plasma membrane. *Cellular Microbiology* 23, 12, e13399. <https://onlinelibrary.wiley.com/doi/full/10.1111/cmi.13399>.
- ZHOU, B., XIA, L., ZHANG, T., YOU, M., HUANG, Y., HE, M., SU, R., TANG, J., ZHANG, J., LI, S., AN, Z., YUAN, Q., LUO, W., AND XIA, N. 2020. Structure guided maturation of a novel humanized anti-HBV antibody and its preclinical development. *Antiviral Research* 180, 104757. <https://www.sciencedirect.com/science/article/pii/S0166354219304723>.
- ZHOU, L., HE, R., FANG, P., LI, M., YU, H., WANG, Q., YU, Y., WANG, F., ZHANG, Y., CHEN, A., PENG, N., LIN, Y., ZHANG, R., TRILLING, M., BROERING, R., LU, M., ZHU, Y., AND LIU, S. 2021. Hepatitis B virus rigs the cellular metabolome to avoid innate immune recognition. *Nat Commun* 12, 1, 98. <https://www.nature.com/articles/s41467-020-20316-8>.

Acknowledgements

First of all I want to thank Prof. Ulrike Protzer for giving me the opportunity to work on these various projects and do my PhD thesis in her lab. You believed in me and supported me when I needed it.

Next, I want to thank Prof. Matthias Feige and Dr. Karin Wisskirchen who were members of my Thesis Committee. You provided valuable input during all the TAC meetings we had, helping me to get back on track.

A major thank you goes to Lisa who supervised me during my first year and who lay the ground for my projects. You helped me to get started and were always there when I had questions. You gave scientific and emotional support and I am so glad to have had the luck of having such a great supervisor in the beginning.

Another big thank you goes to my collaboration partners Zahra, Elena, Dr. Anne Schütz and Prof. Hendrik Dietz. It was always a pleasure to work with you and the projects we worked on really brought this thesis to another level.

I want to thank Philipp Kolb for providing scientific input and cells used in this thesis.

Moreover, I want to thank the students and interns I supervised. Rafi, Nadja and Alex – all of you helped me to become a better supervisor and a better scientist. It was so much fun to work with either of you! Thank you!

Furthermore, I want to thank all the current and former lab members. Especially Sophia, Theresa, Philipp, Kathi, Antje M., Antje H., Lea, Laura, Shubhankar, Cho-Chin, Aaron, Anna, Eda and Zhe. You provided scientific input and made the in-between time a lot of fun with tons of conversations during coffee or lunch breaks about everything and nothing. Thank you for that!

Big thanks go to Basti and Flo. The time with you in the lab (“Fenna and the boys”) will always have a special place in my heart and without you I would not have had half as much fun in and outside the lab as I did. Thank you so much for being there!

Special thanks go to Olli, Martin and Alex. You did not only provide valuable scientific input whenever I asked for it but also gave emotional support in every situation. You really made my time here so much more valuable and fun. I will never forget all the conversations we had or the karaoke nights when we were singing until the next morning. You taught me so many things. I did not only become a better scientist because of you but I also increased my Magic skills a lot! You really carried me through this thesis. From the bottom of my heart: Thank you!

I also want to thank my friends outside of the lab. Especially Maria, Lena and Tabbi. You provided emotional support and never stopped believing in me. With you I could just forget about the challenges I faced and somehow you made everything okay again. Thanks for having my back all these years!

All of this would not have been possible without the support of my parents and my brother. You provided me with the education I needed to even think about starting a PhD thesis. You did not only pay for my whole studies and made it so easy for me to focus on my studies but you also ensured that I knew that you always believed in me. You did not always understand what I was doing but you never doubted my competencies and you supported me unconditionally. Thank you so much!

Lastly, I want to thank Fynn. You always had my back from the start of my bachelor studies. You never doubted me and you supported me unconditionally through all these years. I always knew that I could count on you. Without you I would have never trusted myself to be able to come to this point but you always showed me my strengths and pushed me to go further. I will never forget all the things you've done for me and don't want to miss a single moment. Thank you for everything!

THANK YOU!